

Detergent-Protein and Detergent-Lipid Interactions:
Implications for Two-dimensional Crystallization of Membrane Proteins
and
Development of Tools for High Throughput Crystallography

Inauguraldissertation

zur

Erlangung der Würde eines Doktors der Philosophie

vorgelegt der

Philosophisch-Naturwissenschaftlichen Fakultät

der Universität Basel

von

Thomas Claudio Kaufmann
aus Zürich ZH und Möhlin AG

Basel, 2006

Genehmigt von der Philosophisch-Naturwissenschaftlichen Fakultät
auf Antrag von
Prof. Dr. Andreas Engel & PD Dr. Heiko Heerklotz

Basel, den 24. Januar 2006

Prof. Dr. Hans-Jakob Wirz
Dekan

*To my Parents
and my Brother*

Table of Contents

1	General Introduction	1
1.1	Structural Investigations of Proteins	1
1.2	The Rise of the Enlivened World	1
1.3	Amphiphiles	1
1.3.1	Lipids	2
1.3.2	Detergents	4
1.4	Membrane Proteins	7
1.4.1	Biological membranes	7
1.5	Two-Dimensional Crystallization	8
2	Microscopic analysis of AmtB	13
2.1	Abstract	13
2.2	Introduction	13
2.3	Materials and Methods	14
2.3.1	Crystallization	14
2.3.2	Electron microscopy	14
2.3.3	Image processing	14
2.3.4	Atomic force microscopy	14
2.3.5	Western blotting and cell fractionation	15
2.4	Results	15
2.4.1	AmtB is trimeric in the native cell membrane	15
2.4.2	Crystallization and AFM	15
2.4.3	Cryoelectron microscopy	15
2.5	Discussion	16
2.5.1	Speculation	18
2.5.2	Supplementary information	18
2.5.3	Note added in proof	19
2.6	Acknowledgements	19
2.7	References	19
2.8	Supplementary Information	21
3	A Novel Method for Detergent Concentration Determination	23
3.1	Abstract	23
3.2	Introduction	23
3.3	Materials and Methods	24

3.3.1	Construction of the contact angle measuring device	24
3.3.2	Characterization of the substrate	24
3.3.3	Calibration of the detergents	25
3.3.4	Comparison with radioactively labeled DDM	25
3.3.5	Purification of the galactose/proton symporter of <i>E. coli</i> (GalP)	25
3.4	Results	26
3.4.1	Contact angle measurements	26
3.4.2	Characterization of Parafilm M	27
3.4.3	Calibration of the detergents	27
3.4.4	Comparison with radioactively labeled DDM	29
3.4.5	Controlling the amount of detergent bound to a membrane protein during Ni-NTA affinity chromatography	29
3.5	Discussion	29
3.6	Conclusion	32
3.7	Acknowledgements	32
3.8	References	32
4	The Use of Detergents in Membrane Biochemistry	35
4.1	Abstract	35
4.2	Introduction	35
4.3	Results	36
4.3.1	The stability of the galactose/proton symporter GalP from <i>Escherichia coli</i> in dif- ferent detergents	36
4.3.2	Controlling the amount of detergent bound to GalP	38
4.3.3	Solubilization of <i>E. coli</i> lipids with different detergents	39
4.4	Materials and Methods	41
4.4.1	Detergents	41
4.4.2	The stability of the galactose/proton symporter GalP from <i>Escherichia coli</i> in dif- ferent detergents	42
4.4.3	Controlling the amount of detergent bound to GalP	43
4.4.4	Solubilization of <i>E. coli</i> lipids with different detergents	43
4.5	Discussion	44
5	2D Crystallization Using Cyclodextrin	49
5.1	Abstract	49
5.2	Introduction	49
5.3	Materials and Methods	50
5.3.1	MBCD/detergent titration curves	50
5.3.2	OmpF and SoPIP 2;1 purification and reconstitution	51
5.3.3	Controlled MBCD addition	51
5.3.4	Phospholipase A2 treatment	51
5.3.5	Electron microscopy	53
5.4	Results	53
5.4.1	MBCD/detergent titrations	53

5.4.2	2D Crystallization of the Porin OmpF	53
5.4.3	2D Crystallization of SoPIP2;1	53
5.5	Discussion	54
5.5.1	Cyclodextrin and detergent removal	54
5.5.2	2D crystallization of OmpF	56
5.5.3	2D crystallization of SoPIP2;1	56
5.5.4	Large screenings for 2D crystals using cyclodextrin	56
5.6	Conclusion	57
5.7	Acknowledgments	58
5.8	References	58
6	Development of a Tool for HT 2D Crystallization Using MBCD	61
6.1	Abstract	61
6.2	Introduction	61
6.3	Machine for High Throughput Two-dimensional Crystallization	62
6.3.1	Requirements	62
6.3.2	Construction of the Machine	63
6.3.3	Operation of the Machine	64
6.4	Screening Strategy for High Throughput Crystallization	65
6.5	Discussion	69
7	General Discussion and Conclusions	73
7.1	Scope of this Thesis	73
7.2	Combining Electron Microscopy and Atomic Force Microscopy	73
7.3	Investigating the Role of the Detergent	73
7.4	The Use of Cyclodextrins for High Thoroughput 2D Crystallization of Membrane Proteins	74
A	Acknowledgements	79
B	Curriculum Vitae	81
B.1	Personal Details	81
B.2	Education	81
B.3	Teaching	81
B.4	Publications	82
B.5	Courses	82

List of Figures

1.1	Amphiphiles	2
1.2	Lipid structures	3
1.3	Nonionic detergents	5
1.4	Ionic detergents	6
1.5	Membrane protein ORF's in different genomes	7
1.6	Structures in the protein data bank (PDB)	7
1.7	Functional categorization of the <i>E. coli</i> inner membrane proteome	8
1.9	Two-dimensional crystallization and reconstitution into proteoliposomes of membrane proteins	9
1.8	Membrane solubilization	10
2.1	Western blot of protein extracts from wild-type <i>E. coli</i> strain ET8000 grown under nitrogen limitation to induce expression of AmtB from its native promoter	15
2.2	Morphology of crystals	16
2.3	High-resolution AFM of AmtB	16
2.4	CryoEM projection maps of AmtB to 12 Å resolution, represented as grey levels	17
2.5	Features of the AmtB trimer	18
2.6	Representation of the Fourier transform of an image of an AmtB crystal embedded in glucose	21
3.1	Schematic drawing showing the setup of the contact angle measuring device	24
3.2	Image analysis procedure	26
3.3	$\gamma_{lv} \cos \theta$ as a function of the surface tension γ_{lv} of various liquids for Parafilm M.	27
3.4	Semi-logarithmic plot of the detergent concentration vs. experimental contact angles for all calibrated detergents	28
3.5	Influence of the ionic strength on the properties of LDAO at pH 7.9	28
3.6	Quality assessment of the detergent concentration measurement	29
3.7	Ni-NTA affinity chromatography with GalP using washes of different DDM concentrations	31
4.1	Detergent check with GalP	36
4.2	Single particles of GalP in different detergents	37
4.3	SDS-Page of GalP	38
4.4	Detergent bound to GalP and protein yield after purification	38
4.5	Solubilization experiments with <i>E. coli</i> Polar extract and different detergents	40
4.6	Extrapolated solubilization plots	41
4.7	Cryoelectron microscopic images of <i>E. coli</i> lipid solubilization by DDM	42
4.8	Detergent-to-protein ratio	44

5.1	MBCD-detergent titration curves	52
5.2	OmpF 2D crystallization using the MBCD procedure	54
5.3	SoPIP2;1 2D crystallization using MBCD	55
6.1	Conceptual layout of the machine	63
6.2	Schematic top view of the machine	64
6.3	Schematic front view of the machine	65
6.4	Schematic side view of the machine	66
6.5	Frequency distributions of pI and pH of crystallization	67
6.6	Correlation between pI and pH	68
7.1	Strategy for high throughput screening in 2D crystallography	75

List of Tables

1.1	Hydrophile-lipophile balance (HLB) numbers	4
2.1	Internal phase residuals of one image according to plane group symmetry	21
2.2	Mean phase residuals in resolution shells for merged images in p3 and p321	21
3.1	Surface roughness analysis of Parafilm M	27
3.2	Summary of detergent and calibration plot properties	30
6.1	Jones-Dole viscosity B coefficients follow the Hofmeister series	68

Chapter 1

General Introduction

1.1 Structural Investigations of Proteins

Over the last decades structural investigations of proteins gained more and more scientific attention. The deciphering of increasing numbers of genomes of living organisms –including the human genome– led to a flood of detailed genetic information. The transversion of these informations on the genetic level into detailed knowledge on the structural and functional basis of the resulting transcriptional products, i.e., the proteins, represents one of the most labourous challenges of today's molecular biology. The value of such data is invaluable, as with every structure that gets unravelled, a new piece of the puzzle is added to complete the picture of the structural determinants of life. The more three-dimensional (3D) folds are known, the more reliable become computer assisted predictions of 3D structures of yet structurally unknown sequences. Task-specific protein engineering is only one of the beneficial developments that can emerge from such knowledge. Taken together with the spectacular findings in the field of structural biology on the architectural level of life, it becomes evident why so much effort is invested in the elucidation of protein structures.

1.2 The Rise of the Enlivened World

Whether the appearance of nucleic acids or the evolution of biochemical reactions and pathways was first or not still is subject to controversial discussion. However, a crucial step during evolution of life was the delimitation of compartments of finite size within the prebiotic soup. This provided a means of concentrating newly synthesized molecules, thereby increasing the chance of forming oligomers and polymers, e.g. ribonucleic acids (RNA) and proteins. The possibility of enclosing substrates and metabolic substances within a finite compartment, i.e., the (proto-)cell, represented an evolutionary highly active environment.

The need for exchange and communication between the inside and outside of such prototyped cells arose as an intrinsic consequence of the system. However, the benefits of compartmentalization would be lost in great parts if there wouldn't be tight control of the traffic between the in- and the outside. Simple diffusion would lead to equal distribution of components. Therefore the task to be fulfilled

extends beyond simple opening and closing. It is rather a rigorously controlled reaction to specific substrates accounting for a given context. Nature came up with the concept of enzymes embedded in the membranes –membrane proteins–, i.e., precisely controlled valves directly at the interface between the inside and the outside. These peptides were in fact designed to either act passively as filters or actively as real carriers and transporters using energy sources like concentration gradients, adenosine triphosphate (ATP) and electrochemical gradients.

1.3 Amphiphiles

Amphiphilic molecules are composed of a hydrophobic (lipophilic) part and a hydrophilic (lipophobic) head group. 'Hydrophobic' meaning that this part is soluble in apolar solvents (such as chloroform) and 'hydrophilic', in turn, meaning that this part is soluble in polar solvents (such as water). Due to this dual character they self-assemble in aqueous solution in a variety of morphologically different structures (see Figure 1.1). The driving force

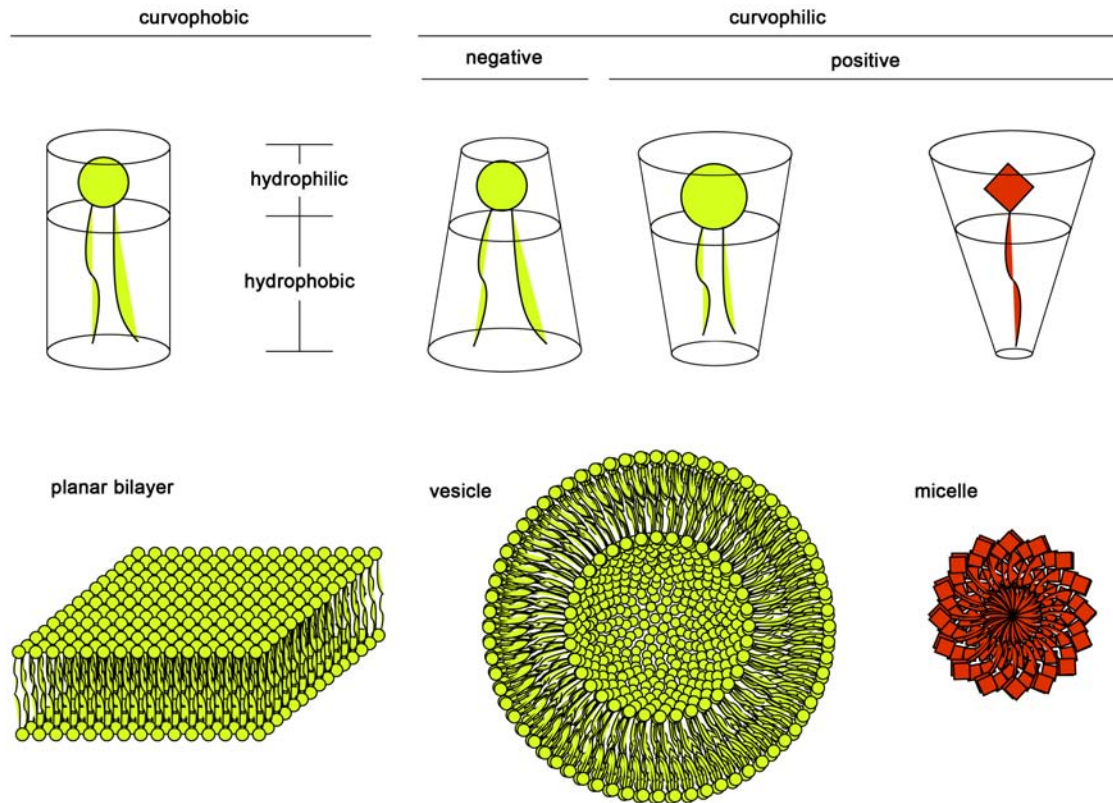


Figure 1.1: **Amphiphiles.** *Upper row:* Shape and properties of Lipids and detergents. *Lower row:* Higher order structures spontaneously formed in aqueous solution.

for this aggregation process is the tendency of the hydrophobic part to minimize contact with water, an effect called the 'hydrophobic effect' (Tanford, 1980) and that is mainly due to the entropic gain of the water structure by not being in contact with the hydrophobic part. A variety of different aggregate shapes are observed that range from spherical and rod-like micelles to amphiphilic bilayers. The actual form assumed by an aggregate depends on the molecular constitution of the amphiphile and can be explained by simple geometric considerations. On the basis of the size of the head group as compared to the hydrophobic tail the overall structure can be described as being of cylindrical or conical shape. Therefore, amphiphilic molecules can be divided in two groups: curvophobic and curvophilic, respectively; whereas the curvophilic comprise either positive or negative curvophilic, depending on the orientation of the cone. This classification is commonly referred to as spontaneous curvature strain.

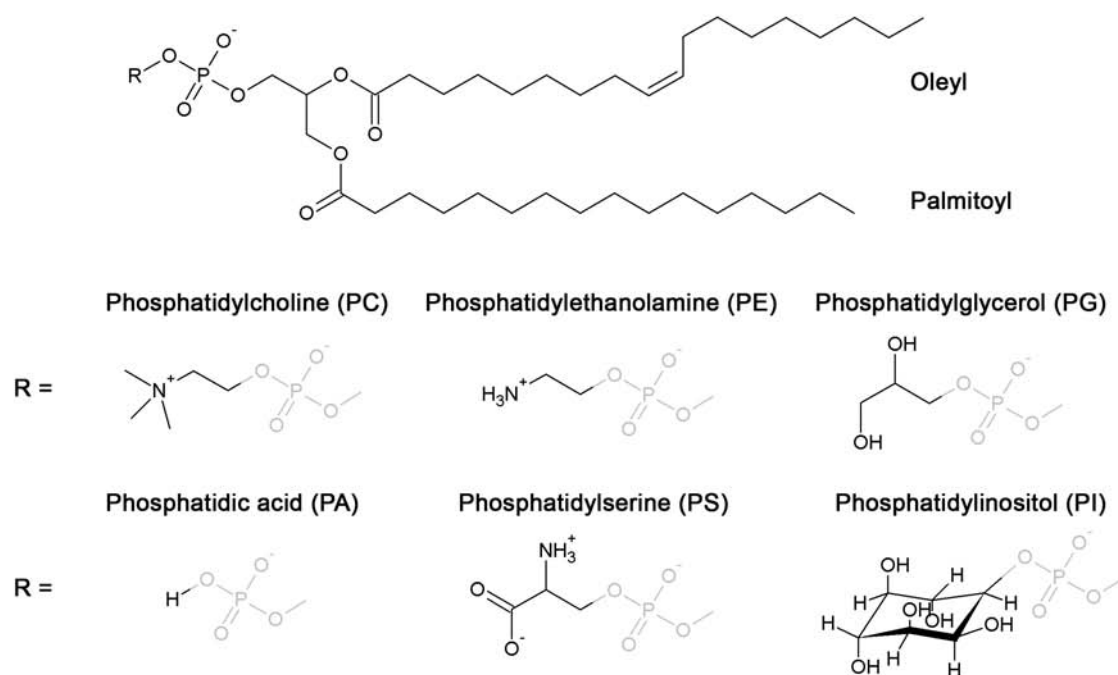
1.3.1 Lipids

Lipids representing the molecular building blocks of biological membranes comprise phospholipids (dia-

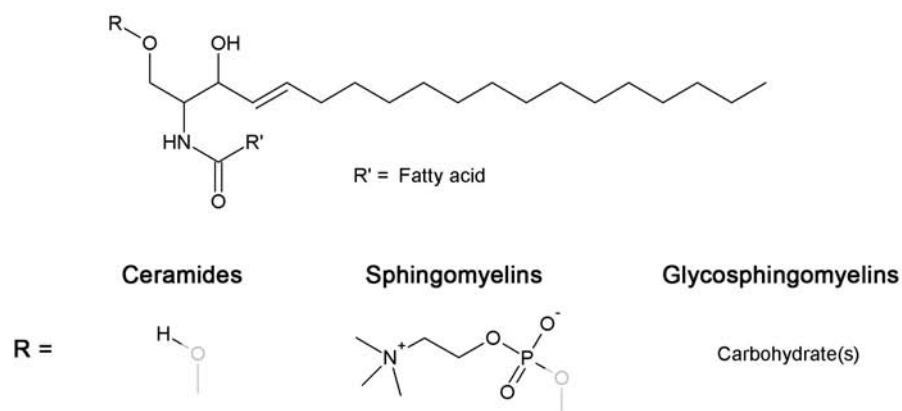
cylglycerides), sphingolipids, glycolipids and cholesterol. Note: No precise definition of the term 'lipid' exists. Therefore, the aforementioned classification is of rudimentary character and for didactic purposes only.

Phospholipids are made from glycerol, two fatty acids and a phosphate group linking to a hydrophilic head group. According to the head group they can further be divided in several subclasses: phosphatidylcholine (PC), phosphatidylethanolamine (PE), phosphatidylglycerol (PG), phosphatidylserine (PS), phosphatidylinositol (PI) and phosphatidic acid (PA). A very special representant of phospholipids is the cardiolipin, which is basically a covalently linked dimer of phosphatidyl glycerol. In order to have a stable bilayer structure phospholipids are indispensable as they spontaneously form bilayers in an aqueous solution. By adopting a vesicular organization all the hydrophobic tails are facing each other elegantly circumventing unfavorable interactions with water molecules which are only faced by the hydrophilic head groups. PC and PE together are most abundant in nature.

Phospholipids (Diacylglycerides)



Sphingolipids



Cholesterol

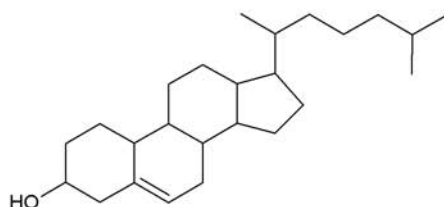


Figure 1.2: **Lipids.** Structures of commonly used lipids in membrane protein research

Sphingolipids carry sphingosine as a common component. They can further be divided into: Ceramides, sphingomyelins, and glycosphingolipids. Ceramides have a fatty acid linked to the amino

group of the sphingosine, sphingomyelins additionally have a phosphoryl choline as a polar head group at the primary alcohol of ceramide and glycosphingolipids have one or more carbohydrates linked to

the primary alcohol of ceramide.

Glycolipids are glycosyl derivatives of lipids such as acylglycerols, ceramides and prenols. They represent a very complex class of lipids as some have carbohydrate chains with more than twenty monosaccharide residues. Normally they are found at the outer surface of cell membranes, e.g. as gly-cocalyx.

Cholesterols are made up of a sterol (steroid carrying a hydroxyl group as hydrophilic moiety) and a short aliphatic chain (opposite to the hydroxyl group). The large body of cholesterol is planar and rigid. At high temperatures cholesterol tends to reduce membrane fluidity, by interacting with the hydrocarbon tails of the lipid molecules. Whereas at low temperatures cholesterol helps to prevent membranes from freezing and thus tends to maintain membrane fluidity. Cholesterol reduces the passive permeability of membranes to solutes as it literally fills in the gaps created by imperfect packing of other lipid species or by proteins are embedded in the membrane.

Some physical properties

The phase transition temperature is defined as the temperature required to induce a change in the lipid physical state from the ordered gel phase, where the hydrocarbon chains are fully extended and closely packed, to the disordered liquid crystalline phase, where the hydrocarbon chains are randomly oriented and fluid (Small, 1986). There are several factors which directly affect the phase transition temperature including hydrocarbon length, unsaturation, charge, and head group species. As the hydrocarbon length is increased, van der Waals interactions become stronger requiring more energy to disrupt the ordered packing, thus the phase transition temperature increases. Likewise, introducing a double bond into the acyl group results in a kink in the chain which requires much lower temperatures to induce an ordered packing arrangement.

Many biological membranes carry a net negative charge on their surface. The charge is generally imparted by the presence of anionic phospholipid species in the membrane. The major naturally occurring anionic phospholipids are phosphatidylserine, phosphatidylinositol, phosphatidic acid, and cardiolipin. Some bacterial systems also contain phosphatidylglycerol. The charge may provide a special function for the membrane. As an example, several steps of the blood coagulation cascade require

HLB number	Property/Function
< 10	Oil soluble
> 10	Water Soluble
4-8	Antifoaming agent
7-11	w/o-Emulsifier
12-16	o/w-Emulsifier
11-14	Wetting agent
12-15	Detergent
16-20	Stabilizer

Table 1.1: **Hydrophile-lipophile balance (HLB) numbers**

a charged lipid membrane. The assembling of protein aggregates on the surface of platelets requires a negatively charged surface. The conversion of prothrombin to thrombin requires not only a negative surface, the requirement is somewhat specific, limited to PS and PA (Jones et al., 1985). Coagulation proteins bind as tightly to negatively charged surfaces containing PG and PI as they do to PS or PA membranes, however, the activity is only a fraction of that obtained with PS or PA membranes. Therefore, in some systems, not only the charge requirement must be satisfied, the system specificity for a particular species must be satisfied too.

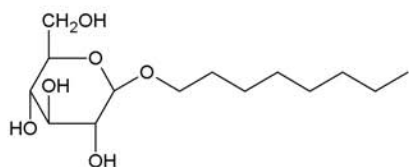
1.3.2 Detergents

Detergents represent another class of amphiphiles. Just like lipids, they can have many different head groups. But since they typically carry only one chain as hydrophobic moiety, their shape is best described by a cone (the broader end of which is located at the head group) and therefore they are very curvophilic (Figure 1.1). Their behavior in an aqueous solution is very characteristic: They exhibit a certain solubility in water as monomers. However, when a critical concentration is exceeded they form aggregates in the form of micelles. This point is usually referred to as critical micellar concentration (cmc). The cmc varies a lot with the size and nature of the head group, the length of the hydrophobic tail and environmental conditions such as the temperature and the ionic strength of the solution.

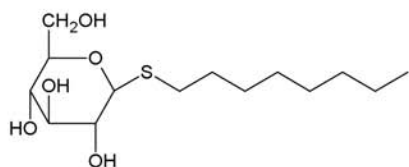
The hydrophilic-lipophilic balance (HLB) number is an empirical expression for the relationship of the hydrophilic and hydrophobic groups of a surfactant. The HLB number provides a semi-quantitative description of the efficacy of surfactants with respect to emulsification of water and oil systems. This scale (ranging from 0-20) was introduced in 1949 by Griffin (Griffin, 1949; 1954) to characterize non-

Nonionic Detergents

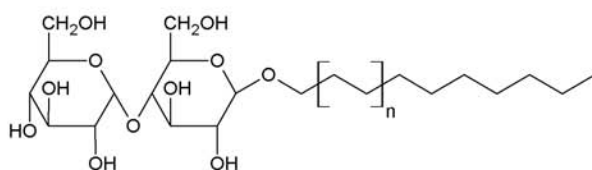
Glycosides



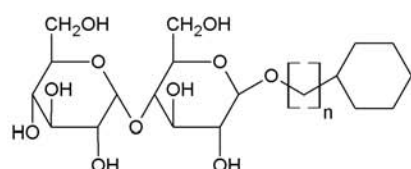
Octyl- β ,D-glucopyranoside
(OG)



Octyl- β ,D-thioglucopyranoside
(OTG)

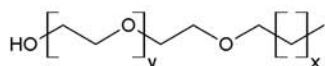


n = 1 Decyl- β ,D-maltopyranoside
(DM)
n = 2 Dodecyl- β ,D-maltopyranoside
(DDM)

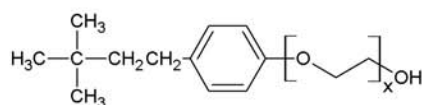


n = 5 CYMAL-5
n = 6 CYMAL-6

Polyoxyethylene detergents

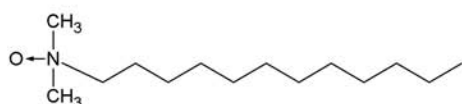


x = 10, y = 22	BRIJ-35
x = 15, y = 19	BRIJ-58
x = 6, y = 0-10	Octyl polyoxyethylene (8-POE)
x = 6, y = 4	Pentaethylene glycol monoethyl ether (C8E5)
x = 6, y = 5	Hexaethylene glycol monoethyl ether (C8E6)
x = 10, y = 7	Octaethylene glycol monododecyl ether (C12E8)
x = 10, y = 8	Nonaethylene glycol monododecyl ether (C12E9)



x = 10 TRITON X-100
x = 8 TRITON X-114

Special case



Lauryl-N,N-dimethylamine oxide
(LDAO)
pH \geq 7 nonionic species
pH \leq 3 cationic species

Figure 1.3: **Nonionic detergents.** Structures of commonly used nonionic detergents in membrane protein research.

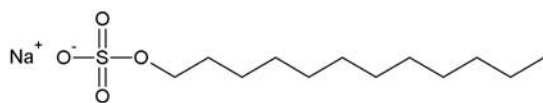
ionic surfactants using oxyethylene oligomers as hydrophilic group. The HLB number for nonionic surfactants can be calculated through the following equation

$$HLB = 20\left(1 - \frac{M_L}{M_T}\right) \quad (1.1)$$

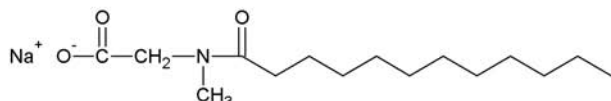
where M_L is the formula weight of the hydropho-

Ionic Detergents

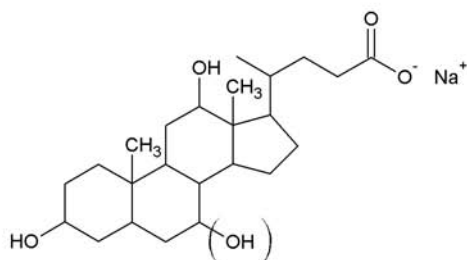
Anionic detergents



Sodium dodecyl sulfate
(SDS)



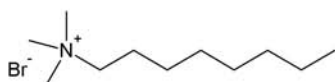
Sodium lauryl sarcosine
(SLS)



Sodium cholate

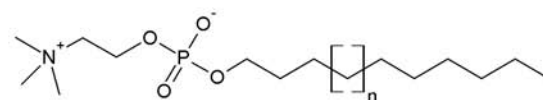
() = Sodium deoxycholate

Cationic detergents

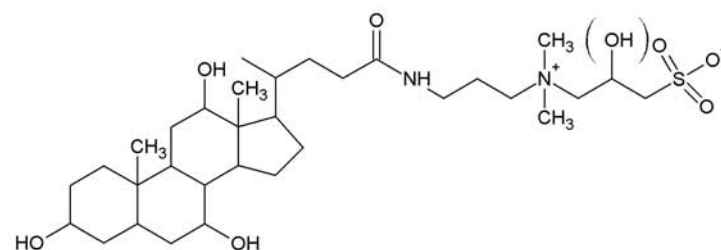


Octyltrimethylammonium bromide
(OTAB)

Zwitterionic detergents

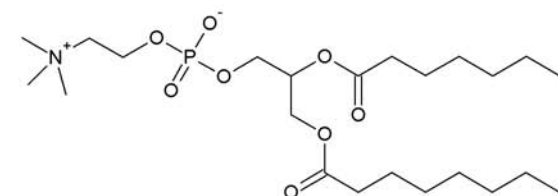


n = 1 N-decylphosphocholine
(FOS-CHOLINE-10)
n = 3 N-dodecylphosphocholine
(FOS-CHOLINE-12)



3-[(3-Cholamidopropyl)
dimethylammonio]-2-
hydroxypropanesulfonic acid
(CHAPSO)

() = 3-[(3-Cholamidopropyl)
dimethylammonio]
propanesulfonic acid
(CHAPS)



Diheptanoyl phosphatidylcholine
(DHPC)

Figure 1.4: **Ionic detergents.** Structures of commonly used ionic detergents in membrane protein research.

bic portion of the molecule and M_T is the total formula weight of the surfactant molecule. Table 1.1 lists HLB values along with the typical use of the corresponding compounds. Egan *et al.* (Egan *et al.*, 1976) demonstrated that there is a correlation between the HLB values of Triton surfactants

and their ability to disrupt mitochondrial membranes. Maximum protein and phospholipid extraction occurred at HLB values between 12.5 and 13.5.

1.4 Membrane Proteins

About a third of all encoded proteins are membrane embedded or at least membrane bound proteins (Wallin and von Heijne, 1998) (see Figure 1.5). They represent the most important fraction of pharmaceutically relevant targets (up to 70%) as many diseases are directly linked to a dysfunction of a certain receptor or transporter. To date (as of 18-Oct-2005) 33'152 protein structures are available from the protein databank (PDB). However, only a tiny fraction of which are membrane protein structures (see Figure 1.6). The striking discrepancy between the availability of membrane protein structures and the need for them is due to the peculiarities of this class of proteins.

Natural abundance/over-expression

First of all they are not as abundant in a cell as soluble proteins. The first membrane protein structures were recovered from proteins which have a high natural abundance. An other major set of structures available is from bacterial proteins, as until recently over-expression of proteins was greatly performed in bacterial host cells. However, today's challenges in over-production comprise mammalian and human proteins, which are much more intricate to produce. Large-scale cultivation of mammalian cells is not as straight-forward as for bacterial cells. Post-transcriptional and post-translational modifications are very common to mammalian proteins and make it very delicate to over-express them: A host cell might simply not be able to correctly process the nascent polypeptide chain as required for the protein to mature. As a consequence, the protein is left in the wrong cellular compartment or in an unfinished state, ultimately leading to its degradation. Therefore, protein production for structural biology not only has to cope with the demand for milligram quantities but more importantly with the need for stable protein in its native state.

Stability of membrane proteins

There are major differences in the biophysical properties of membrane proteins compared to those of soluble cytoplasmic proteins. The most prominent one is the hydrophobic character of a large part of the membrane protein structure.

Membrane proteins come in two major classes: α -helical and β -barrel proteins. Within the α -helical class the proteins with up to six and

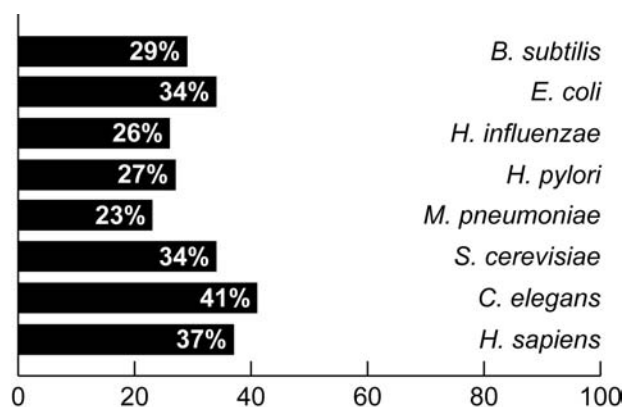


Figure 1.5: **Membrane protein ORF's in different genomes.** (Wallin and von Heijne, 1998)

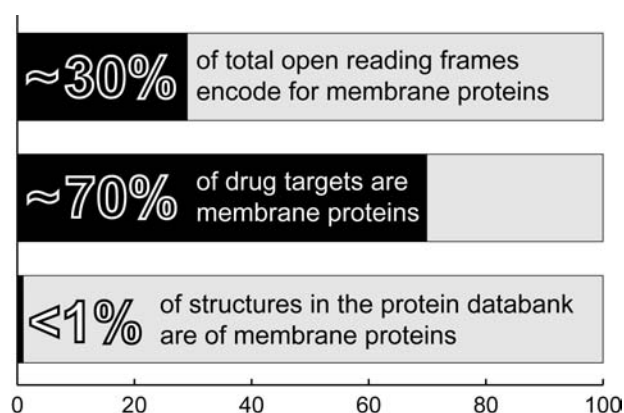


Figure 1.6: **Structures in the protein data bank (PDB).** Figures as of 18-Oct-2005.

twelve transmembrane segments are predominantly present (Daley et al., 2005) indicating an evolutionary appearance through gene duplication (see Figure 1.7). In eucaryotic organisms (e.g. *homo sapiens*) seven transmembrane segments are prominent too (G-protein coupled receptors) (Wallin and von Heijne, 1998). β -Barrel proteins are usually found in the outer membrane and stand out through a good stability in the detergent solubilized state. It is therefore not surprising that a lot of their structures have been solved and were among the first to be available.

1.4.1 Biological membranes

Biological membranes are commonly described as two-dimensional (2D) apolar solvents providing an environment for amphiphilic molecules and peptides. Membrane proteins have been designed to reside within the membrane by thermodynamically anchoring the water-insoluble hydrophobic parts of the polypeptide chain within the so-called hy-

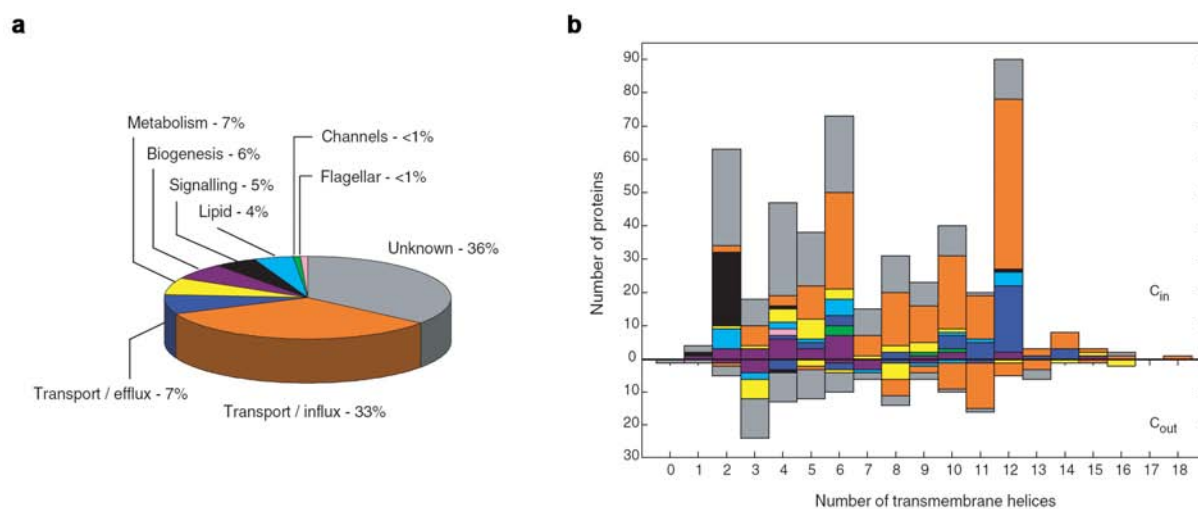


Figure 1.7: **Functional categorization of the E. coli inner membrane proteome.** (Daley et al., 2005) (a) The fractions of the inner membrane proteome (737 proteins) assigned to different functional categories. (b) The number of proteins with assigned C-terminal location (C_{in} (cytoplasmic), C_{out} (periplasmic)) in each functional category for different topologies (601 proteins in total). C_{in} topologies are plotted upward, C_{out} downward. For C_{in} proteins, even numbers of transmembrane helices are three times as common as odd numbers; for C_{out} proteins, odd and even numbers of transmembrane helices are roughly equal.

drophobic core of the membrane bilayer. Nevertheless they are able to freely diffuse in-plane within this 2D array.

Membrane solubilization

In order to get a membrane protein into solution one has to protect the hydrophobic portion, as they would immediately aggregate upon transfer into an aqueous medium. This is achieved by using detergents which accommodate the protein in a micelle-like structure (Garavito and Ferguson-Miller, 2001) (protein-detergent complex, see Figure 1.8). Once solubilized the protein can be purified and used for further experiments. However, in many cases detergents have only a limited capacity to mimic the protective surrounding of a lipid bilayer keeping the protein in its native state (Bowie, 2001). This is further discussed in Chapter 2.

Lipid rafts

Cells have found ways of confining particular membrane proteins to localized areas within the bilayer, thereby creating functionally specialized regions, or membrane domains, on the cell surface. How the proteinaceous constituents of the bilayer are organized into higher ordered domains within so-called lipid rafts still is subject of controversial discussions. A special difficulty associated to these investigations is the possibility of artificially creating membrane domains by the experimental

procedure applied: For a long time a key property in the identification of lipid rafts has been the resistance of certain membrane components to detergent treatment. These (artificial) domains have been termed detergent resistant membranes (DRM's). In practice, however, this has led to a great confusion as the term DRM is often taken as a synonym for lipid rafts (Lichtenberg et al., 2005).

1.5 Two-Dimensional Crystallization

In two-dimensional (2D) crystallization purified membrane proteins are reconstituted into a lipid bilayer (for a comprehensive review on membrane protein reconstitution see (Rigaud et al., 1995)). This is achieved by mixing the purified protein with solubilized lipids and subsequently removing the detergent, hopefully yielding crystalline arrays (for a comprehensive review on 2D crystallization of membrane proteins see (Mosser, 2001)). There are numerous factors influencing the outcome of a 2D crystallization experiment.

The lipid-to-protein ratio (LPR)

Depending on the LPR proteins are more or less tightly packed after reconstitution. At high LPR the proteins are loosely distributed within a vesicle. If the LPR is too low, there are not enough

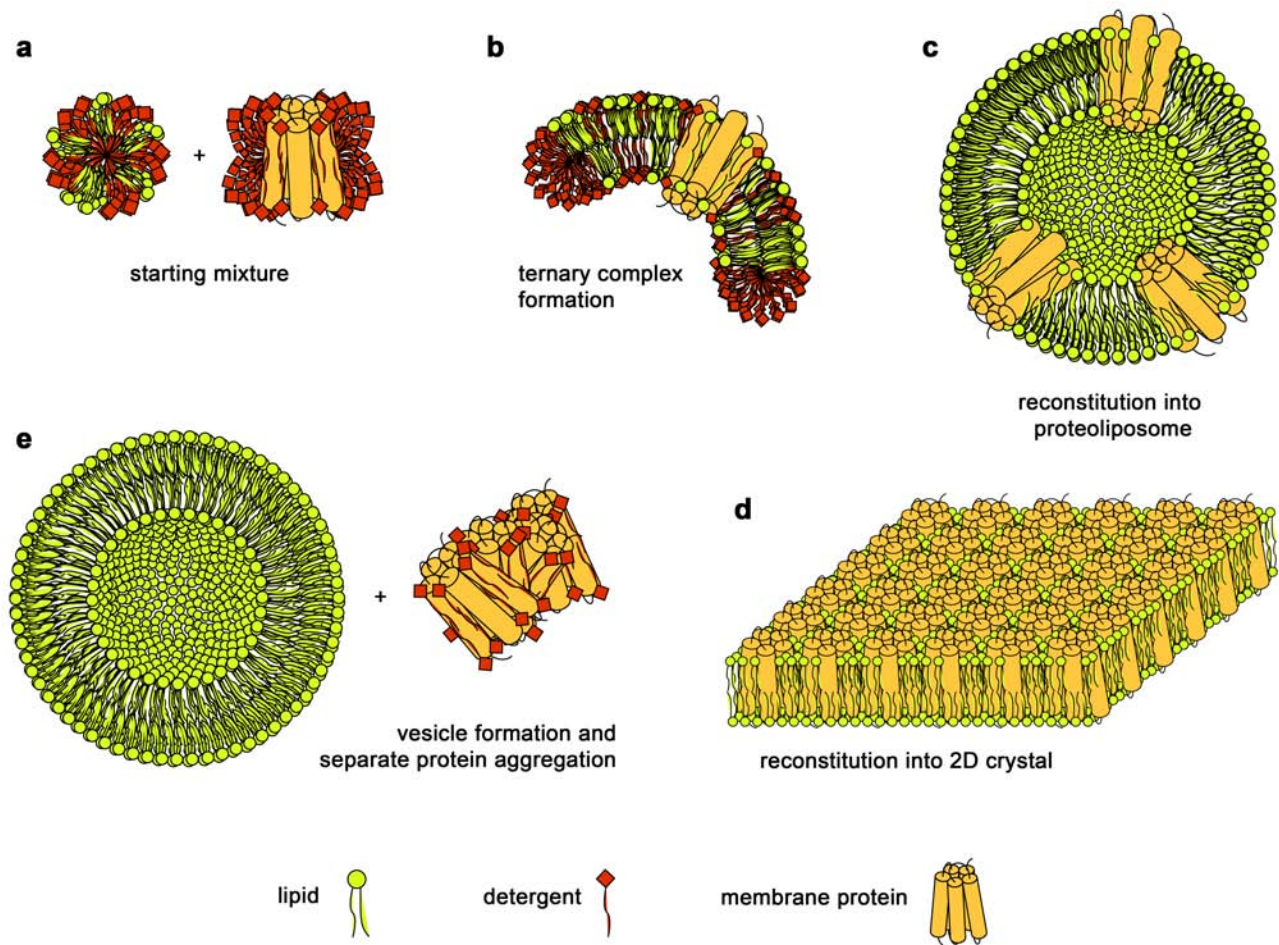


Figure 1.9: **Two-dimensional crystallization and reconstitution into proteoliposomes of membrane proteins.** (a) Components of the starting mixture for detergent mediated reconstitution. (b) Ideally, ternary micelles are formed upon equilibration in the starting mixture. After subsequent detergent removal different structures in the assay mixture are formed: (c) At a higher lipid-to-protein ratio (LPR) the membrane protein is reconstituted into proteoliposomes. (d) At a sufficiently low LPR 2D crystals can assemble. (e) In unfavorable circumstances the ternary micelles don't form or vesicle formation and protein aggregation occur temporally separated at different concentrations of the free detergent.

lipid molecules to incorporate all membrane proteins, thereby leading to protein aggregation. Just in between lies the LPR leading to crystalline packing within a bilayer.

Type of lipid

As already mentioned in section 1.3.1 specific lipids might be required for membrane protein function (White et al., 2001; Bowie, 2001). The morphology of 2D crystals can vary from sheets over tubes to vesicles, depending on the molecular shape of the lipid molecule used for reconstitution (see Figure 1.1).

Type of detergent

Not every detergent is able to stabilize the na-

tive structure of a membrane protein (Bowie, 2001). Additionally, detergents affect the kinetics of the reconstitution process because of their different cmc's and association constants with different lipids and proteins.

The amount of detergent

An excess of detergent can cause loss of quaternary and tertiary structure, and protein aggregation. Moreover, an excess slows down the kinetics of detergent removal.

The temperature

The temperature affects the lipid phase and the protein stability. Additionally it acts on the kinetics of the experiment. At higher temperature the

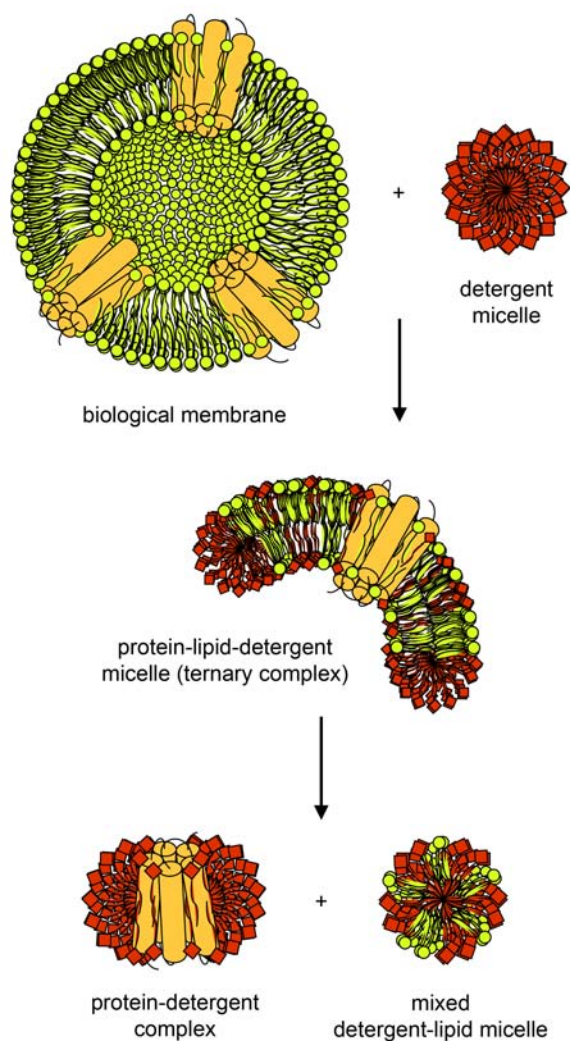


Figure 1.8: **Membrane solubilization.** The use of detergents for membrane (protein) solubilization.

diffusion controlled removal of detergents is faster than at lower temperatures.

The pH

The pH of a solution affects the protein by dictating the net charge of the polypeptide chain. When the pH corresponds to the so-called isoelectric point (pI) of a protein, it carries a net charge of approximately zero. At either sides of the pI the protein is charged (positively: $\text{pH} < \text{pI}$, or negatively: $\text{pH} > \text{pI}$). The same is true for lipids and detergents as they can be neutral or charged depending on the pH (see e.g. LDAO in Figure 1.3).

The ionic strength

The nature and amount of ions present in the assay solution steer the interactions of proteins with each other. The possibility of counterions to interact with charged residues on proteins as well

as lipids (head group) governs the electrostatics of intermolecular association. Divalent cations are mainly acting on the intrastuctural level of a protein providing stability to charged regions. Furthermore, ions affect the water structure, thereby implicating thermodynamical aspects. Thus, the effects of increasing the salt concentration in a protein solution are:

1. Changes to the hydration of the protein, because the ions themselves need water for solvation.
2. Decrease of repulsive electrostatic protein/protein interactions, allowing the molecules to come closer together.
3. Direct interaction of ions with residues at the surface of the protein to form a protein salt.

In 1888, Hofmeister observed that the ability of salts to precipitate hen egg white proteins follows a series. With the major protein (ovalbumin) being negatively charged the series is:

Sulphate²⁻ > phosphate²⁻ > acetate¹⁻ > citrate³⁻ > tartrate²⁻ > bicarbonate¹⁻ > chromate²⁻ > chloride¹⁻ > nitrate¹⁻ > chlorate¹⁻.

With solubility measurements of positively charged proteins the order of the anion series is reversed:

Thiocyanate¹⁻ ~ para-toluene sulphonate¹⁻ > nitrate¹⁻ > chloride¹⁻ > acetate¹⁻ > phosphate¹⁻ > citrate²⁻

Sulphate ions are said to be kosmotropic (lyotropic) and thiocyanate chaotropic. Such series have been used in classic "salting in", "salting out" purifications and are now applied in the growth of crystals to modify macromolecular interactions. For reviews on the effects of the so-called Hofmeister series see Cacace et al. (1997); Riès-Kautt and Ducruix (1999); Collins (2004).

The art of 2D crystallization

The discipline of 2D crystallization consists of directing the detergent solubilized membrane protein on a narrow path of ideally adjusted parameters through the entanglement of kinetic, thermodynamical and electrostatic effects. Unfortunately, only little is understood on how these different parameters have to be weighted and on how they interact/interfere. Therefore, a wide multidimensional space has to be illuminated experimentally in order to find appropriate crystallization conditions. This

is why structural biology of membrane proteins belongs to the most challenging and tedious efforts in molecular biology.

References

- J. U. Bowie. Stabilizing membrane proteins. *Curr. Opin. Struct. Biol.*, 11:397–402, 2001.
- M. G. Cacace, E. M. Landau, and J. J. Ramsden. The Hofmeister series : Salt and solvent effects on interfacial phenomena. *Quart. Rev. Biophys.*, 30:241–277, 1997.
- K. D. Collins. Ions from the Hofmeister series and osmolytes: Effects on proteins in solution and in the crystallization process. *Methods*, 34:300–311, 2004.
- D. O. Daley, M. Rapp, E. Granseth, K. Melen, D. Drew, and G. von Heijne. Global topology analysis of the *Escherichia coli* inner membrane proteome. *Science*, 308:1321–1323, 2005.
- R. W. Egan, M. A. Jones, and A. L. Lehninger. Hydrophile-lipophile balance and critical micelle concentration as key factors influencing surfactant disruption of mitochondrial membranes. *J. Biol. Chem.*, 251:4442–4447, 1976.
- R. M. Garavito and S. Ferguson-Miller. Detergents as tools in membrane biochemistry. *J. Biol. Chem.*, 276:32403–32406, 2001.
- W. C. Griffin. Classification of surface-active agent by HLB. *J. Soc. Cosmetic Chem.*, 1:311, 1949.
- W. C. Griffin. Calculation of HLB values of non-ionic surfactants. *J. Soc. Cosmetic Chem.*, 5:259, 1954.
- M. E. Jones, B. R. Lentz, F. A. Dombrose, and H. Sandberg. Comparison of the abilities of synthetic and platelet-derived membranes to enhance thrombin formation. *Thromb. Res.*, 39:711, 1985.
- D. Lichtenberg, Felix M. Goni, and H. Heerklotz. Detergent-resistant membranes should not be identified with membrane rafts. *Trends Biochem. Sci.*, 30:430–436, 2005.
- G. Mosser. Two-dimensional crystallogenesis of transmembrane proteins. *Micron*, 32:517–540, 2001.
- J.-L. Rigaud, B. Pitard, and D. Levy. Reconstitution of membrane proteins into liposomes: application to energy-transducing membrane proteins. *Biochim. Biophys. Acta*, 1231:223–246, 1995.
- M. Riès-Kautt and A. Ducruix. *From solution to crystals with physico-chemical aspects. in: Crystallization of Nucleic acids and proteins: A practical approach.* IRL/Oxford Press, 1999.
- D. M. Small. *Handbook of Lipid Research: The Physical Chemistry of Lipids, From Alkanes to Phospholipids*, volume 4. Plenum Press, New York, 1986.
- C. Tanford. *The Hydrophobic Effect.* John Wiley & Sons, Inc., New York, 1980.
- E. Wallin and G. von Heijne. Genome-wide analysis of integral membrane proteins from eubacterial, archaean, and eukaryotic organisms. *Protein Science*, 7:1029–1038, 1998.
- S. H. White, A. S. Ladokhin, S. Jayasinghe, and K. Hristova. How membranes shape protein structure. *J. Biol. Chem.*, 276:32395–32398, 2001.

In the following the publication "Electron and atomic force microscopy of the trimeric ammonium transporter AmtB" is appended as published in EMBO Reports 2004, volume 5, pages 1153–1158. Contribution to this work was the atomic force microscopic measurement.

Chapter 2

Electron and atomic force microscopy of the trimeric ammonium transporter AmtB

Matthew J. Conroy¹, Stuart J. Jamieson^{1,4}, Daniel Blakey², **Thomas Kaufmann**³, Andreas Engel³, Dimitrios Fotiadis³, Mike Merrick^{2,5} & Per A. Bullough^{1,6}

2.1 Abstract

Escherichia coli AmtB is an archetypal member of the ammonium transporter (Amt) family, a family of proteins that are conserved in all domains of life. Reconstitution of AmtB in the presence of lipids produced large, ordered two-dimensional crystals. From these, a 12 Å resolution projection map was determined by cryoelectron microscopy, and high-resolution topographs were acquired using atomic force microscopy. Both techniques showed the trimeric structure of AmtB in which each monomer seems to have a pseudo-two-fold symmetry. This arrangement is likely to represent the in vivo structure. This work provides the first views of the structure of any member of the Amt family.

2.2 Introduction

The transport of ammonium across the cell membrane is important in nearly all organisms, although the mechanism is not fully understood. It is known, however, that high-affinity ammonium transporters

(Amt) constitute a distinct protein family found in all domains of life (von Wirén & Merrick, 2004). Many organisms encode several Amt paralogues that show different affinities for ammonium (or methylammonium), and in higher eukaryotes, these paralogues are expressed in a tissue-specific fashion (von Wirén *et al*, 2000).

In animals, the Amt proteins are represented by the Rhesus (Rh) proteins (Marini *et al*, 2000). In humans, some Rh paralogues are expressed in the erythrocyte membrane (Eyers *et al*, 1994) and others are expressed in the kidney, liver and skin, the main organs of ammonia genesis (Quentin *et al*, 2003). Evidence is accumulating that the Rh proteins facilitate the transport of ammonium (Westhoff *et al*, 2002).

Escherichia coli contains a single Amt gene (amtB), which encodes a 428-amino-acid polypeptide (AmtB) with a deduced molecular mass of 44.5 kDa. The protein was predicted to have 12 trans-

¹Department of Molecular Biology and Biotechnology, Krebs Institute for Biomolecular Research, University of Sheffield, Firth Court, Western Bank, Sheffield S10 2TN, UK

²Department of Molecular Microbiology, John Innes Centre, Colney Lane, Norwich NR4 7UH, UK

³ME Müller Institute for Structural Biology, Biozentrum, University of Basel, Klingelbergstrasse 50/70, 4056 Basel, Switzerland

⁴Present address: Avecia Biotechnology, Belasis Avenue, Billingham, Cleveland TS23 1YN, UK

⁵Present address: Department of Human Anatomy and Genetics, University of Oxford, South Parks Road, Oxford OX1 3QX, UK

⁶Corresponding author. Tel: +44 114 2224245; Fax: +44 114 2222800; E-mail: p.bullough@shef.ac.uk

membrane alpha-helices (TMH) with both termini located in the cytoplasm (Thomas *et al*, 2000). However, recent work indicates that the first predicted TMH is actually a signal sequence, which is cleaved to leave a mature, 11 TMH protein of 406 residues with a periplasmic N-terminus (von Wirén & Merrick, 2004). This 11 TMH structure is characteristic of Amt proteins from bacteria, fungi and plants but not of Rh proteins, which have 12 TMH (Eyers *et al*, 1994).

E. coli AmtB purifies in detergent solution as a homotrimeric complex with a molecular mass of 135 kDa (Blakey *et al*, 2002). So far, *E. coli* AmtB is the only Amt protein to have been purified, but genetic and biochemical evidence indicates that Amt proteins from fungi and higher plants also form oligomeric complexes (Marini & Andre, 2000; Monahan *et al*, 2002; Ludewig *et al*, 2003). The erythroid Rh proteins have been proposed to form hetero-oligomers (Eyers *et al*, 1994).

Despite their important role in cellular metabolism, there have been no structural studies on Amt proteins. In this paper, we report the first structural view of a member of this protein family. We describe the reconstitution of *E. coli* AmtB into two-dimensional (2D) crystals and their imaging by cryoelectron microscopy (cryoEM) and atomic force microscopy (AFM), both of which show the likely *in vivo* structure when viewed perpendicular to the membrane.

2.3 Materials and Methods

2.3.1 Crystallization

C-terminally histidine-tagged AmtB was expressed in *E. coli* and purified as described by Blakey *et al* (2002) with the exception that the construct did not contain a linker between the native sequence and the tag. AmtB was concentrated to 0.5 mg/ml using Amicon Centricon concentrators (molecular weight cut-off 100'000). Purified protein was mixed with DMPC (Avanti Polar Lipids, Alabaster, AL, USA) solubilized in 2% decyl- β -D-maltoside to yield LPRs of between 0.4 and 1.4 (w/w) at a final protein concentration of 0.4 mg/ml and total volume of 100 μ l. The solution was dialysed against 50 mM Tris buffer at pH 8.0, 250 mM NaCl and 0.005% sodium azide in a home-built dialysis machine (Jap *et al*, 1992) at 20°C for 10 days.

2.3.2 Electron microscopy

Crystals were embedded in 1% (w/v) glucose. Micrographs were recorded on a Philips CM200 FEG EM. Grids were mounted on an Oxford cold stage and cooled to around -180°C. Images were recorded at 200 kV at a magnification of about \times 50,000 and a total dose of \sim 10 e \AA^{-2} on Kodak SO-163 film, developed in concentrated D19 developer for 12 min.

2.3.3 Image processing

Micrographs were digitized in steps of 7 μ m on a Zeiss SCAI densitometer. Image processing followed procedures described previously (Henderson *et al*, 1986; Crowther *et al*, 1996). Origin and phase CTF refinement were performed with Fourier terms limited to 12 \AA resolution and symmetry analysis was carried out using ALLSPACE (Valpuesta *et al*, 1994). Amplitudes from individual images were corrected by temperature factors of between 110 and 967 \AA^2 with SCALIMAMP3D (Schertler *et al*, 1993) before averaging. Rotational correlation coefficients were calculated using IMAGIC (van Heel *et al*, 1996).

2.3.4 Atomic force microscopy

A stock solution of crystals was diluted tenfold in 20 mM Tris-HCl, 150 mM KCl and 15 mM MgCl₂ at pH 8.1 (imaging buffer) and adsorbed for > 60 min on freshly cleaved muscovite mica. After adsorption, the sample was gently washed with imaging buffer. AFM experiments were performed using a Nanoscope Multimode microscope equipped with an infrared laser head, fluid cell and oxide-sharpened silicon nitride cantilevers of 100 and 200 μ m length, and nominal spring constants of 0.08 and 0.06 N m⁻¹ from Olympus Optical Co. (Tokyo, Japan) and Digital Instruments (Santa Barbara, CA, USA), respectively. Topographs were acquired in contact mode at minimal loading forces (\leq 100 pN). Trace and retrace signals were recorded simultaneously at line frequencies ranging between 4.1 and 5.5 Hz. Correlation averages were calculated from AFM topographs with the SEMPER image processing system (Saxton, 1996). Perspective views were prepared using the SXM program (University of Liverpool, UK).

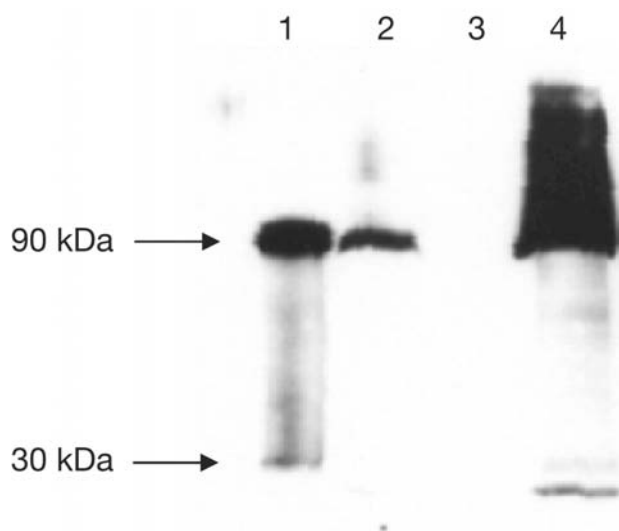


Figure 2.1: **Western blot of protein extracts from wild-type *E. coli* strain ET8000 grown under nitrogen limitation to induce expression of AmtB from its native promoter.** Lane 1 is from a His-tagged construct, while all other lanes are wild type. Lane 1: purified AmtB; lane 2: whole-cell extract; lane 3: cytoplasmic fraction; lane 4: membrane fraction. Samples were separated on a 10% SDS-polyacrylamide gel and visualized with a rabbit polyclonal anti-AmtB antibody.

2.3.5 Western blotting and cell fractionation

These were carried out as described by Coutts *et al.* (2002).

2.4 Results

2.4.1 AmtB is trimeric in the native cell membrane

Polyclonal antibodies prepared against purified AmtB were used in a western blot of cellular fractions from wild-type *E. coli* grown under nitrogen limitation. This blot identified a principal band with an apparent molecular mass of ~ 90 kDa and a mobility identical to that of purified trimeric AmtB. A minor fraction ($< 5\%$) was observed as a monomeric species of about 30 kDa. AmtB is completely localized in the membrane fraction (Figure 2.1). These data confirm that *E. coli* AmtB is almost exclusively trimeric when expressed at normal levels from the native *amtB* promoter, and that it is extremely stable in the presence of SDS.

2.4.2 Crystallization and AFM

The best-ordered 2D crystals were formed from a mixture of AmtB and 1,2-dimyristoyl-sn-glycero-3-phosphatidylcholine (DMPC) at a lipid-to-protein ratio (LPR) of 1.0 (w/w). Crystals formed as ($> 3 \mu\text{m}$ on an edge) angular edged sheets. AFM of AmtB crystals showed that the majority are $127 \pm 3 \text{ \AA}$ thick (labelled '3' in Figure 2.2), sufficient to accommodate two bilayers stacked together, although $63 \pm 2 \text{ \AA}$ 'single' thicknesses (labelled '2' in Figure 2.2) could sometimes be seen at the margins of these sheets. Adjacent particles were of the same height, suggesting that all molecules in the crystal have the same orientation relative to the membrane plane. While the 127-\AA -thick layers showed much greater crystalline order than the 63 \AA layers, it is apparent from Figure 2.2 B that particles in both types of layer show the same surface characteristics, implying that both 'single' and 'double' layers show the same surface of the protein to the AFM tip. Thus, double-layered crystals are most likely to be composed of two membranes stacked 'head-to-tail'. At a higher magnification, AFM topographs (Figure 2.3) showed ordered arrays of particles each of which showed three prominent protrusions (arrows) 15 \AA from the three-fold symmetry center and a further three more peripheral protrusions (arrowheads) 34 \AA from the center. Correlation averages of 213 trimers (Figure 2.3 C,D) show these features clearly.

2.4.3 Cryoelectron microscopy

CryoEM showed crystals with unit cell dimensions $a=b=157.5 \pm 1.5 \text{ \AA}$ and $\gamma=119 \pm 0.7^\circ$. The Fourier components of one image are represented in supplementary Figure 2.6 online. Analysis of predicted symmetry-related phases to 12 \AA resolution showed the data to be consistent with p3 and p321 symmetry (see supplementary data online). Amplitudes and phases from the six best images were averaged with p3 or p321 symmetry imposed, giving phase residuals to 12 \AA resolution of 59.4° and 59.2° , respectively (see supplementary data online for a more detailed analysis). Projection maps are shown in Figure 2.4. Both maps show similar features; one unit cell (outlined in Figure 2.4 A) contains four triangular particles, approximately 53 \AA on a side. One particle, 'b', lies on a strict three-fold crystallographic symmetry axis. The three remaining (crystallographically equivalent) particles, 'a', do not lie on a crystallographic symmetry axis

in the p3 map, but are each bisected by an in-plane crystallographic two-fold axis in the p321 map. In this instance, three such two-fold axes also bisect particle 'b'.

In both maps, those particles ('a') that do not lie on a crystallographic three-fold axis nevertheless seem to show three-fold symmetry, confirmed by determining rotational correlation coefficients for these particles. An unambiguous three-fold symmetry is shown for particles from both maps (Figure 2.5 A). The similarity of the two crystallographically independent particles is even more apparent when three-fold averaging is applied to particle 'a' from either map (Figure 2.4 C,D), and was confirmed by a rotational alignment of particle 'a' on 'b', giving maximum correlations of 98.7% and 98.4% for p3 and p321 maps, respectively.

The density features common to both particles are indicated in Figure 2.5 B. Each particle contains a central region of low density, marked 'w', surrounded by a ring of three density peaks (marked 'x'). Six regions of lower density, marked 'y' and 'z', in turn encircle this central arrangement.

2.5 Discussion

Here we present the first structural view of a member of the Amt family. CryoEM and AFM of 2D

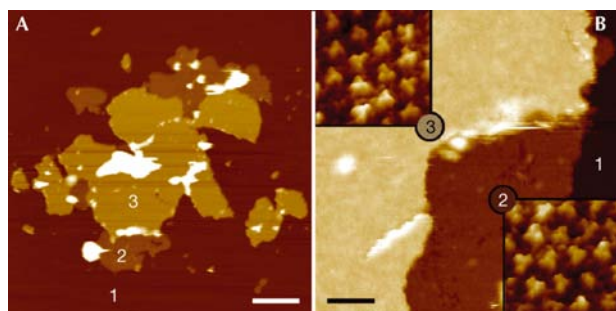


Figure 2.2: **Morphology of crystals.** (A) Overview AFM topograph of single- and double-layered AmtB sheets adsorbed on mica. Regions denoted with numbers 1, 2 and 3 correspond to mica, single-layered sheets and double-layered sheets, respectively. (B) AFM image of a crystal recorded at the border between single- and double-layered sheets. The insets show scans of regions 2 and 3 at higher magnification. The topographs in the insets of (B) are shown in relief, tilted by 2° . Scale bars represent $2\ \mu\text{m}$ (A) and $120\ \text{nm}$ (B). Vertical brightness ranges: $25\ \text{nm}$ (A) and $20\ \text{nm}$ (B). Frame sizes are $32\ \text{nm}$ for the insets in (B).

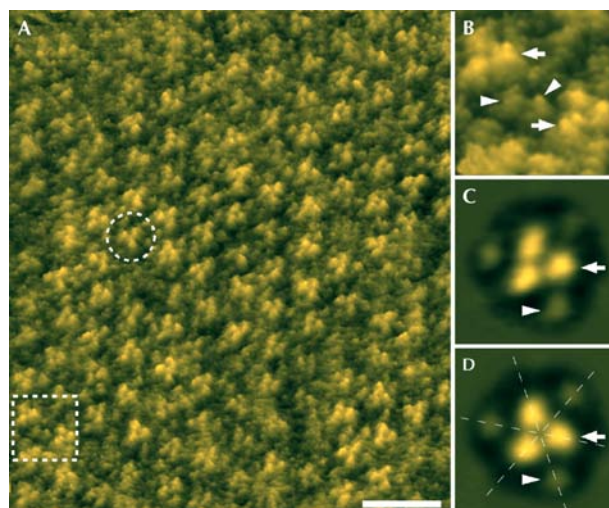


Figure 2.3: **High-resolution AFM of AmtB.** (A) Height image of the upper layer of a double-layered 2D crystal. An AmtB trimer is marked by the broken circle. The area indicated by the broken frame is magnified in (B). (C) Correlation average of 213 AmtB trimers and (D) with three-fold symmetrization. The arrows mark the prominent protrusions near the three-fold axis of the AmtB trimer and the arrowheads indicate the smaller, peripheral protrusions; the dashed lines indicate apparent pseudo-two-fold symmetry axes. The topographs in (A,B) are shown in relief, tilted by 15° . Scale bar in (A): $15\ \text{nm}$. Frame size in (B): $12.3\ \text{nm}$. Vertical brightness ranges: $1.3\ \text{nm}$ (A,B) and $1.2\ \text{nm}$ (C,D). Frame sizes in (C,D): $11.2\ \text{nm}$.

crystals showed particles with three-fold symmetry when viewed perpendicular to the membrane plane. The two crystallographically independent views indicate that the most likely molecular envelope is as shown in Figure 2.4 A. AmtB thus seems to form a trimeric structure, consistent with the trimeric nature of the purified protein observed by analytical ultracentrifugation (Blakey *et al*, 2002). Each particle of projected density occupies an area of approximately $4900\ \text{\AA}^2$, which is entirely consistent with a single trimer of AmtB containing 33 TMH (Thomas *et al*, 2000; von Wirén & Merrick, 2004), assuming an average projected area of approximately $140\ \text{\AA}^2$ per TMH (Veenhoff *et al*, 2002).

Determination of the oligomeric state of membrane proteins is a topic of growing interest, particularly as the structure of the protein in detergent may not always reflect the physiologically relevant state (Veenhoff *et al*, 2002). However, in this case, the unusually stable state of AmtB in SDS allowed

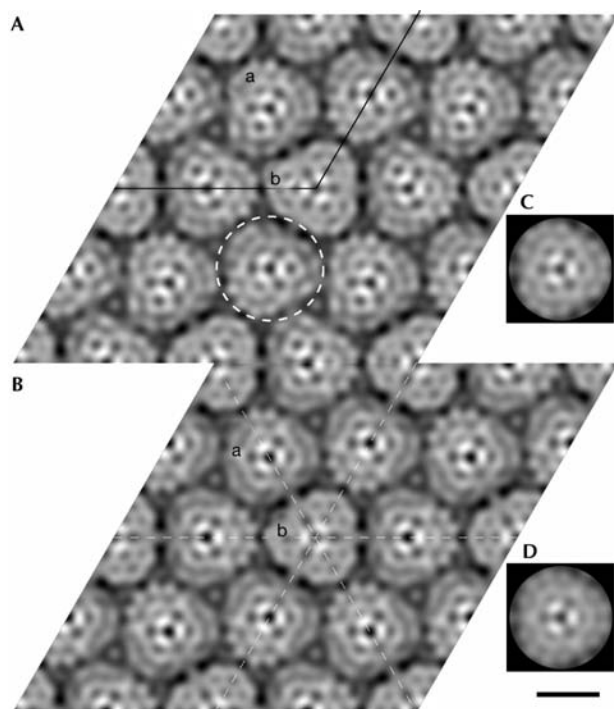


Figure 2.4: **CryoEM projection maps of AmtB to 12 Å resolution, represented as grey levels.** White corresponds to maximum density. (A) Map from six merged images of AmtB crystals with p3 symmetry imposed. One unit cell is outlined. The dashed circle denotes one trimeric particle of AmtB. (B) Projection map as in (A), but with p321 symmetry imposed. The unit cell is not outlined but is the same as in (A). The dashed lines show two-fold symmetry axes. In both maps, the two crystallographically independent particles are labelled 'a' and 'b'. (C,D) Three-fold rotationally averaged density maps of particle 'b' from the p3 and p321 maps, respectively. Scale bar, 50 Å.

us to confirm that the protein is a trimer in the membrane of wild-type *E. coli* cells. Consequently, we can be reasonably confident that the trimeric crystal structure reported here reflects not only the structure of the purified protein in solution but also the native state of the protein.

With our data limited to 12 Å resolution, the EM projection maps fit both p3 and p321 symmetry. The apparent p321 symmetry could arise through one of two routes: either the crystal is composed of two oppositely oriented layers of protein related by an in-plane intermolecular two-fold axis, or there exists an intramolecular pseudo-two-fold symmetry indistinguishable from a crystallographic two-fold at the current resolution. AFM measurements of the thickness of most crystalline

sheets are consistent with the notion of a double layer, but the surface topography of the single layers seems similar to that of the double layers, albeit more disordered. If so, both layers are oriented in the same way and therefore not related by a two-fold symmetry. On the other hand, an intramolecular pseudo-two-fold axis in the crystal plane could also be caused by an internal homology between N- and C-terminal halves of the protein (Dutzler *et al*, 2002; Murakami *et al*, 2002; Van den Berg *et al*, 2004). However, multiple alignments of over 100 Amt sequences showed no obvious evidence of such internal homology in this family at the sequence level (M. Merrick, unpublished). It is interesting to note that AFM images, showing only the surface features of the molecule, rather than projected density, also seem to have an internal two-fold symmetry (Figure 2.3 D). This apparent symmetry can only arise as a pseudo-symmetry manifested at the limited resolution currently attained.

AFM and cryoEM show complementary structural information, namely, surface features and internal structure, respectively. In AFM experiments, it is likely that the cytoplasmic face of the protein, with an overall positive charge, binds to the negatively charged mica substrate. Therefore, the surface features observed are in all probability those of the periplasmic face of AmtB, and the most likely cause of the prominent feature near the three-fold axis is the 31-residue loop between helices II and III (Thomas *et al*, 2000).

AFM showed that double-layered crystals were generally better ordered, as EM images were selected for computer processing on the basis of diffraction quality, it is likely that these were from double layers. The 12 Å projection map of these AmtB crystals (Figure 2.5 B) shows several low-density regions that may represent pores in the protein and several high-density regions that may represent projected alpha-helical density. However, given the uncertainty of the nature of the superposition of densities from different crystal layers in the projections of Figure 2.4, a definite identification of such features is not possible. The one feature that must be coincident in both layers of protein (that is, the center of each particle at the three-fold axis) is also the lowest density feature within each AmtB particle ('w' in Figure 2.5 B). This is of a comparable density to that of the lipid surrounding the protein, suggesting that it is not a perpendicular channel running right through the protein, because such a feature would be expected

to have considerably lower density (Mindell *et al*, 2001).

Of the known quaternary structures of membrane transport proteins, a trimeric architecture seems comparatively rare. For example, the majority of secondary transporters studied in detail seem to be monomeric, dimeric or tetrameric (Veenhoff *et al*, 2002), and channels of known structure are all dimeric, tetrameric, pentameric or heptameric (Chang *et al*, 1998; Doyle *et al*, 1998; Bass *et al*, 2002; Dutzler *et al*, 2002). We are not aware of any trimeric channels. However, we are aware of structural data for three secondary transporters that are trimeric: the multidrug-proton antiporter, AcrB (Murakami *et al*, 2002); the tetracycline-proton antiporter, TetA (Yin *et al*, 2000); and the sodium-glycine betaine symporter, BetP (Ziegler *et al*, 2004). In the case of AcrB, it is clear that the trimeric assembly is necessary for function, as drugs are transported through a channel formed at the interface of the three subunits. In the case of TetA, it is more likely that, by analogy to other major facilitator superfamily (MFS) proteins, each monomer contains a transport channel (Abramson *et al*, 2003) so that the role of the trimeric architecture in function is less clear. BetP is notable in that the monomers within the trimer seem to have different conformations. We have found no evidence for this type of conformational heterogeneity in AmtB. Both AcrB and members of the MFS, which includes TetA, lactose permease and the glycerol-3-phosphate antiporter, show a pseudo-two-fold symmetry within the monomer. We see evidence for a similar pseudo-symmetry in our projection structures of AmtB.

2.5.1 Speculation

In bacteria and archaea, *amtB* is invariably linked to the gene *glnK*, and in *E. coli* we have shown that AmtB activity is regulated by interaction with GlnK, which is also a trimer (Coutts *et al*, 2002; Javelle *et al*, 2004) and has a similar footprint to AmtB when viewed down the three-fold axis (Xu *et al*, 1998). It is possible that the trimeric structure of both proteins may reflect a symmetry required for interaction between the two proteins. Whether the trimeric state of AmtB is necessary for function is as yet unknown, but we would speculate that each monomer contains an ammonium channel. Furthermore, as Amt proteins from bacteria, archaea, fungi and plants show a high degree of ho-

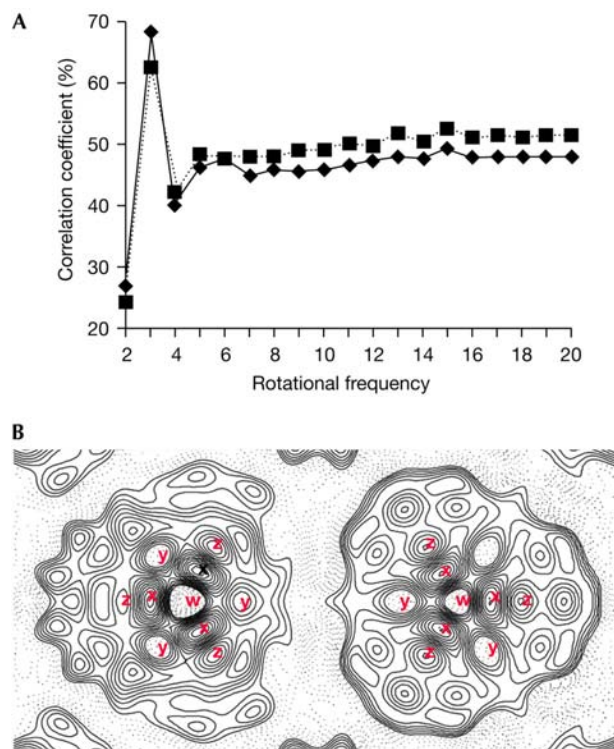


Figure 2.5: **Features of the AmtB trimer.** (A) Rotational correlation analysis of particles 'a' from p3 (solid line) and p321 (dotted line) maps that do not lie on a crystallographic three-fold axis. (B) Contour plot of particles from the p321 map, one of which (right) lies on the crystallographic three-fold axis while the other (left) is bisected by a single two-fold axis only. Both particles show a low-density region (w), surrounded by three peaks of high density (x) and a ring of six areas of lower density (y and z); those marked with the same letter are related by either crystallographic (right) or noncrystallographic (left) three-fold symmetry.

mology, it is tempting to suggest that this conservation could be reflected in the tertiary and quaternary structures. Fungal and plant Amt proteins and human Rh proteins are thought to be oligomeric (Eyers *et al*, 1994; Marini & Andre, 2000; Ludewig *et al*, 2003) and may also occur as homo- or heterotrimers.

2.5.2 Supplementary information

Supplementary information (see Section 2.8) is available at EMBO reports online (<http://www.nature.com/embor/journal/v5/n12/extref/7400296-s1.pdf>).

2.5.3 Note added in proof

Since submission of this manuscript, the 3D crystal structure of AmtB has been published by two groups (Khademi *et al* (2004) *Science* 305: 1587-1594; Zheng *et al* (2004) *Proc Natl Acad Sci USA*, in press). These crystal structures confirm and extend the findings presented here.

2.6 Acknowledgements

We thank Dr P. Wang for excellent microscopy support, Mr J. Thornton for preparation of the AmtB antibody, Dr A. Javelle for Figure 2.1 and Dr A. Durand for constructive criticism of the manuscript. P.B., M.C., D.B. and M.M. acknowledge generous support from the BBSRC (UK). A.E. acknowledges support by the Swiss National Research Foundation, the ME Müller Foundation, the Swiss National Center of Competence in Research (NCCR) 'Structural Biology' and the NCCR 'Nanoscale Science'.

2.7 References

- Abramson J, Smirnova I, Kasho V, Verner G, Kaback HR, Iwata S (2003) Structure and mechanism of the lactose permease of *Escherichia coli*. *Science* 301:610-615
- Bass RB, Strop P, Barclay M, Rees DC (2002) Crystal structure of *Escherichia coli* MscS, a voltage-modulated and mechanosensitive channel. *Science* 298:1582-1587
- Blakey D, Leech A, Thomas GH, Coutts G, Findlay K, Merrick M (2002) Purification of the *Escherichia coli* ammonium transporter AmtB reveals a trimeric stoichiometry. *Biochem J* 364:527-535
- Chang G, Spencer RH, Lee AT, Barclay MT, Rees DC (1998) Structure of the MscL homolog from *Mycobacterium tuberculosis*: a gated mechanosensitive ion channel. *Science* 282:2220-2226
- Coutts G, Thomas G, Blakey D, Merrick M (2002) Membrane sequestration of the signal transduction protein GlnK by the ammonium transporter AmtB. *EMBO J* 21:1-10
- Crowther RA, Henderson R, Smith JM (1996) MRC image processing programs. *J Struct Biol* 116:9-16
- Doyle DA, Morais Cabral J, Pfuetzner RA, Kuo A, Gulbis JM, Cohen SL, Chait BT, MacKinnon R (1998) The structure of the potassium channel: molecular basis of K⁺ conduction and selectivity. *Science* 280:69-77
- Dutzler R, Campbell EB, Cadene M, Chait BT, MacKinnon R (2002) X-ray structure of a ClC chloride channel at 3.0 Å reveals the molecular basis of anion selectivity. *Nature* 415:287-294
- Eyers SA, Ridgwell K, Mawby WJ, Tanner MJ (1994) Topology and organization of human Rh (rhesus) blood group-related polypeptides. *J Biol Chem* 269:6417-6423
- Henderson R, Baldwin JM, Downing KH, Lepault J, Zemlin F (1986) Structure of purple membrane from *Halobacterium halobium*-recording, measurement and evaluation of electron-micrographs at 3.5 Å resolution. *Ultramicroscopy* 19:147-178
- Jap BK, Zulauf M, Scheybani T, Hefti A, Baumeister W, Aebi U, Engel A (1992) 2D crystallization: from art to science. *Ultramicroscopy* 46:45-84
- Javelle A, Severi E, Thornton J, Merrick M (2004) Ammonium sensing in *E. coli*: the role of the ammonium transporter AmtB and AmtB-GlnK complex formation. *J Biol Chem* 279:8530-8538
- Ludewig U, Wilken S, Wu B, Jost W, Obrdlik P, El Bakkoury M, Marini AM, Andre B, Hamacher T, Boles E, von Wiren N, Frommer WB (2003) Homo- and hetero-oligomerization of ammonium transporter-1 NH₄⁺-uniporters. *J Biol Chem* 278:45603-45610
- Marini A-M, Andre B (2000) In vivo N-glycosylation of the Mep2 high-affinity ammonium transporter of *Saccharomyces cerevisiae* reveals an extracytosolic N-terminus. *Mol Microbiol* 38:552-564
- Marini A-M, Matassi G, Raynal V, Andre B, Cartron J, Cherif-Zahar B (2000) The human Rhesus-associated RhAG protein and a kidney homologue promote ammonium transport in yeast. *Nat Genet* 26:341-344
- Mindell JA, Maduke M, Miller C, Grigorieff N (2001) Projection structure of a ClC-type chloride channel at 6.5 Å resolution. *Nature* 409:219-223
- Monahan BJ, Unkles SE, Tsing IT, Kinghorn JR, Hynes MJ, Davis MA (2002) Mutation and functional analysis of the *Aspergillus nidulans* ammonium permease MeaA and evidence for interaction with itself and MepA. *Fungal Genet Biol* 36:35-46
- Murakami S, Nakashima R, Yamashita E, Yamaguchi A (2002) Crystal structure of bacterial multidrug efflux transporter AcrB. *Nature* 419:587-593
- Quentin F, Eladari D, Cheval L, Lopez C, Goossens D,

- Colin Y, Cartron JP, Paillard M, Chambrey R (2003) RhBG and RhCG, the putative ammonia transporters, are expressed in the same cells in the distal nephron. *J Am Soc Nephrol* 14:545-554
- Saxton WO (1996) SEMPER: distortion compensation, selective averaging, 3-D reconstruction, and transfer function correction in a highly programmable system. *J Struct Biol* 116:230-236
- Schertler GF, Villa C, Henderson R (1993) Projection structure of rhodopsin. *Nature* 362:770-772
- Thomas GH, Mullins JG, Merrick M (2000) Membrane topology of the Mep/Amt family of ammonium transporters. *Mol Microbiol* 37:331-344
- Valpuesta JM, Carrascosa JL, Henderson R (1994) Analysis of electron microscope images and electron diffraction patterns of thin crystals of phi 29 connectors in ice. *J Mol Biol* 240:281-287
- Van den Berg B, Clemons WMJ, Collinson I, Modis Y, Hartmann E, Harrison SC, Rapoport TA (2004) X-ray structure of a protein-conducting channel. *Nature* 427:36-44
- van Heel M, Harauz G, Orlova EV (1996) A new generation of the IMAGIC image processing system. *J Struct Biol* 116:17-24
- Veenhoff LM, Heuberger EHML, Poolman B (2002) Quaternary structure and function of transport proteins. *Trends Biochem Sci* 27:242-249
- von Wirén N, Merrick M (2004) Regulation and function of ammonium carriers in bacteria, fungi and plants. *Top Curr Genet* 9:95-120
- von Wirén N, Lauter FR, Ninnemann O, Gillissen B, Walch-Liu P, Engels C, Jost W, Frommer WB (2000) Differential regulation of three functional ammonium transporter genes by nitrogen in root hairs and by light in leaves of tomato. *Plant J* 21:167-175
- Westhoff CM, Ferreri-Jacobia M, Mak DO, Foscett JK (2002) Identification of the erythrocyte Rh-blood group glycoprotein as a mammalian ammonium transporter. *J Biol Chem* 277:12499-12502
- Xu Y, Cheah E, Carr PD, van Heeswijk WC, Westerhoff HV, Vasudevan SG, Ollis DL (1998) GlnK, a PII-homologue: structure reveals ATP binding site and indicates how the T-loops may be involved in molecular recognition. *J Mol Biol* 282:149-165
- Yin CC, Aldema-Ramos ML, Borges-Walmsley MI, Taylor RW, Walmsley AR, Levy SB, Bullough PA (2000) The quaternary molecular architecture of TetA, a secondary tetracycline transporter from *Escherichia coli*. *Mol Microbiol* 38:482-492
- Ziegler C, Morbach S, Schiller D, Kramer R, Tziatzios C, Schubert D, Kuhlbrandt W (2004) Projection structure and oligomeric state of the osmoregulated sodium/glycine betaine symporter BetP of *Corynebacterium glutamicum*. *J Mol Biol* 337:1137-1147

2.8 Supplementary Information

Plane group	Phase residual versus other spots ($^{\circ}$) (90 $^{\circ}$ =random)	Phase residual versus theoretical ($^{\circ}$) (45 $^{\circ}$ =random)	Target residual ($^{\circ}$)
p1	31.3 (140)	–	
p2	55.6* (70)	27.8 (140)	46.6
p3	29.3* (33)	–	31.3
p312	51.2 (219)	28.6 (14)	31.8
p321	31.5* (223)	29.3 (22)	32.1
p6	55.2 (246)	37.9 (140)	35.7
p622	51.9 (512)	38.0 (140)	33.4

Table 2.1: **Internal phase residuals of one image according to plane group symmetry.** Internal phase residuals were determined using ALLSPACE for reflections of $IQ \leq 5$ to 12 \AA resolution. Number of comparisons is shown in parentheses. Asterisks indicate where the calculated residual is better than the target.

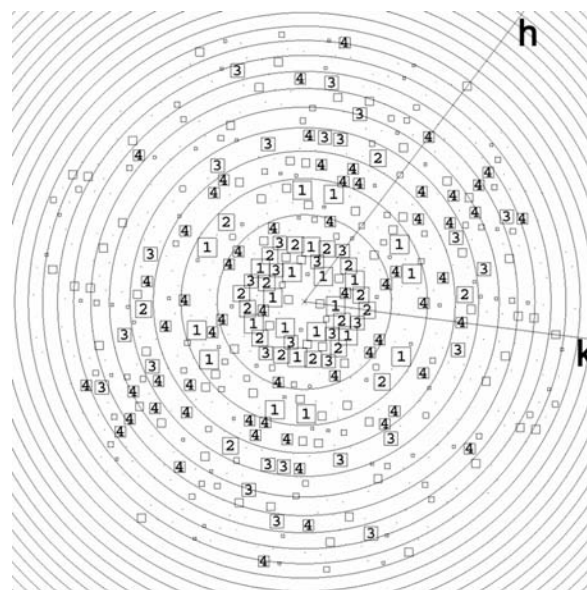


Figure 2.6: **Representation of the Fourier transform of an image of an AmtB crystal embedded in glucose.** The circles represent zero transitions of the phase contrast transfer function (CTF) and the boxed numbers depict the IQ values of the individual reflections. Reflections are shown to 10 \AA^{-1} resolution.

Resolution (\AA)		IQ Value ¹								IQ weighted residuals
From	To	1	2	3	4	5	6	7	8	
p3 symmetry										
∞	25	11.5	15.3	20.3	44.3	59.4	66.6	79.5	77.8	47.5
		16	47	21	29	25	16	17	53	224
25	18	7.8	15.9	26.3	40.4	53	72.4	28.3	72.5	50.4
		18	17	18	23	24	22	14	81	217
18	12	18.3	18.1	50.3	41.8	62.3	55.2	89.3	83.7	70.6
		6	12	26	54	38	35	47	231	449
∞	12	13.4	15.8	29.7	45.9	57.2	66.3	76	78.2	59.4
		40	76	65	106	87	73	78	365	890
p321 symmetry										
∞	25	11.4	14.5	21.3	48.1	44.1	68.7	91.2	73.8	46.3
		16	47	21	29	25	16	17	53	224
25	18	8.1	13.8	30.7	43.9	40	76.2	60.7	75.4	53.2
		18	17	18	23	24	22	14	81	217
18	12	21	19.4	36.3	41.2	72	64.2	92.8	87.4	73.7
		6	12	26	54	38	35	47	231	449
∞	12	13.2	16.2	30	43.8	61.6	66.8	67.8	78.5	59.2
		40	76	65	106	87	73	78	365	890

¹ Phase residuals in degrees (top line) and number of spots (bottom line) in each class are given for different resolution ranges

Table 2.2: **Mean phase residuals in resolution shells for merged images in p3 and p321 (random=90 $^{\circ}$).**

In the following the publication "A Novel Method for Detergent Concentration Determination" is appended as published in Biophysical Journal 2006, volume 90, pages 310–317.

Chapter 3

A Novel Method for Detergent Concentration Determination

Thomas C. Kaufmann¹, Andreas Engel¹ & Hervé-W. Rémigy^{1,2}

3.1 Abstract

A fast and precise method for detergent concentration determination is presented³. A small droplet of the detergent solution is deposited on a piece of Parafilm M and side views are recorded by two orthogonally arranged TV cameras. The droplet contours are then approximated by ellipses to determine the contact angles. Comparison of the observed contact angle values to calibrated standard curves of known detergent concentrations gives the concentration of the detergent assessed. A range of commonly used detergents was studied to demonstrate the reproducibility and precision of this simple method. As a first application the detergent binding capacity of GalP, the *E. coli* galactose/proton symporter was assessed. Aggregation of GalP was observed when less than 260 ± 5 dodecyl- β ,D-maltoside molecules were bound to one GalP molecule. These measurements document the efficacy of the drop-shape based detergent concentration determination described.

3.2 Introduction

Knowing the exact detergent concentration is an important prerequisite for working with solubilized membrane proteins. Protein purification steps such as affinity chromatography and procedures to increase the protein concentration can affect the detergent concentration (1), and high detergent concentrations can induce loss of the quaternary and tertiary protein structure. Moreover, the kinetics of

detergent removal during reconstitution and two-dimensional (2D) crystallization of membrane proteins is strongly dependent on the initial detergent concentration (2-4), and three-dimensional (3D) crystallization may depend on the amount of detergent present (5, 6). Therefore, the detergent concentration needs to be accurately measured. While quite a few methods exist for the determination of detergent concentrations, they are impractical for many routine applications. They include the use of radiolabeled detergents (7), Fourier transform infrared spectroscopy (8), quantitative thin-layer chromatography (9), analytical ultracentrifugation (10, 11), equilibrium column desorption (1), a modified phenol-sulfuric acid assay (12) to measure sugar moieties of some detergents (13), the falling drop method and the sitting drop method (14). All these methods are in general slow and often require large sample volumes to obtain ac-

¹M.E. Müller Institute for Microscopy at the Biozentrum, University of Basel, Klingelbergstrasse 70, CH-4056 Basel, Switzerland

²Corresponding author. Tel: +41 61 267 22 57 Fax: +41 61 267 21 09 Email: herve.remigy@unibas.ch

³Patent applications for the method described here have been submitted (EP05011904 and US60/702,261). Depending on the interest of the scientific community, the system will be commercialized. For further information contact Hervé-W. Rémigy (herve.remigy@unibas.ch)

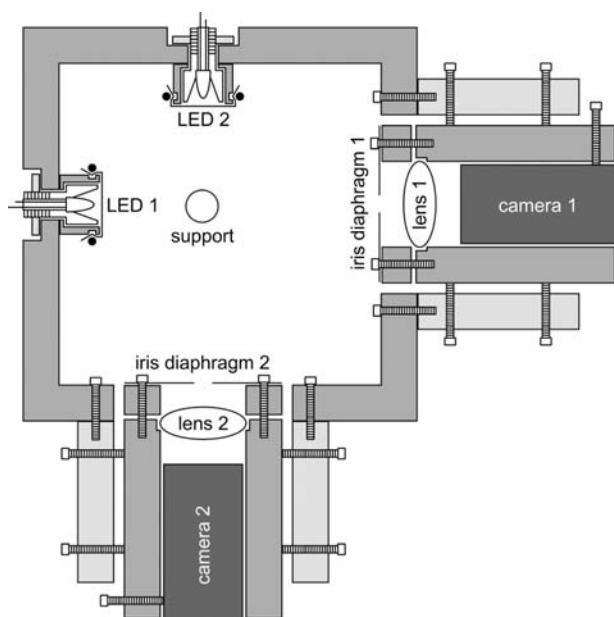


Figure 3.1: Schematic drawing showing the setup of the contact angle measuring device.

curate results, making them unsuitable for routine measurements. The related time-loss may be critical for membrane proteins, which are often destabilized by exposure to detergents. Detergents reduce the surface tension of any aqueous solution by partitioning to the air-water interface. This disturbs the ordered arrangement of water molecules at the surface and diminishes the force of attraction between them. The surface tension is steadily reduced until the critical micellar concentration (cmc) is reached. Above this point the concentration of free (monomeric) detergent molecules in solution does not further increase, because addition of more detergent results in the formation of micelles. Here we take advantage of the intrinsic surface activity of detergents to set up a device for their concentration determination. As a first application we have studied the behavior of the *E. coli* galactose/proton symporter (GalP) solubilized in dodecyl- β ,D-maltoside. The method allowed the detergent binding capacity of GalP and its related aggregation behavior to be determined quickly and with excellent accuracy.

3.3 Materials and Methods

3.3.1 Construction of the contact angle measuring device

A box (Figure 3.1) made of standard PVC holds two cameras with their optics (including iris diaphragms

made of aluminum) and a plexiglass cylinder for depositing the drop. C-MOS black and white camera modules with a resolution of 628 pixels horizontally times 582 pixels vertically have been purchased from Conrad (Hirschau, Germany (Article Nr. 150334)). Bi-convex lenses with a focal length of 25.4 mm and f-number 1 purchased from Thorlabs Inc. (Grünberg, Germany (Article Nr. LB1761)) magnify the drop image. The two cameras acquire side views of the drop from orthogonal directions to detect drop asymmetry. Two frame grabber cards (Brooktree BT 848 chipset based acquisition cards) control the image acquisition. The diffuse illumination of the droplet is achieved by Teflon tape covered LEDs (standard 5 mm round white 60 mW LED) mounted opposite to the cameras. To ensure reproducible surface properties for each measurement, a fresh piece of Parafilm M was mounted on the plexiglass support using double sided tape (Scotch 665, 12.7 mm). The image analysis software was programmed in C under the GNU general public license (for further information see: <http://www.gnu.org/copyleft/gpl.html>). The ellipsoid approximation is achieved by GNU PLOT and the results are displayed using XVIEW.

3.3.2 Characterization of the substrate

The substrate in this study was Parafilm M and is a product of Pechiney Plastic Packaging (Chicago, USA). Atomic force microscopy (AFM) measurements were performed in air using a Nanoscope III microscope equipped with an infrared laser head and oxide-sharpened silicon nitride cantilevers of 200 μm length and a nominal spring constant of 0.06 N/m from Veeco Metrology (Santa Barbara, USA). Topographs were acquired in contact mode at minimal loading forces (≤ 100 pN). Line frequencies ranged between 4.1 and 5.5 Hz. Surface roughness calculations were performed using the analyze/roughness subroutine in the Nanoscope software package (v5.12r2). The Parafilm was fastened by double sided tape (Scotch 665, 12.7 mm) on a ferromagnetic steel disc with a glued-on Teflon disc. The solid surface tension (γ_{sv}) of Parafilm was determined by the equation of state approach (15-17) from the experimentally determined contact angles of different liquids with known surface tension values (γ_{lv}). The liquids used were water, glycerol, ethylene glycol, polyethylene glycol 200, pyridine, N,N-dimethyl formamide, 1,4-dioxane, 2-ethoxyethanol and ethanol. The correspond-

ing surface tensions at 26°C are 71.89 mJ/m², 63.64 mJ/m², 47.17 mJ/m², 42.80 mJ/m², 37.18 mJ/m², 36.26 mJ/m², 32.17 mJ/m², 28.05 mJ/m² and 21.60 mJ/m² respectively (18). Experimental contact angle values were used in conjunction with the following equation of state (16):

$$\cos\vartheta = -1 + 2\sqrt{\gamma_{sv}/\gamma_{lv}} e^{-\beta(\gamma_{lv}-\gamma_{sv})^2} \quad (3.1)$$

where γ_{lv} and γ_{sv} are the interfacial tensions of the liquid-vapor and solid-vapor interfaces respectively; ϑ is the Young contact angle as defined by Young's equation:

$$\cos\vartheta = \frac{\gamma_{sv} - \gamma_{sl}}{\gamma_{lv}} \quad (3.2)$$

and β is a fit parameter.

3.3.3 Calibration of the detergents

The detergents used in this study were octyl- β ,D-glucoside (OG), octyl- β ,D-thiogluconide (OTG), decyl- β ,D-maltoside (DM), dodecyl- β ,D-maltoside (DDM), CYMAL-5, dodecyl-N,N-dimethylamine-N-oxide (LDAO), nonaethylene glycol monododecyl ether (C12E9), N-dodecylphosphocholine (FOSCh12), which all were purchased from Anatrace (Ohio, USA), Triton X-100 (TX-100) and octyltrimethylammonium bromide (OTAB) from Sigma-Aldrich (Missouri, USA), 3[(3-Cholamidopropyl) dimethyl-ammonio] propane-sulfonic acid (CHAPS) from Dojindo Molecular Technology (Maryland, USA) and sodium dodecyl sulfate (SDS) from Bio-Rad Laboratories (California, USA). All detergents were of high purity grade ($\geq 98\%$) and were used without further purification. Aqueous solutions of these detergents in the range of 0-7.5 x cmc were prepared by dilution from the corresponding stock solutions (15x cmc) with reagent-grade water produced by a Milli-Q filtration system ($\geq 18 \text{ M}\Omega$). The pipetted volumes were weighed on a balance (Mettler AE50) purchased from Mettler-Toledo (Greifensee, Switzerland). One calibration curve represents the mean of three measured curves for each detergent. The cmc's were determined from the intersection of a 3rd polynomial fit to the descending part of the curve and a linear fit to the plateau.

3.3.4 Comparison with radioactively labeled DDM

The concentration of radiolabeled [¹⁴C]DDM (a generous gift from J.L. Rigaud) was determined by liquid scintillation counting using a Packard Tricarb 2000 CA (Canberra-Packard, Zürich, Switzerland). These concentrations were plotted against measured contact angles (see Figure 3.6).

3.3.5 Purification of the galactose/proton symporter of *E. coli* (GalP)

1.5 ml membranes from *E. coli* strain JM1100 (pPER3) overexpressing GalP (kindly provided by P.J.F. Henderson) were resuspended in 13.5 ml solubilization buffer (20 mM Tris pH 8.0, 300 mM NaCl, 20% (v/v) glycerol, 20 mM imidazole). Solubilization was achieved at 4°C within 2 hours after addition of 1% (w/v) DDM as powder. The solubilization mixture was centrifuged at 4°C and 150'000 g to remove all unsolubilized material. 3.2 ml Ni-NTA agarose slurry were pre-equilibrated using wash buffer without detergent (20 mM Tris pH 8.0, 20 mM imidazole) and then incubated overnight at 4°C with the solubilized membranes. The column binding mixture was partitioned between 8 columns, which were washed with 20ml (100 times column volume) wash buffer containing different concentrations of DDM (0.001 / 0.003 / 0.005 / 0.006 / 0.008 / 0.011 / 0.022 / 0.043 % (w/v)). The quasi totality of the wash buffers was removed by suction. As a control, the same experiment was performed without protein, ruling out the possibility of detergent retention/accumulation by the column material (data not shown). Elution was achieved by immediate incubation with 250 μ l of elution buffer (200 mM imidazole pH 8.0 containing different concentrations of DDM (see washes)) for 1 hour and subsequent centrifugation at 4°C. The weight of the column resin and the volumes of elution buffer added and recovered were determined and taken into account in the calculations for the protein yield. Protein concentrations were determined using the Bio-Rad protein assay from Bio-Rad Laboratories (California, USA), correcting for the presence of DDM after calibration of the assay with BSA/DDM mixtures of different concentrations. The amount of DDM bound to GalP was determined by calculating the difference between the DDM concentration in the loaded elution buffers and the DDM concentration in the eluted samples. This was possible

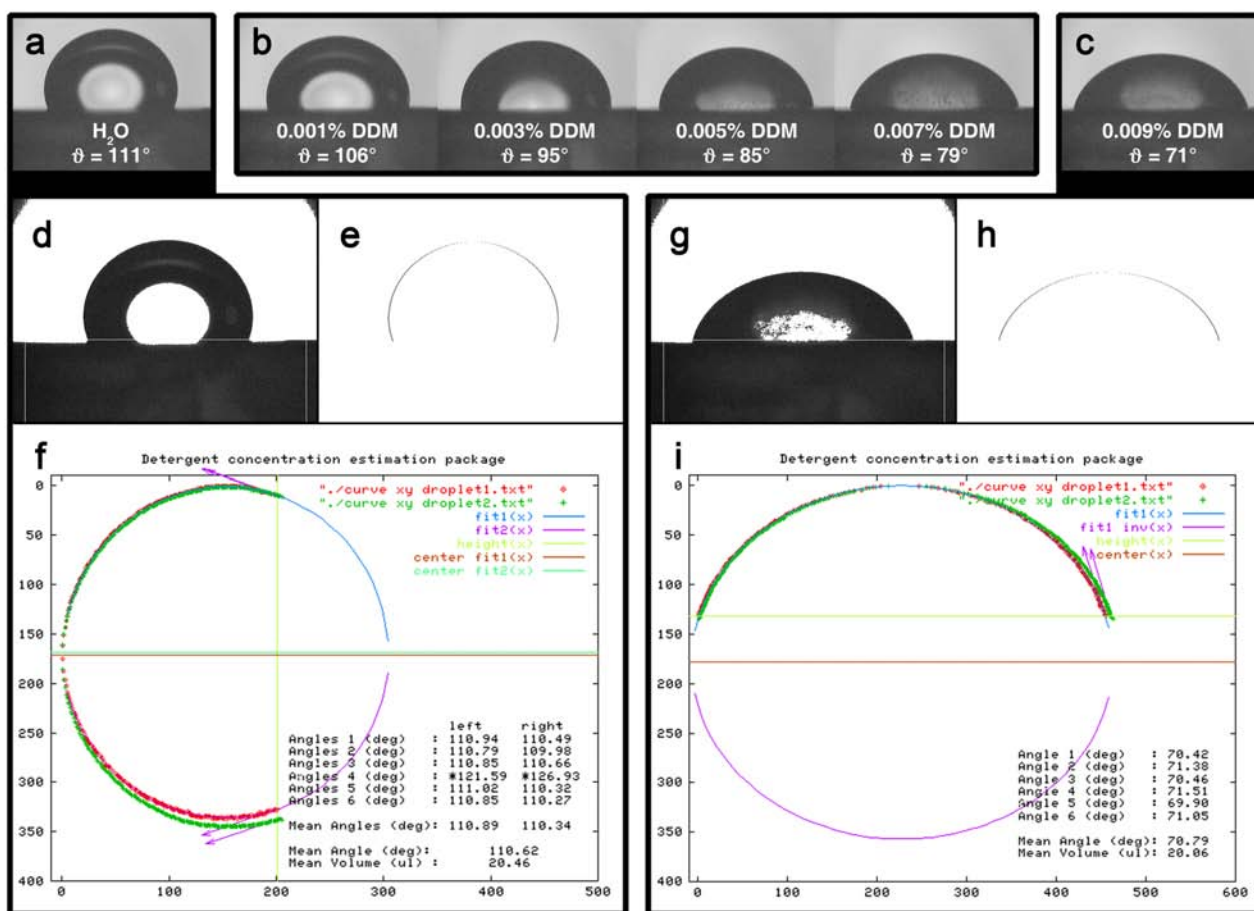


Figure 3.2: **Image analysis procedure.** (a-c) Raw images of the droplet series for DDM. (d) and (g) Pictures (a) and (c) respectively, with applied threshold. (e) and (h) Extracted droplet contours. (f) and (i) Output file from GNUPLOT displaying contact angles and mean volume. Note: In (f) the contour has been rotated by 90° with respect to (e).

assuming that total detergent concentrations are measured. Additionally it was assumed that the same monomeric and micellar detergent concentrations were present in the eluted samples as in the corresponding elution buffers and therefore the differences in detergent concentrations were due to detergent brought along by the protein. For the measurements the eluted samples had to be diluted typically between 50 and 100 times to release the detergent from the protein, which precipitated out of solution.

3.4 Results

3.4.1 Contact angle measurements

A $20 \mu\text{l}$ droplet is gently deposited onto a piece of Parafilm M fastened on the support. After 30 seconds each camera records 3 images, which are independently processed. Characteristic drop shapes

are displayed in Figure 3.2 a-c, while the processing steps are documented for two typical drops in Figure 3.2 d-i.

The software analyses the drop images in three steps: First a threshold is applied to determine the drop contour (Figure 3.2 d and g). Second, the droplet is cut out according to a predefined frame including the baseline. The coordinates of the contour (Figure 3.2 e and h) are extracted to an xy-coordinates file and used to calculate the drop volume. Third, an ellipse is fitted to the contour. Initial fit parameters such as the width and height of the droplet are read out from the xy-coordinates file. If, based on the preliminary approximation values, the contact angle is expected to be larger than 90 degrees the contour will be treated as two independent halves to solve the ellipsoid equation (see Figure 3.2 f and i). As a consequence angles larger than 90 degrees will have separate values for the left and the right contact angle (Figure 3.2 f). The el-

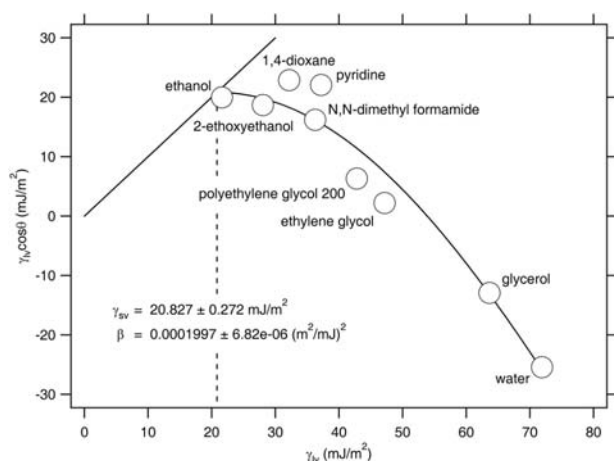


Figure 3.3: $\gamma_w \cos \vartheta$ as a function of the surface tension γ_w of various liquids for Parafilm M. The 45° line, $\gamma_w \cos \vartheta = \gamma_w$, i.e., the limiting condition $\vartheta = 0$, is also shown on the graph. The surface energy of Parafilm is given by the intersection between the two lines.

liptical fitting of the contour is then performed and terminated when the relative difference between the last two fitting cycles is smaller than 10-11. The contact angles are obtained by calculating the ellipse tangent at the intersection with the baseline. At the end the mean angle and the volume are calculated and the results together with the contours of the droplet are plotted in a graph, enabling the user to decide whether the fit should be included into the dataset of measurements. When contact angles determined from the orthogonal images differ more than $\pm 5\%$ the values are not taken into account for the mean angle calculation, thereby ensuring that the droplet is sufficiently symmetric or that the image does not exhibit any electronic noise or baseline uncertainty.

3.4.2 Characterization of Parafilm M

To assess the surface roughness of Parafilm M atomic force microscopic (AFM) measurements were carried out. Table 3.1 summarizes the different values for the averaged roughness (Ra) and the root mean squared roughness (Rms or Rq) obtained at different scan sizes. The main difference between the two values is that the Rms is sensitive to extreme peaks or valleys, whereas Ra averages them out. Ra has been designated by the International Standards Organizations (ISO) as standard for characterizing the roughness of a machined surface. Images were recorded on three individual pieces of Parafilm and different regions for scan-

Scan size ($\mu\text{m} \times \mu\text{m}$)	20 x 20	10 x 10	5 x 5	1 x 1
Number of Images ¹	9	11	8	8
Root mean square Rms or Rq \pm SD (nm)	60 \pm 17	33 \pm 15	14 \pm 9	3 \pm 5
Roughness average Ra \pm SD (nm) (ISO)	40 \pm 8	24 \pm 10	10 \pm 6	2 \pm 3

¹ Images have been taken from 3 individual pieces of Parafilm and different regions

Table 3.1: **Surface roughness analysis of Parafilm M.**

ning were chosen arbitrarily. The resulting differences in the roughness are within a range of about 10-15 nm as documented by the standard deviations. The experimentally determined value of 60 ± 17 nm for the Rms (see Table 3.1) at a frame size of $20 \mu\text{m}$ compares well with a previously published value of 42-51 nm (19). The solid surface tension of Parafilm M was determined to be 20.8 mJ/m^2 (see Figure 3.3) reflecting its hydrophobic character. Parafilm consists mainly of polyolefins and paraffin waxes, the exact composition, however, has not been released by the manufacturer. Literature values for the surface energy of paraffin waxes range from 23 to 25 mJ/m^2 , that of polyolefins are much more diverse, depending on their functionalization. They can range from 18 mJ/m^2 for polytetrafluoroethylene to 31 mJ/m^2 for polyethylene (see e.g. (20, 21)).

3.4.3 Calibration of the detergents

As can be seen from Figure 3.4 all calibration curves exhibit the same shape characteristics. The contact angle gradually decreases with increasing detergent concentration until a plateau is reached with a sharp break. The cmc is the concentration where the break occurs and after which there is no further significant reduction in the contact angle. There are clear differences in the amount of surface tension reduction between the different detergents (vertical shift on the graph). The degree of surface tension reduction seems to mainly depend on the properties of the headgroup. In particular, the surface excess, i.e., the number of detergent molecules covering the surface, predominates the surface tension lowering effect. Nonionic detergents

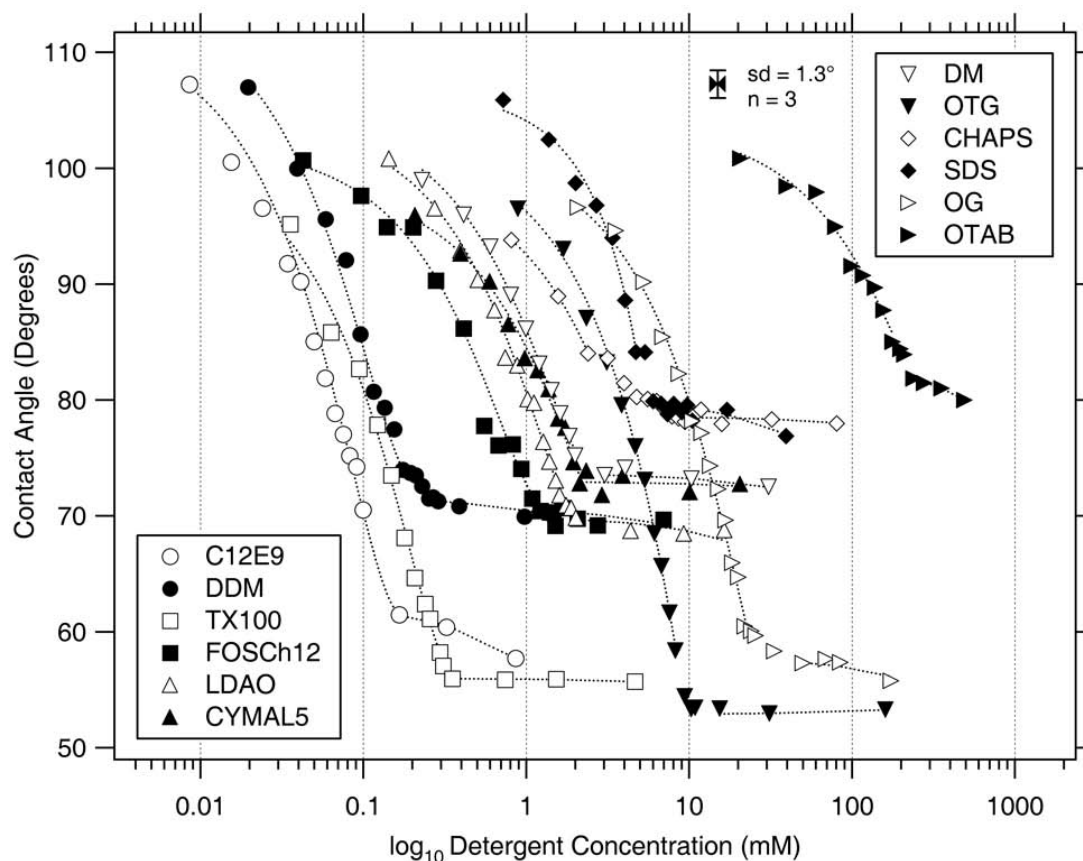


Figure 3.4: **Semi-logarithmic plot of the detergent concentration vs. experimental contact angles for all calibrated detergents.**

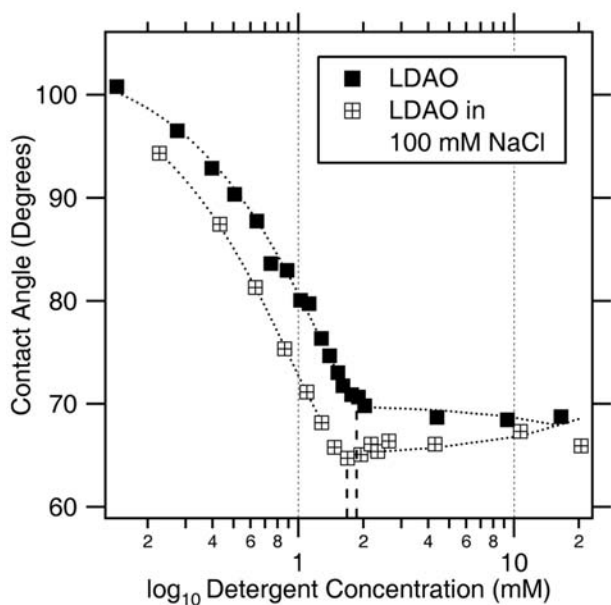


Figure 3.5: **Influence of the ionic strength on the properties of LDAO at pH 7.9.** By adding 100 mM NaCl to the calibration standards the cmc drops from 1.9 mM to 1.7 mM and the contact angle is decreased from 70° to 65° giving evidence for a higher surface excess in the latter case.

(see " $\theta @ \text{cmc}$ " in Table 3.2) are more efficient in reducing the surface tension than charged ones (OTAB/SDS). Charged detergents seem to have a limited capacity to adsorb to the air-water interface due to repulsion between equally charged species. Since the N-O bond in the headgroup of LDAO has a polar character, it exhibits an intermediate behavior. Depending on the pH LDAO is present as nonionic (pH = 7) or cationic (pH = 3) species, accompanied by a significant increase in the cmc for the latter (22). Additionally, it has been shown that the cmc of cationic LDAO strongly depends on the ionic strength of the aqueous solution (23). For ionic surfactants this is a known influence mainly due to electrostatic interactions of the counterions with the charged headgroups. Interestingly the addition of NaCl also affects the cmc and the adsorption behavior of the nonionic species (see Figure 3.5). Even though this has been reported for nonionic detergents, such as polyoxyethylene derivatives (24) and others (25), the observed effect on LDAO is considerably larger and cannot only be explained by the salting out effect, i.e. the dehydration (22, 23). It is most likely that additionally, par-

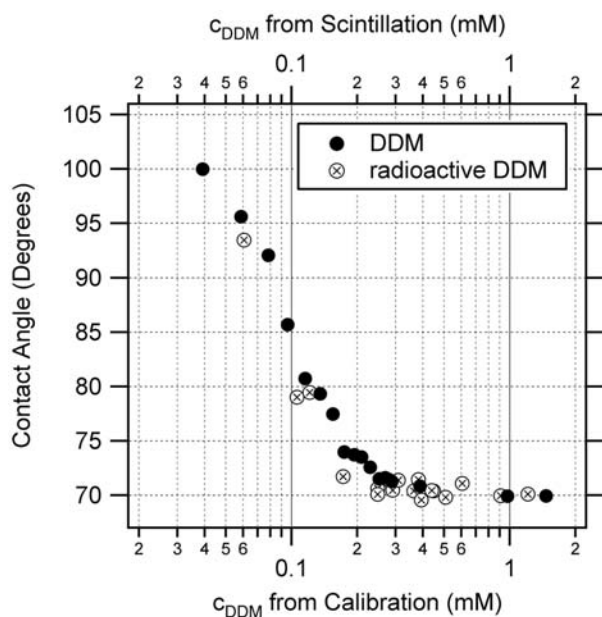


Figure 3.6: **Quality assessment of the detergent concentration measurement.** Concentrations from the DDM calibration have been calculated from the preparation of the standards, concentrations from the radioactive DDM have been taken from scintillation counting.

tial charges in the amine oxide group get shielded resulting in an increase of the surface excess of the surfactant and therefore in an appreciable decrease in surface tension upon addition of NaCl. NaCl on its own is known to increase the surface tension of an aqueous solution. This effect is negligible at concentrations used in biological buffers (100 mM) (data not shown). The bulkier the headgroup (e.g., CHAPS), the less they reduce the surface tension. The length of the hydrophobic tail (DM/CYMAL-5/DDM) does not seem to have a great impact on the adsorption behavior. However, increasing the chain length results in a lower cmc (horizontal shift on the graph).

3.4.4 Comparison with radioactively labeled DDM

As an independent quality test for the presented concentration determination, radioactively labeled DDM has been assessed. Precise [^{14}C]DDM concentrations of the samples were measured using a liquid scintillation counter. The calibration curves of DDM and radioactive DDM overlay very well (see Figure 3.6), demonstrating the accuracy of the sitting drop method.

3.4.5 Controlling the amount of detergent bound to a membrane protein during Ni-NTA affinity chromatography

After membrane solubilization with an excess of detergent, the hydrophobic parts of membrane proteins are completely covered by detergent molecules, shielding them from the aqueous surrounding (2, 4). However, in order to keep the proteins soluble, less detergent would be sufficient (26). In view of membrane protein stability one wants to minimize the amount of detergent present in a solution before reconstitution to favor lipid-protein contacts in the ternary solution (lipid-protein-detergent). In the case of low cmc detergents dialysis takes considerably longer if excess detergent is present. This means that the reconstitution process takes longer and the protein is kept in a non-native environment for a longer time. Here we show that it is possible to adjust the amount of detergent bound to the protein during Ni-NTA affinity chromatography by using washes of different near-cmc detergent concentrations (see Figure 3.7). Based on the assumption that the protein is saturated with detergent after solubilization (P_{sat}), one would expect that when lowering the detergent concentration in the wash, the detergent-to-protein ratio (DPR) would decrease before the protein elution yield decreases. This is the range where excess detergent molecules are drawn off the protein without affecting its solubility (between D_{free} and D_{agg}). When a critical DPR is reached (P_{sol}) the protein yield starts to decrease too, indicating that part of the protein aggregates and that there is not enough detergent to keep all the protein soluble. As was shown by Møller and le Maire the amount of detergent binding by membrane proteins can be seen as a measure for their hydrophobicity and the size of their hydrophobic sector. The obtained solubility range (P_{sol} to P_{sat}) of 260 to 290 DDM molecules per GalP monomer (i.e., the molar ratio) in this study is an indication for a strong hydrophobicity, since it is higher compared with other published values, which range from 148 to 215 molecules for other membrane proteins (1).

3.5 Discussion

When depositing a droplet onto a hydrophobic surface (Parafilm M) the spreading of the droplet over the surface is merely dominated by three phenom-

Detergent	Calibration Plot Properties			Physical Properties				
	Nr. of Points	sd (°)	ϑ @ cmc (°)	Type ¹	MW (g/mole)	Aggregation Nr. ^{2,4}	Critical Micellar Concentrations (mM)	
							This Work	Literature Values
C12E9	15	1.9	61.8	N	583.1		0.16	0.05 ² , 0.08 ^{3,4} , 0.1 ⁶
DDM	18	1	74.1	N	510.6	78-149	0.17	0.15 ⁶ , 0.17 ^{2,3} , 0.18 ⁷ , 0.1-0.6 ⁴
TX-100	15	1.1	56	N	647	100-155	0.37	0.23 ² , 0.24 ⁶ , 0.9 ³ , 0.2-0.9 ⁴
FOSCh12	18	2.3	70.5	Z	351.5	50-60	1.3	1.5 ^{2,3}
LDAO	19	1.1	69.7	N/C	229.4	76	1.9	1 ² , 1.4 ⁶ , 2 ³ , 2.2 ⁷ , 1-2 ⁴
CYMAL-5	16	2	72.9	N	494.5	66	2.2	2.4 ^{2,3}
DM	14	0.8	73.5	N	482.6	69	2.5	1.6 ^{4,6} , 1.8 ^{2,3,5} , 2.2 ⁷
OTG	17	0.9	52.9	N	308.4		9.5	9 ^{2,3,4,5,6}
CHAPS	18	1	78.5	Z	614.9	10	3.4	8 ^{2,3} , 2-10 ⁶ , 3-10 ⁷ , 4.2-6.3 ⁵ , 6-10 ⁴
SDS	17	0.9	79.7	A	288.4	62-101	5.3	2.6 ² , 1.2-7.1 ⁷ , 7-10 ⁴
OG	20	1.4	57.6	N	292.4	78	25	18 ² , 24.5 ³ , 30.3 ⁶ , 18-20 ⁵ , 19-25 ⁷ , 20-25 ⁴
OTAB	15	1.4	81.9	C	252.2		230	220 ⁸ , 241 ⁹

¹ Types of detergents: A = Anionic / C = Cationic / N = Nonionic / Z = Zwitterionic

² (Anatrace Catalog, Maumee, USA, 2004)

³ (Hampton Research, Laguna Niguel, USA, 2002)

⁴ (33)

⁵ (Glycon Biochemicals Catalog, Luckenwalde, Germany, 2004)

⁶ (34)

⁷ (35)

⁸ (36)

⁹ (37)

Table 3.2: Summary of detergent and calibration plot properties.

ena: The molecules at the surface are energetically less favorable than the molecules in the interior of the droplet and hence the droplet tries to minimize its surface. On the other hand, adsorption of surfactant molecules to the liquid-vapor interface disturbs the ordering of the water molecules, thereby reducing the surface tension. Adsorption of surfactant to the solid-liquid interface hydrophilizes the hydrophobic substrate by adsorption of the hydrophobic tails and exposure of the hydrophilic headgroup. The latter two adsorption processes favor the spreading of the droplet.

To ensure a (quasi-) equilibrium Young contact angle and good reproducibility, images are taken after 30 seconds time. In many studies (19, 27-31) it has been shown that the spreading of surfactant solutions due to detergent adsorption to the liquid-

vapor and solid-liquid interface reaches a plateau at the latest within 30 seconds.

The use of 20 μl droplets ensures a high reproducibility because all adverse effects, such as evaporation and bulk concentration depletion are minimized. In addition, such drops are sufficiently small to assure the validity of the elliptical shape approximation. Assuming a cross-sectional area of 0.4 nm^2 per detergent molecule, a mean surface (including the base) of 40 nm^2 for a 20 μl droplet can accommodate an absolute maximum of 10^{14} detergent molecules. This corresponds to a maximum depletion of about 8.3 μM , which in turn corresponds to an error in the cmc of 5% for a detergent with a cmc of 0.17 mM like DDM. This error would get worse with smaller volumes, since the volume scales with r^3 while the surface only scales with r^2 .

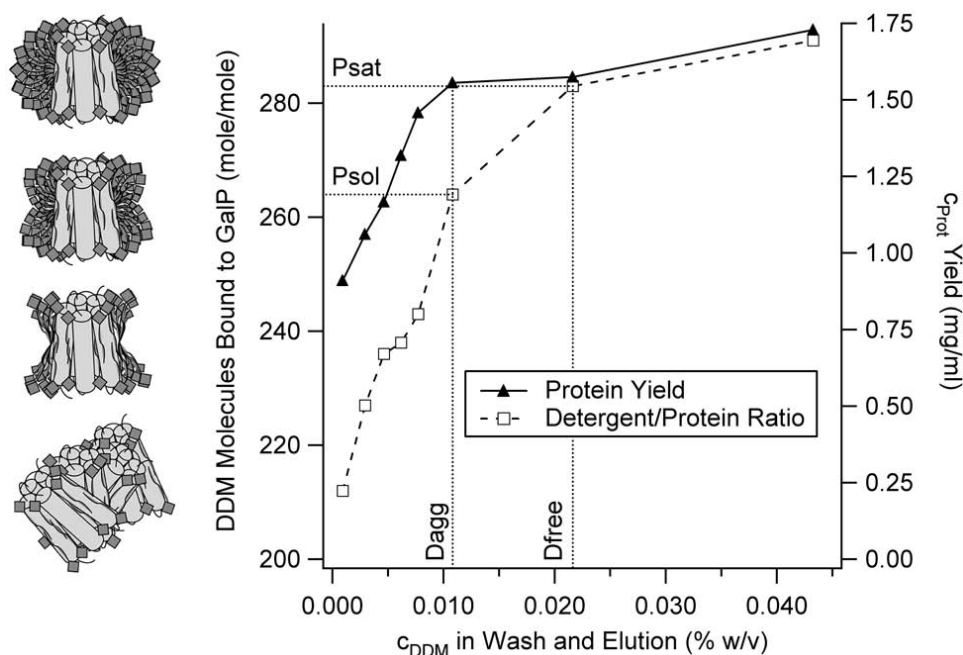


Figure 3.7: Ni-NTA affinity chromatography with GalP using washes of different DDM concentrations.

The only interfering substances are other surface active reagents like glycerol and polyethylene glycols. Lipids slightly affect the measurement since they exhibit a somewhat similar behavior as detergents in that they possess a cmc (10 mg/ml Dimyristoyl-phosphatidylcholine (DMPC) and 10 mg/ml Dioleoyl-phosphatidylcholine/Dioleoyl-phosphatidic acid (DOPC/DOPA) 70:30 exhibit contact angles of 106.1° and 107.1° , respectively, compared to 110.7° for water alone). However, for the measurement one has to dilute the sample typically between 50 and 100 times in order to be below the cmc. In doing so the concentrations of interfering compounds usually drop below a critical concentration and the disturbing effect can be neglected. Another possibility is to perform calibrations in the presence of interfering substances, thereby implementing their contribution to the reduction in surface tension already in the calibration. Furthermore, it might be possible by generating calibration curves containing multiple surface active components at different ratios to decompose the resulting curves in terms of single components. For precision purposes it is advisable to weigh the pipetted volumes on a balance to prevent errors arising from small pipetting volumes.

The low surface energy of Parafilm M provides a suitable range for the measured contact angles. If the substrate is too hydrophilic the contact an-

gles would be much lower and hence within a narrower range. The ease with which a fresh and clean surface can be prepared by the use of disposable Parafilm makes it a perfect candidate for the substrate. The reproducibility of the surface properties from one piece of Parafilm to another is excellent (see Table 3.1).

Solubilizations of membranes are often performed with an excess of detergent to ensure complete recovery of the over-expressed membrane protein(s). From a quantitative point of view this is valid. However, from a qualitative point of view there is no need for excess detergent. On the contrary, when working with low cmc detergents it is even desirable to use the minimal amount of detergent in view of an efficient detergent removal (2). During membrane protein reconstitution the lipid headgroups should come in contact with the polar protein surface. However, if the detergent monolayer around the protein is too large and the polar residues are concealed, the bilayer recognition may be hindered (4). Similarly, in x-ray crystallography the size of the detergent collar is of fundamental importance too, since an oversized micelle is obstructive to the formation of crystal contacts because of steric hindrance (32).

Over the last decades DDM has proven to be a good choice as a solubilizer for a wide range of membrane proteins, since it is relatively mild to the

protein, keeping its native tertiary structure intact. It is therefore frequently used in 3D crystallography. However, with its large micellar size DDM tends to concentrate during protein concentration procedures. Moreover, its low cmc makes DDM unsuitable for dialysis-driven 2D crystallization. Nevertheless, we believe that by learning the subtleties in how this detergent behaves and how to adjust the size of the protecting belt around the protein, DDM and other low cmc detergents can well be used for 2D membrane protein crystallization.

3.6 Conclusion

The speed and ease of use of the presented detergent concentration determination procedure are unique. The mean standard deviation for three contact angle measurements of 1.3° for a large set of detergents (see Figure 3.4) and the additional comparison of the calibrated DDM curve with radiolabeled DDM underline the reproducibility and accuracy of the measurements. The universality of surface tension reduction by surfactants makes this method suitable for all types of detergents and the robustness of the procedure with respect to interfering substances even allows for their concentration to be determined in tertiary mixtures.

3.7 Acknowledgements

We are grateful to P.L.T.M. Frederix and T. Braun for helping us with the camera layout and the iris diaphragm calculation. We are indebted to J.L. Rigaud for kindly providing us with radioactive DDM and to M. Chami for fruitful discussions on the results obtained with GalP. We would like to thank S. Bürgi for the calibration of OTAB, M. Duckely for the calibration of FOSCh12 and G. Martin for helping with the liquid scintillation counter. Last but not least we are thankful to H. Heerklotz for reading and discussing the manuscript.

This work was supported by the Swiss National Center for Competence in Research in Nanoscale Sciences and the Swiss National Center for Competence in Research in Structural Biology and the M.E. Müller Foundation.

3.8 References

1. Moller, J.V., and M. le Maire. 1993. Detergent binding as a measure of hydrophobic surface area of integral membrane proteins. *J Biol Chem* 268(25):18659-18672.
2. Remigy, H.W., D. Caujolle-Bert, K. Suda, A. Schenk, M. Chami, and A. Engel. 2003. Membrane protein reconstitution and crystallization by controlled dilution. *FEBS Lett* 555(1):160-169.
3. Dolder, M., A. Engel, and M. Zulauf. 1996. The micelle to vesicle transition of lipids and detergents in the presence of a membrane protein: towards a rationale for 2D crystallization. *FEBS Lett* 382(1-2):203-208.
4. Jap, B.K., M. Zulauf, T. Scheybani, A. Hefti, W. Baumeister, U. Aebi, and A. Engel. 1992. 2D crystallization: from art to science. *Ultramicroscopy* 46(1-4):45-84.
5. Caffrey, M. 2003. Membrane protein crystallization. *J Struct Biol* 142(1):108-132.
6. Ai, X., and M. Caffrey. 2000. Membrane protein crystallization in lipidic mesophases: detergent effects. *Biophys J* 79(1):394-405.
7. Le Maire, M., S. Kwee, J.P. Andersen, and J.V. Moller. 1983. Mode of interaction of polyoxyethyleneglycol detergents with membrane proteins. *Eur J Biochem* 129(3):525-532.
8. daCosta, C.J., and J.E. Baenziger. 2003. A rapid method for assessing lipid:protein and detergent:protein ratios in membrane-protein crystallization. *Acta Crystallogr D Biol Crystallogr* 59(Pt 1):77-83.
9. Eriks, L.R., J.A. Mayor, and R.S. Kaplan. 2003. A strategy for identification and quantification of detergents frequently used in the purification of membrane proteins. *Anal Biochem* 323(2):234-241.
10. Reynolds, J.A., and C. Tanford. 1976. Determination of molecular weight of the protein moiety in protein-detergent complexes without direct knowledge of detergent binding. *Proc Natl Acad Sci U S A* 73(12):4467-4470.
11. Noy, D., J.R. Calhoun, and J.D. Lear. 2003. Direct analysis of protein sedimentation equilibrium in detergent solutions without density matching. *Anal Biochem* 320(2):185-192.
12. Dubois, M., K. Gilles, J.K. Hamilton, P.A. Rebers, and F. Smith. 1951. A colorimetric method for the determination of sugars. *Nature* 168(4265):167.
13. Lau, F.W., and J.U. Bowie. 1997. A method for assessing the stability of a membrane protein. *Biochemistry* 36(19):5884-5892.
14. Ringler, P., B. Heymann, and A. Engel. 2000. Two-dimensional crystallization of membrane proteins. In *Membrane Transport*. S.A. Baldwin, editor. Oxford University Press, New York. 229-268.

15. Neumann, A.W., R.J. Good, C.J. Hope, and M. Sejjal. 1974. An equation-of-state approach to determine surface tensions of low-energy solids from contact angles. *Journal of Colloid and Interface Science* 49(2):291-304.
16. Kwok, D.Y., and A.W. Neumann. 2000. Contact Angle Interpretation in Terms of Solid Surface Tension. *Colloids and Surfaces A: Physicochemical and Engineering Aspects* 161:31-48.
17. Li, D., and A.W. Neumann. 1992. Contact angles on hydrophobic solid surfaces and their interpretation. *Journal of Colloid and Interface Science* 148(1):190-200.
18. Surface tension values of some common test liquids for surface energy analysis. 2004. <http://www.surface-tension.de>
19. Dutschk, V., K.G. Sabbatovskiy, M. Stolz, K. Grundke, and V.M. Rudoy. 2003. Unusual wetting dynamics of aqueous surfactant solutions on polymer surfaces. *J Colloid Interface Sci* 267(2):456-462.
20. Myers, D. 1991. *Surfaces, Interfaces, and Colloids: Principles and Applications*. VCH Publishers, New York.
21. Janczuk, B., T. Bialopiotrowicz, and A. Zdzienicka. 1999. Some Remarks on the Components of the Liquid Surface Free Energy. *J Colloid Interface Sci* 211(1):96-103.
22. Ikeda, S., M.A. Tsunoda, and H. Maeda. 1978. The application of the gibbs adsorption isotherm to aqueous solutions of a nonionic-cationic surfactant. *J Colloid Interface Sci* 67(2):336-348.
23. Ikeda, S., M.A. Tsunoda, and H. Maeda. 1979. The effects of ionization on micelle size of dimethyldodecylamine oxide. *J Colloid Interface Sci* 70(3):448-455.
24. Schick, M.J. 1962. Surface films of nonionic detergents - I. Surface tension study. *J Colloid Sci* 17(9):801-813.
25. Walter, A., G. Kuehl, K. Barnes, and G. Vander-Waerdt. 2000. The vesicle-to-micelle transition of phosphatidylcholine vesicles induced by nonionic detergents: effects of sodium chloride, sucrose and urea. *Biochim Biophys Acta* 1508(1-2):20-33.
26. Koning, R.I. 2003. *Cryo-electron crystallography - from protein reconstitution to object reconstruction*. University of Groningen, Groningen.
27. von Bahr, M., F. Tiberg, and B.V. Zhmud. 1999. Spreading dynamics of surfactant solutions. *Langmuir* 15(20):7069-7075.
28. Starov, V.M., S.R. Kosvintsev, and M.G. Velarde. 2000. Spreading of surfactant solutions over hydrophobic substrates. *Journal of Colloid and Interface Science* 227:185-190.
29. Stoebe, T., R.M. Hill, M.D. Ward, and H.T. Davis. 1997. Enhanced spreading of aqueous films containing ionic surfactants on solid substrates. *Langmuir* 13(26):7276-7281.
30. Stoebe, T., Z. Lin, R.M. Hill, M.D. Ward, and H.T. Davis. 1997. Enhanced spreading of aqueous films containing ethoxylated alcohol surfactants on solid substrates. *Langmuir* 13(26):7270-7275.
31. von Bahr, M., F. Tiberg, and V. Yaminski. 2001. Spreading dynamics of liquids and surfactant solutions on partially wettable hydrophobic substrates. *Colloids and Surfaces A: Physicochemical and Engineering Aspects* 193:85-96.
32. Marone, P.A., P. Thiagarajan, A.M. Wagner, and D.M. Tiede. 1999. Effect of detergent alkyl chain length on crystallization of a detergent-solubilized membrane protein: correlation of protein-detergent particle size and particle-particle interaction with crystallization of the photosynthetic reaction center from *Rhodobacter sphaeroides*. *Journal of Crystal Growth* 207:214-225.
33. Bhairi, S.M. 2001. *A guide to the properties and uses of detergents in biological systems*. Calbiochem-Novabiochem Corporation.
34. Zulauf, M., and H. Michel. 1990. Properties of commonly used nonionic and zwitterionic detergents for membrane protein solubilization and crystallization. In *Crystallization of membrane proteins*. H. Michel, editor. CRC Press, Boca Raton. 209-211.
35. le Maire, M., P. Champeil, and J.V. Moller. 2000. Interaction of membrane proteins and lipids with solubilizing detergents. *Biochim Biophys Acta* 1508(1-2):86-111.
36. Jang, J., J.H. Oh, and X.L. Li. 2004. A novel synthesis of nanocapsules using identical polymer core/shell nanospheres. *J Mater Chem* 14:2872-2880.
37. Ruso, J.M., and F. Sarmiento. 2000. The interaction between n-alkyl trimethylammonium bromides with poly(L-aspartate): a thermodynamics study. *Colloid Polym Sci* 278:800-804.

Chapter 4

The Use of Detergents in Membrane Biochemistry

4.1 Abstract

Detergents serve as tools to solubilize, isolate and manipulate membrane proteins for subsequent biochemical and physical characterization. The choice of detergent and experimental conditions will have an enormous impact on whether or not a technique (e.g. solubilization, purification, concentrating) can be successfully applied to a specific membrane protein. An understanding of detergent behavior and of the structure of micelles and protein-detergent complexes (PDC's) is thus a prerequisite for membrane biochemistry. In this chapter the influence of different detergents on the galactose/proton symporter (GalP) of *E. coli* is examined. In addition, the use of octyl- β ,D-glucoside (OG), octyl- β ,D-thiogluconide (OTG), undecyl- β ,D-maltoside (UDM) and dodecyl- β ,D-maltoside (DDM) for the solubilization of *E. coli* lipids is described.

4.2 Introduction

Integral membrane proteins, by definition, are embedded in biological membranes *in vivo*. The non-polar interior of a fluid bilayer, approximately 30 Å thick (Wiener and White, 1992), shields the hydrophobic membrane-spanning portions of the protein. Thus, the ideal medium for working with membrane proteins is the lipid bilayer. Unfortunately, current technology for protein purification necessitates extraction from the membrane into detergent micelles. To preserve the integrity of a membrane protein, the best we can do is to provide an environment similar to the bilayer. The bilayer, however, is very complex, with large variations in lateral pressure, polarity and charge throughout (White and Wimley, 1999; Curran et al., 1999; Gruner, 1985; White and Wimley, 1998), and is essentially impossible to mimic very well. Consequently, detergent extraction is likely to be, at best, mildly destabilizing.

The aggregation properties of detergents are described in terms of the hydrophobic effect (Tanford, 1980), an entropy-driven process. In the presence of membrane proteins, three states of the detergent

are in equilibrium: detergent monomers, protein-free detergent micelles, and detergent bound to the protein. The detergent bound to the protein is micelle-like in that it is a hydrophobic effect-driven aggregation of detergent molecules that sequester the nonpolar portions of the detergent and the protein away from aqueous solvent. However, the actual form of this detergent torus may not be micellar; evidence suggests that it may be more like a monolayer of detergent wrapped around the protein (Moller and le Maire, 1993). This protein-detergent complex (PDC) is the entity that is crystallized either by adding additional lipids (2D crystallization) or by precipitation (3D crystallization).

For a solution of detergent at a total concentration D_{tot} , the detergent will exist in an equilibrium between monomers (mon) and micelles (mic) so that

$$D_{tot} = D_{mon} + D_{mic} \quad (4.1)$$

Above the cmc, the concentration of monomers is approximately equal to the cmc (Zulauf, 1991). Then

$$D_{tot} \approx cmc + D_{mic} \quad (4.2)$$

The number of detergent molecules in a micelle is given by its aggregation number N_{agg} (typically 50-100), so that the actual concentration of micelles is D_{mic}/N_{agg} . For a purified membrane protein, the ratio of micelles to membrane protein molecules should be fairly small, as low as 1.5-2 (Helenius et al., 1979). If there is too much detergent, there will be too many free micelles along with detergent monomers and PDC's. Excess detergent can be denaturing and/or leads to complications during detergent removal by dialysis.

Some simple calculations illustrate the general trend. Lets consider a 50kDa membrane protein at a concentration of 10 mg/ml (0.2mM). A 1.5-fold excess of micelles to protein would require a micelle concentration of 0.3mM. A typical high-cmc detergent used in membrane protein crystallization is OG ($N_{agg} \approx 80$, $cmc \approx 18mM$). For this detergent, $D_{mic} \approx (0.3mM)(80) = 24mM$; therefore, $D_{tot} = 42mM$ (2.3 times the cmc of OG). A typical low-cmc detergent used in membrane protein crystallization is DDM ($N_{agg} \approx 85$, $cmc \approx 0.17mM$). For this detergent, $D_{mic} \approx (0.3mM)(85) = 25.5mM$; therefore, $D_{tot} = 25.7mM$ (151 times the cmc of DDM). Admittedly, these crude calculations tend to overestimate the amount of detergent required. However, they provide some indication of the observed trend that low-cmc detergents are required at a higher concentration (in terms of their cmc) than are high-cmc detergents. OG can be used at a typical concentration of 25-35mM; DDM can be used at a concentration of 1-10mM (or even higher). In fact, when solubilizing a native membrane, not only the protein but also the lipid need to be considered.

Lipid solubilization can be described in a general way by a 'three-stage model' (Lichtenberg et al., 1983; Lichtenberg, 1985; Rigaud et al., 1995). When at constant lipid concentration the detergent concentration is increased, three stages can be distinguished. In stage I both the monomeric detergent concentration in the aqueous phase and the partial detergent concentration in the liposomal phase increase, up to the point where detergent micelles start to form. At this detergent/lipid ratio, called R_{sat} , all liposomes are saturated with detergent. Upon further addition of detergent the saturated liposomes enter stage II and gradually solubilize into mixed lipid-detergent micelles until the solution contains only mixed micelles. This point is

called R_{sol} and marks the start of stage III, in which the free detergent is in equilibrium with the detergent in the mixed micelles. The detergent concentrations at which both R_{sat} and R_{sol} appear are linearly dependent on the lipid concentration (Rigaud et al., 1988).

Here we explore different detergents with respect to their ability to stabilize GalP, as well as solubilize different lipids.

4.3 Results

4.3.1 The stability of the galactose/proton symporter GalP from Escherichia coli in different detergents

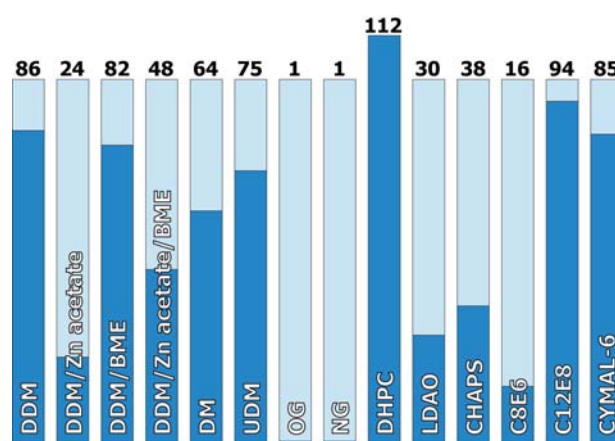


Figure 4.1: **Detergent check with GalP.** The percentage of GalP in the supernatant after 6 days at 4°C is indicated above the bars.

After purifying GalP in DDM the protein was aliquoted into 14 samples, each of which was mixed with different detergents and/or additives. In order to determine the long term stability the aliquots were left at 4°C for six days. After centrifugation of the samples the protein concentration of the supernatants, i.e., the soluble fraction was determined. Fig. 4.1 shows the percentage of GalP still remaining in the supernatant. Clearly the alkyl glucosides (OG/NG) failed in keeping the protein in a stably in solution. The alkyl maltoside series (DM/UDM/DDM) follows the alkyl chain length with respect to stabilization (64%/75%/86%). In general detergents with shorter hydrophobic moieties tend to be less successful in keeping the protein stable. The addition of β -mercaptoethanol (BME) to protect any cysteine residues present in the sequence did not show any effect on protein

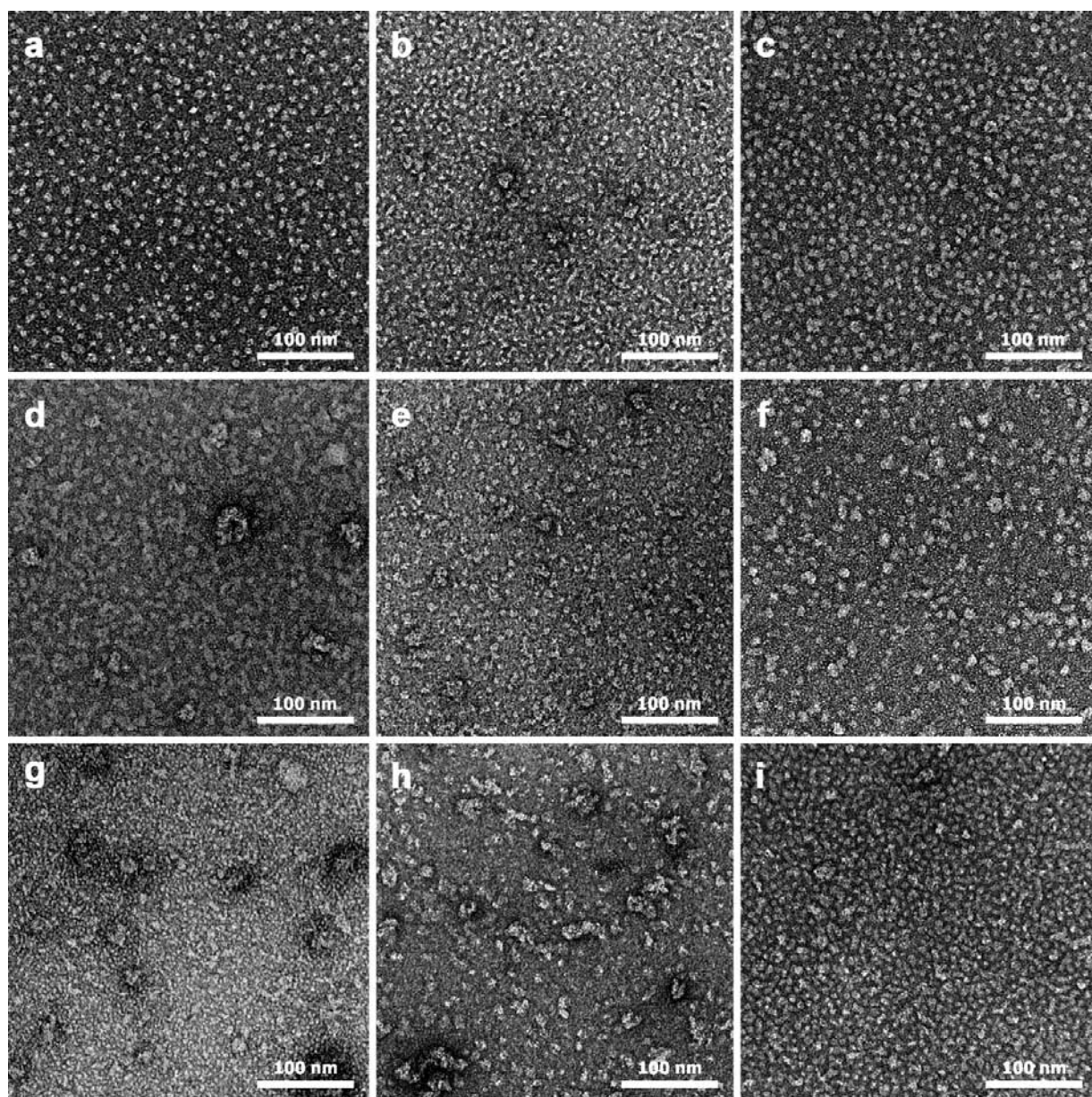


Figure 4.2: **Single particles of GalP in different detergents.** (a) DDM, (b) DM, (c) UDM, (d) DHPC, (e) LDAO, (f) CHAPS, (g) C8E6, (h) C12E8, (i) CYMAL-6. After 6 days at 4°C samples were centrifuged at 100'00 g. Samples were taken from the supernatants and negatively stained. The detergent concentration was kept over the respective cmc.

stability. It is noteworthy however, that BME was able to reduce part of the zinc from zinc acetate ($\text{Zn}^{2+} \rightarrow \text{Zn}$), thereby protecting GalP from the negative effects of zinc acetate. In fact, as the two were added at the same concentration (2mM) and an oxidized zinc ion needs two electrons in order to be reduced, only half of the zinc was reduced, compatible with the observed effect of BME. CYMAL-6 and C12E8 were as efficient as DDM to maintain the protein's solubility. DHPC representing a very short-chained lipid (acting like a detergent due to its highly curvophilic nature) seemed

to be the best choice. However, the fact that there should be 112% of the original protein concentration present in the supernatant lead to the suspicion that there may be an interference of DHPC with the protein assay. In order to clarify this question negatively stained single particles of the samples were visualized by electron microscopy (see Fig. 4.2). DHPC clearly exhibits non-homogenous dispersion (Fig. 4.2d). This is also true for C12E8 (Fig. 4.2h) which –with respect to the gel– seemed just as suitable as DDM for the solubilization of GalP. When evaluating the single particles, then

only UDM and perhaps CYMAL-6 can measure up to DDM. All other preparations showed clear heterogeneity. This underlines the importance of visually controlling the state of a protein preparation by electron microscopy. One could be misled by simple concentration determination, since the aggregates formed in solution might be too small to be pelleted during centrifugation.

4.3.2 Controlling the amount of detergent bound to GalP

As one uses excess detergent to solubilize biological membranes in order to completely recover the protein present in the membranes, it is very likely that the protein is saturated with detergent molecules. However, this might represent an additional stress on the protein besides the poor substitution of the bilayer environment by detergents. The use of excess detergent can also lead to protein aggregation via a delipidation of the protein, thereby stripping off native lipids necessary for the protein to be stable (le Maire et al., 2000).

To determine the amount of DDM bound to GalP after purification the detergent measuring device described in Chapter 3 was used (Kaufmann et al., 2006). Moreover this amount was adjusted during purification to examine whether differently saturated species exist. Here, the experiment already presented in Chapter 3 (Figure 3.7) is further detailed and discussed.

First, membranes of an *E. coli* overproducing GalP were solubilized in DDM and the recombinant His-tagged protein was bound to the column material. Then, eight separate columns were loaded with equal amounts of column material and washed with differently concentrated detergent solutions. After subsequent elution the detergent concentrations as well as the protein concentrations of each elution were assessed. Fig. 4.3 shows the SDS-Page run after elution of the eight columns. In each slot $10\mu\text{l}$ of the eluted sample were loaded. Fig. 4.4 displays the protein yield after elution and the amount of DDM bound per GalP monomer. The protein yield decreases as the concentration in the wash falls below the cmc of DDM. In contrast, the amount of DDM bound to GalP is being decreased already before the cmc is reached (D_{free}) suggesting that detergent molecules are ripped off the protein at a higher concentration without affecting its solubility. It is only after the solubility limit (P_{sol}) is reached that the protein starts to aggregate on the column.

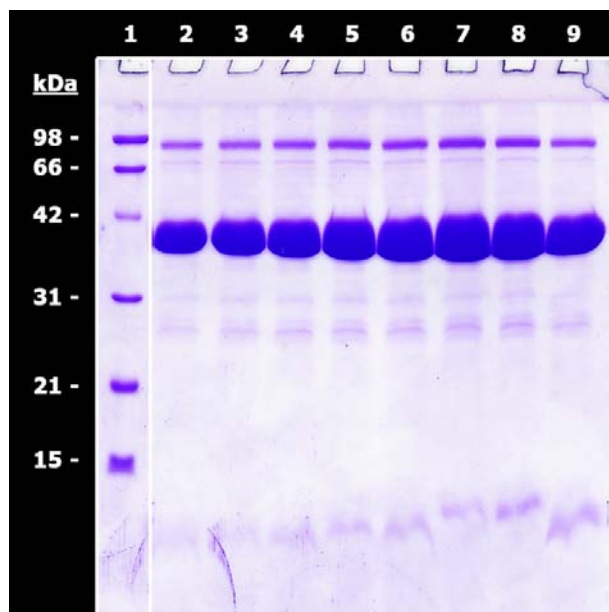


Figure 4.3: **SDS-Page of GalP.** Lanes 2-9 correspond to 0.001 / 0.003 / 0.005 / 0.006 / 0.008 / 0.011 / 0.022 / 0.043% (w/v) DDM in the wash buffer and the elution buffer respectively (see section 4.4.3). Cmc of DDM = 0.0087% (w/v).

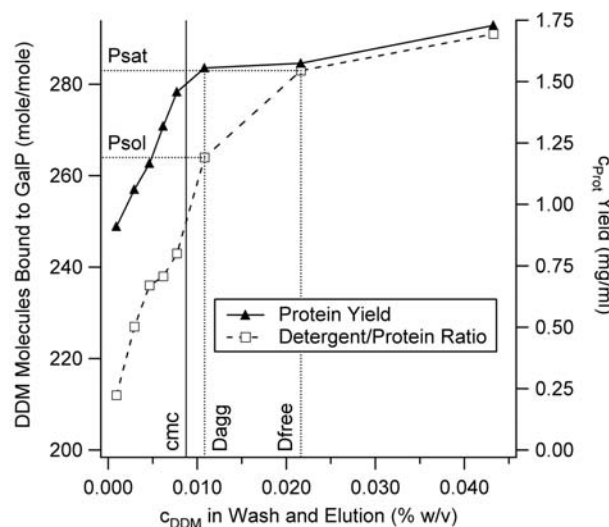


Figure 4.4: **Detergent bound to GalP and protein yield after purification.** The points correspond to the eluted fractions from Fig. 4.3.

The gel in Fig. 4.3 is somewhat misleading from lanes 7 to 9 as the protein concentration seems lower in the lanes 8 and 9 compared to lane 7. However, when weighing the column material after elution it became apparent that the last two columns were less loaded. When the protein yield was corrected for the amount of column material present and for the volume of the elutions, the re-

sults are consistent with the expected outcome of the experiment (see Fig. 4.4). The detergent-to-protein ratio is independent of the volumes of column material and elution buffer present. Of course the amount of sub-cmc wash buffer that is used affects the outcome of such an experiment. Therefore, the volume of the washing step should be fixed with respect to the volume of the column material (e.g., 100 × column volume in this case).

4.3.3 Solubilization of *E. coli* lipids with different detergents

In these experiments the amount of detergent needed to solubilize *E. coli* polar lipid extract was examined. Four detergents were tested for their solubilizing capacity, namely, OG, OTG, UDM and DDM. The first two were chosen because of their high cmc and their known ability to promote the formation of large vesicles upon detergent removal. The latter two were chosen because in section 4.3.1 they had proven to be fairly mild to GalP in keeping it in a monodisperse state over 6 days at 4°C.

In order to perform these solubilization measurements, small unilamellar vesicles (SUV's) of *E. coli* polar lipid extract were produced by sonication. These were subsequently injected into cuvettes using motor-driven syringes controlled by solenoids allowing precise addition of small amounts of the vesicle solution (Remigy et al., 2003). Simultaneous recording of the turbidity of the solution enabled the observation of the end of solubilization and in some cases the onset of solubilization (see Figs. 4.5 and 4.6).

Injection of vesicles into detergent rather than detergent into vesicles was chosen for kinetic reasons: DDM is known to preferentially bind to the outer leaflet of sonicated vesicles (Heerklotz and Seelig, 2000) and to show limited translocation across the membrane, thereby imposing a kinetic limit to the solubilization process. This can be overcome by assuring that the initial detergent concentration in the cuvette is much higher than the amount of detergent needed for solubilization. That way the detergent will initially completely disrupt the added vesicles and mixed lipid-detergent micelles are formed. As the lipid content increases, micelles will be found in coexistence with membranes, and finally, at a sufficiently high lipid concentration, micellar structures will cease to exist and only the vesicular phase remains.

A distinctive feature in Fig. 4.5 is the absence of

larger structures for OG and OTG at the beginning of the solubilization of SUV's by excess detergent. This suggests that injected vesicles are rapidly dissolved by these detergents to form small mixed lipid-detergent micelles, although wormlike micelles have been reported for egg phosphatidylcholine and OG mixtures (Vinson et al., 1989). In contrast to this the solubilization by UDM and DDM exhibit an immediate increase in the size of present structures. In order to clarify this situation cryoelectron microscopic analysis was performed on the solubilization series with DDM (Fig. 4.7). The samples examined are indicated in Panels (d) of Figs. 4.5 and 4.6. The visual inspection of Sample 4 revealed that long thread-like micelles are present along with small spherical micelles at the beginning of the experiment (Fig. 4.7 (d) and (e)) accounting for the rapid increase in turbidity. The curve in Fig. 4.5 (d) tends towards a first plateau after which the addition of more vesicles results in a second steep increase of the turbidity. During this increase mixed lipid-detergent micelles coexist with detergent containing bilayers. When the curve reaches a second plateau only vesicles (exhibiting a detergent-to-lipid ratio below R_{sat}) are observed under the microscope. It is noteworthy to point out the difference in vesicular size at the end of the experiment compared to the starting material (see scale bars in Panels (a) and (b) of Fig. 4.7). This attests to the detergent-induced vesicle size growth as described by Lichtenberg *et al.* (Lichtenberg et al., 2000). Additionally, even larger vesicular structures can be observed in the coexistence range (Panel (c) of Fig. 4.7) together with very small vesicles enclosed in the large ones. These have already been observed by others (Ueno et al., 1997) and might be formed via partial solubilization of the large vesicles followed by revesiculation of part of the resultant mixed micelles (Lichtenberg et al., 2000).

An intriguing feature of Fig. 4.6 is the fact that the extrapolated lines don't cross the y-axis at the cmc of the respective detergent (see for e.g. Remigy et al., 2003). However, slight variations in the intercept are not uncommon and usually the shift occurs towards a lower concentration. Several factors may play a role in this context:

First, the vesicles in this study are a mixture of different lipids. Preferential solubilization of different membrane components might influence the outcome of the experiment.

Secondly, in other published studies (Majhi and

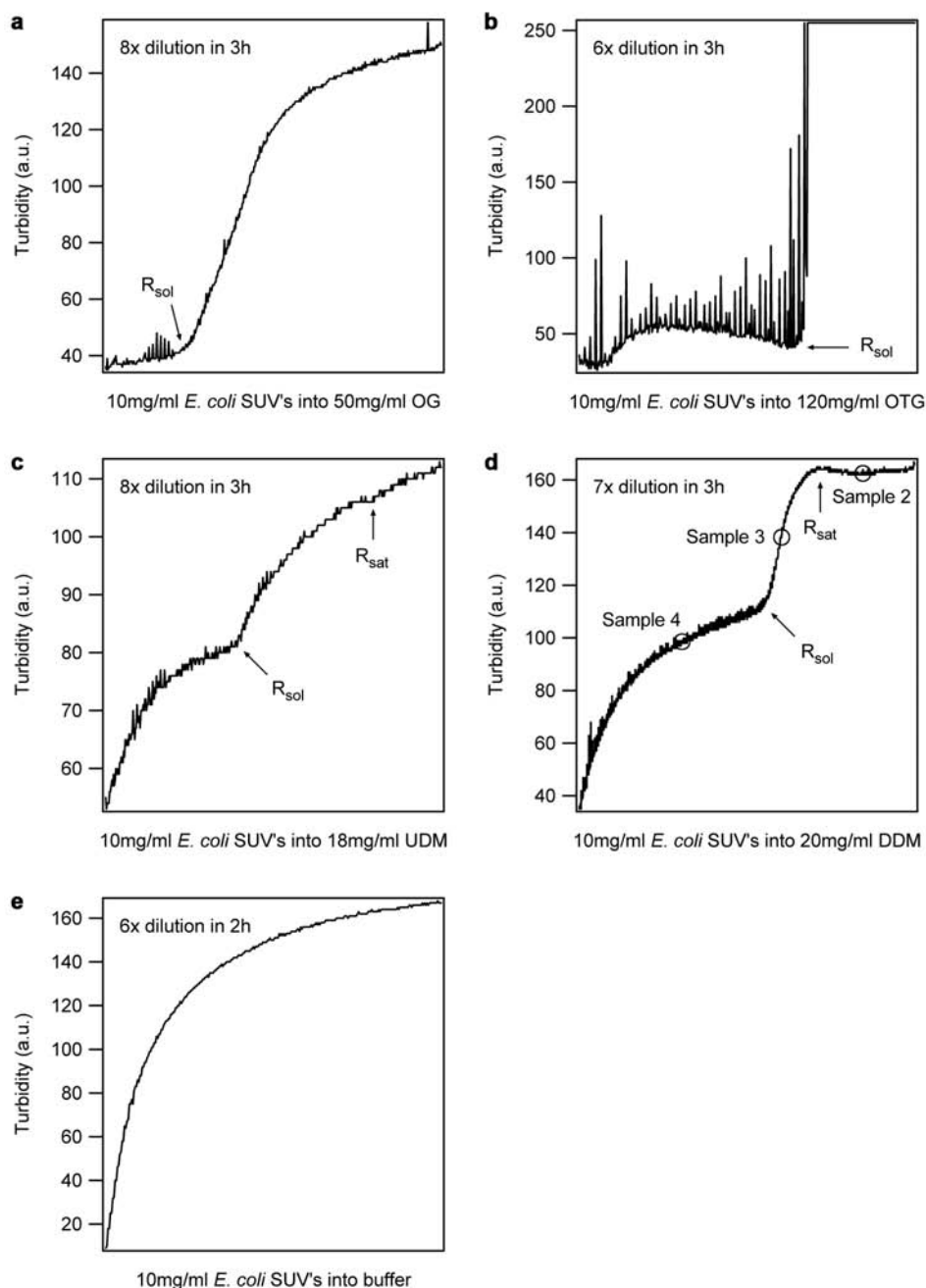


Figure 4.5: **Solubilization experiments with *E. coli* Polar extract and different detergents.** Representative saturation curves are shown displaying the course of a solubilization experiment as observed by turbidimetry. R_{sol} and R_{sat} are indicated where possible. (a) - (d) Addition of 10mg/ml small unilamellar vesicles (SUV's) of *E. coli* polar lipids to 50mg/ml OG, 120mg/ml OTG, 18mg/ml UDM and 20mg/ml DDM respectively. In panel (d) the samples taken for cryoelectron microscopic analysis (see Fig. 4.7) are indicated. (e) Control experiment, where 10mg/ml SUV's were added to detergent-free buffer.

Blume, 2002; Meister and Blume, 2004) similar behavior has been shown where the intercept is much lower than the cmc of the corresponding detergent even for charged DMPG and even for pure DMPC vesicles. This would simply mean that the detergent readily partitions into the bilayer phase already at very low sub-cmc concentrations and con-

sequently less free detergent is present in solution.

Thirdly, the precision of these measurements is somewhat limited, due to the precision of simple turbidimetry, and due to the number of points for each curve.

However, the purpose of this study was to find the minimal concentration for solubilization of *E.*

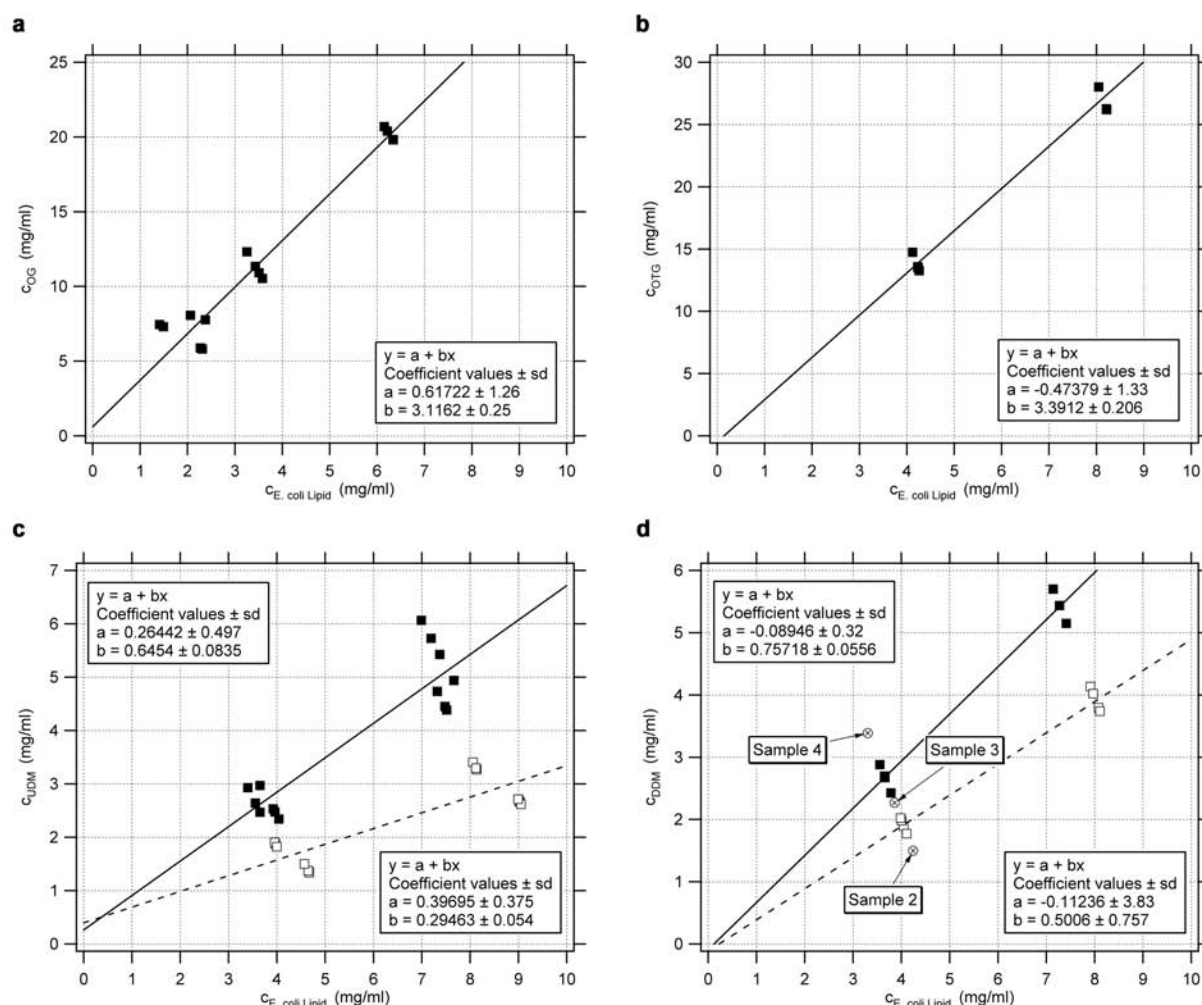


Figure 4.6: **Extrapolated solubilization plots** for (a) OG, (b) OTG, (c) UDM and (d) DDM. Solid lines depict the detergent concentration required for complete lipid solubilization R_{sol} , broken lines represent the detergent concentration at the onset of solubilization R_{sat} , both as a function of lipid concentration. In part these plots represent a phase diagram, however for OG and OTG it was not possible to determine R_{sat} based on the observed curves in Fig. 4.5. In (d) samples taken for cryoelectron microscopy (Fig. 4.7) are indicated: Sample 2 corresponds to Panel (b), Sample 3 to Panel (c) and Sample 4 to Panels (d) and (e) in Fig. 4.7.

coli polar lipid extract with different detergents. This goal has been achieved.

4.4 Materials and Methods

4.4.1 Detergents

The detergents used in this study were octyl- β ,D-glucoside (OG), nonyl- β ,D-glucoside (NG), octyl- β ,D-thiogluconate (OTG), decyl- β ,D-maltoside (DM), undecyl- β ,D-maltoside (UDM), dodecyl- β ,D-maltoside (DDM), CYMAL-6, dodecyl-N,N-dimethylamine-N-oxide (LDAO), hexaethylene glycol mono-octyl ether (C8E6), octaethylene glycol monododecyl ether (C12E8),

which all were purchased from Anatrache (Ohio, USA), 3[(3-Cholamidopropyl) dimethyl-ammonio] propanesulfonic acid (CHAPS) from Dojindo Molecular Technology (Maryland, USA) and diheptanoyl phosphatidylcholine (DHPC) from Avanti Polar Lipids (Alabama, USA). All detergents were of high purity grade ($\geq 98\%$) and were used without further purification. Aqueous solutions of these detergents were prepared with reagent-grade water produced by a Milli-Q filtration system ($\geq 18 \text{ M}\Omega$).

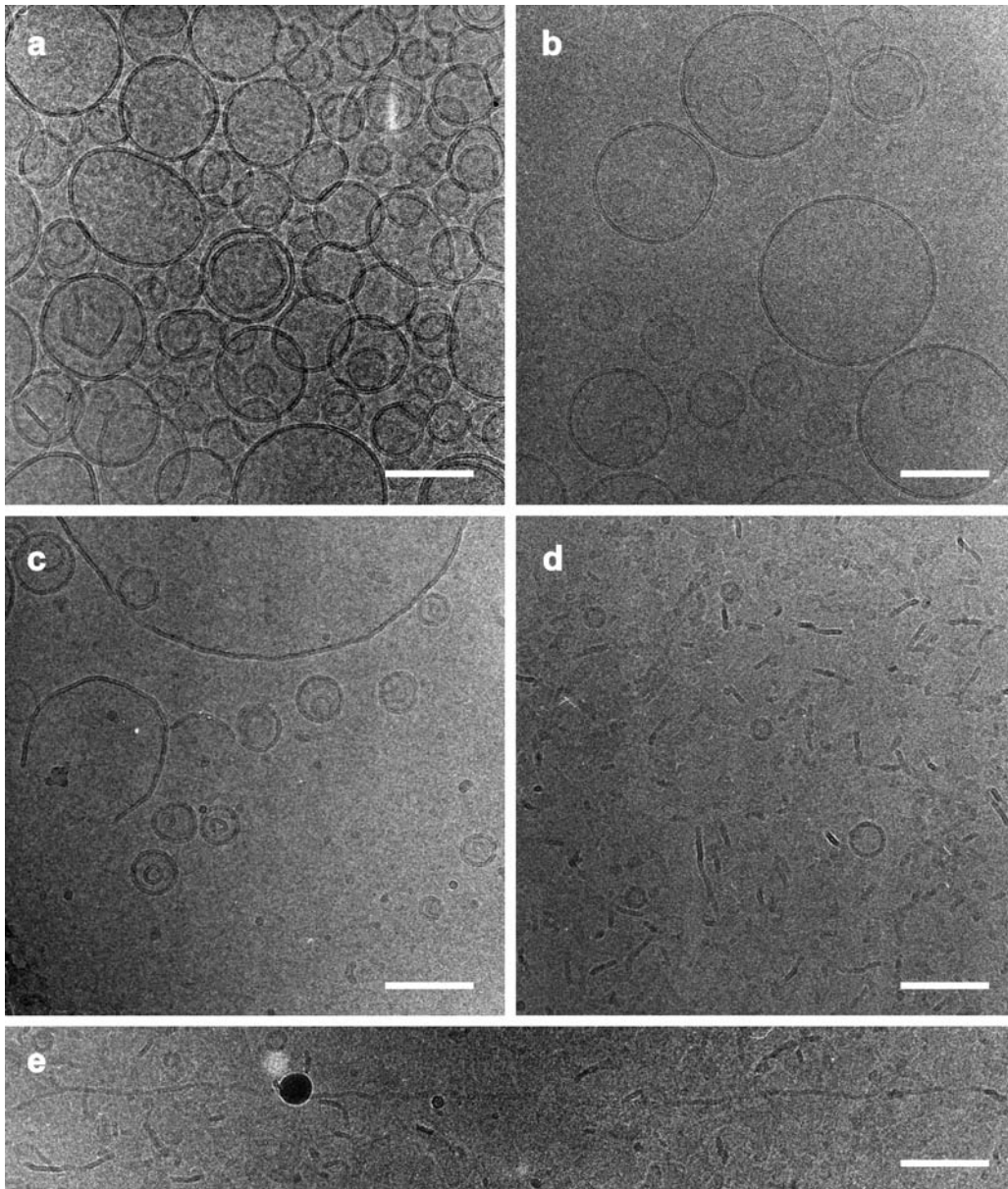


Figure 4.7: **Cryoelectron microscopic images of E.coli lipid solubilization by DDM.** (a) Starting material: Small unilamellar vesicles (SUV's). (b) Vesicles increase in size due to detergent mediated fusion (Sample 2 Figs. 4.5 and 4.6). (c) Coexistence of vesicles with incorporated DDM, open bilayer structures (top left) and micelles (small structures in bottom half) (Sample 3 Figs. 4.5 and 4.6). (d) and (e) Solubilized material with spherical micelles (d) and long thread-like micelles (d) and (e) (Sample 4 Figs. 4.5 and 4.6). Scale bars represent 100 nm.

4.4.2 The stability of the galactose/proton symporter GalP from *Escherichia coli* in different detergents

0.3 ml membranes from *E. coli* strain JM1100 (pPER3) overexpressing GalP (kindly provided by P.J.F. Henderson) were resuspended in 2.7 ml solubilization buffer (20 mM Tris pH 8.0, 300 mM NaCl, 20% (v/v) glycerol, 20 mM imidazole). Solubilization was achieved at 4°C within 1 hour af-

ter addition of 1% (w/v) DDM as powder. The solubilization mixture was centrifuged at 4°C and 150'000 g to remove all unsolubilized material. 2 ml Ni-NTA agarose slurry were pre-equilibrated using wash buffer (20 mM Tris pH 8.0, 10% (v/v) glycerol, 20 mM imidazole, 0.05% (w/v) DDM) and then incubated for 2 hours at 4°C with the solubilized membranes.

Column washes have been carried out in 15 ml Falcon tubes by adding ~ 15 ml of wash buffer and

subsequent centrifugation for 1 minute at 1'000 rpm and 4°C. This was repeated 10 times. Finally, the material was loaded on a spin column and 1 ml elution buffer (200 mM Imidazole pH 8.0, 20% (v/v) glycerol, 0.05% (w/v) DDM) was added. After an incubation of 45 minutes at 4°C the protein was eluted by centrifugation at 3'000 rpm for 2 minutes. Protein concentrations were determined using the protocol of Schaffner and Weissman (Schaffner and Weissman, 1973). The eluted protein was mixed 1:1 with detergent solutions containing different detergents to reach final detergent concentrations of 3.75% OG, 2% NG, 0.75% DM, 0.5% UDM, 5% DDM, 0.3% CYMAL-6, 0.2% LDAO, 3% C8E6, 0.1% C12E8, 2.5% CHAPS and 0.5% DHPC respectively. These mixtures were incubated for 6 days at 4°C. Protein stability was assessed after centrifugation at 100'000 g and 4°C by measuring the protein concentration in the supernatant. Single particle images were taken using a Hitachi H-8000 electron microscope after negative staining of diluted samples. The samples have been diluted prior to adsorption on the grid keeping the detergent concentration above the respective cmc.

4.4.3 Controlling the amount of detergent bound to GalP

1.5 ml membranes from *E. coli* strain JM1100 (pPER3) overexpressing GalP (kindly provided by P.J.F. Henderson) were resuspended in 13.5 ml solubilization buffer (20 mM Tris pH 8.0, 300 mM NaCl, 20% (v/v) glycerol, 20 mM imidazole). Solubilization was achieved at 4°C within 2 hours after addition of 1% (w/v) DDM as powder. The solubilization mixture was centrifuged at 4°C and 150'000 g to remove all unsolubilized material. 3.2 ml Ni-NTA agarose slurry were pre-equilibrated using wash buffer without detergent (20 mM Tris pH 8.0, 20 mM imidazole) and then incubated overnight at 4°C with the solubilized membranes. The column binding mixture was partitioned between 8 columns, which were washed with 20ml (100 times column volume) wash buffer containing different concentrations of DDM (0.001 / 0.003 / 0.005 / 0.006 / 0.008 / 0.011 / 0.022 / 0.043% (w/v)). The quasi totality of the wash buffers was removed by suction. As a control, the same experiment was performed without protein, ruling out the possibility of detergent retention/accumulation by the column material (data not shown). Elution was achieved by immediate incubation with 250 μ l of elution buffer

(200 mM imidazole pH 8.0 containing different concentrations of DDM (see washes)) for 1 hour and subsequent centrifugation at 4°C. The weight of the column resin and the volumes of elution buffer added and recovered were determined and taken into account in the calculations for the protein yield. Protein concentrations were determined using the Bio-Rad protein assay from Bio-Rad Laboratories (California, USA), correcting for the presence of DDM after calibration of the assay with BSA/DDM mixtures of different concentrations. The amount of DDM bound to GalP was determined by calculating the difference between the DDM concentration in the loaded elution buffers and the DDM concentration in the eluted samples. This was possible assuming that total detergent concentrations are measured. Additionally it was assumed that the same monomeric and micellar detergent concentrations were present in the eluted samples as in the corresponding elution buffers and therefore the differences in detergent concentrations were due to detergent brought along by the protein. For the measurements the eluted samples had to be diluted typically between 50 and 100 times to release the detergent from the protein, which precipitated out of solution.

4.4.4 Solubilization of *E. coli* lipids with different detergents

E. coli Polar lipid extract was purchased from Avanti Polar Lipids (Alabama, USA). The chloroform of the lipid solution was evaporated under argon and desiccated overnight in a vacuum desiccator. The dried lipids were then rehydrated with buffer (20mM Tris pH 7.5, 100mM NaCl, 0.01% (w/v) NaN₃) to reach a final concentration of 5 mg/ml and 10 mg/ml. Small unilamellar vesicles (SUV's) were produced by sonication of the liposome solution on ice with a Branson Sonifier 250 tip for 3 minutes at 30% of the maximum output power, followed by 2 minutes at 40% output power and finally for 1 minute at 50% output power. Lipid solubilization curves were recorded using a home built dilution machine with an integrated system for turbidimetry (Remigy et al., 2003). Experiments were made at room temperature and lasted for 3 hours. During the experiments a constant mixing was applied (about 300 rpm). Depending on detergent solubilization capabilities, final dilutions of 6x (OTG), 7x (UDM/DDM) and 8x (OG) were performed. Dilution series with different de-

tergent concentrations (30 and 50 mg/ml for OG; 60 and 120 mg/ml for OTG; 9 and 18 mg/ml for UDM; 10 and 20 mg/ml for DDM) and two different lipid concentrations (5 and 10 mg/ml) were carried out in parallel using the eight channels of the dilution machine. The liposome solutions were injected into detergent containing cuvettes in order to circumvent kinetic restrictions (Heerklotz and Seelig, 2000; Lichtenberg et al., 2000).

Cryoelectron microscopic images of the solubilization series with DDM have been taken on a Philips CM-200 FEG microscope at 200kV using holey carbon film grids (generously performed by M. Chami).

4.5 Discussion

The experiments performed with GalP clearly demonstrate the profound effect of detergents on membrane proteins. The choice of the right detergent is the first prerequisite for successful reconstitution and crystallization. A homogenous preparation is absolutely vital to the crystallization process and this can only be verified to satisfaction by single particle analysis.

Moreover, the results show that the amount of detergent bound to a protein can be controlled during purification. Keeping the detergent collar around the protein at its minimum circumvents the adverse effect of low-cmc detergents during dialysis and might even help to reduce the stress in terms of destabilization exerted on the protein. At the same time, less favorable detergents in terms of the protein stability could still be successfully applied to crystallization by using minimal amounts for lipid solubilization. This would combine the beneficial behavior of detergents such as OG or OTG in 2D crystallization with non-denaturing conditions for the protein.

Reconstitution of membrane proteins with lipids into protein-containing liposomes (proteoliposomes) can be regarded as the reverse process of liposome solubilization in the presence of a membrane protein. Two mechanisms have been proposed for reconstitution (Helenius et al., 1981; Eytan, 1982; Rigaud et al., 1988). Membrane proteins are either reconstituted during the transition from ternary micelles to proteoliposomes by growing into the membranes of open vesicles, or they are incorporated into preformed liposomes that are destabilized by detergent in conditions that promote bilayer fusion. Bilayer fusion is mediated by the expo-

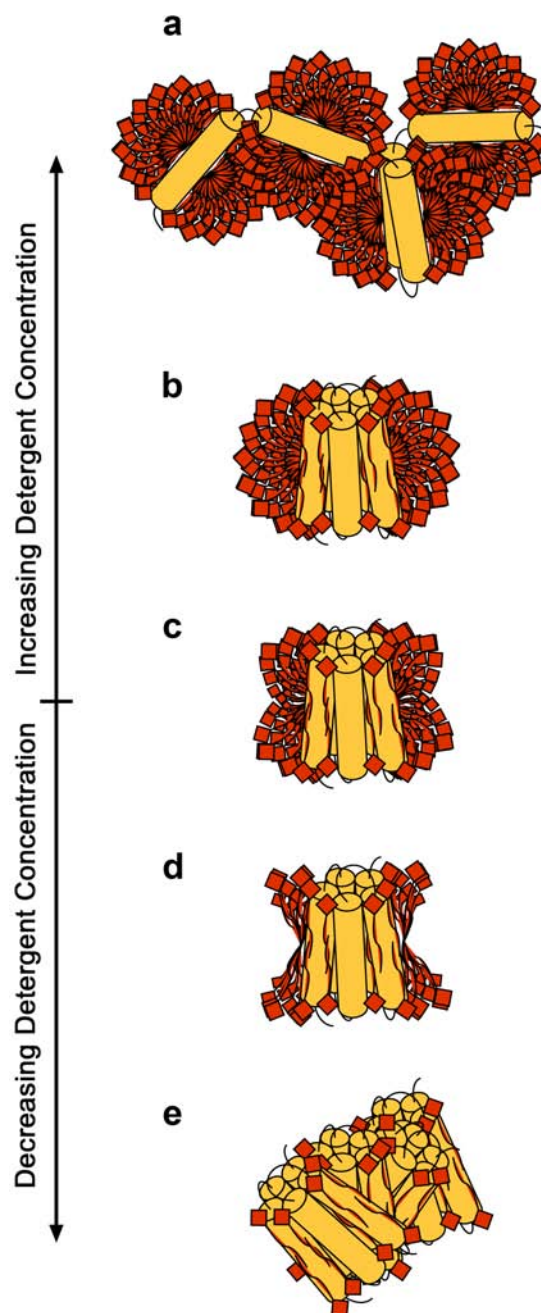


Figure 4.8: **Detergent-to-protein ratio.** Depending on the amount of detergent present during purification the protein is differently decorated by detergent molecules. (a) At very high concentrations the protein can be unfolded. (b) At P_{Sat} the protein is saturated with detergent. (c) Intermediate decoration with detergent (between P_{Sat} and P_{sol}). (d) At P_{sol} the protein is just at its solubility limit. (e) If there is not enough detergent proteins are forced to bury their hydrophobic surfaces by aggregation.

sure of hydrophobic regions to the aqueous phase (Jain and Zakim, 1987). When these circumstances of proteoliposome formation are compared to the

three-stage model for the solubilization of lipids, membrane protein reconstitution either takes place in stage II, where they can insert into the membrane at the same time when the liposomes are formed from mixed micelles, or proteoliposome formation occurs around R_{sat} , where the membrane proteins may spontaneously insert into detergent-saturated liposomes. This insertion as found around R_{sat} is not possible at a detergent/lipid ratio corresponding to the beginning of stage I of lipid solubilization or after segregation of the protein and lipid systems (Kühlbrandt, 1992; Dolder et al., 1996). Insertion of membrane proteins around R_{sat} is normally performed by titration of the lipids with detergent to R_{sat} followed by the addition of detergent solubilized protein (Paternostre et al., 1988; Rigaud et al., 1988). In some cases however, where the lipid-to-protein ratios are low, the addition of a relatively large amount of protein will lead to further solubilization of the lipids. Therefore we focused on the reconstitution of membrane proteins from completely solubilized lipids in stage II of the solubilization, between R_{sat} and R_{sol} .

It has been proposed earlier by Scarborough (Scarborough, 1994), that participation of the hydrophobic surfaces in protein-protein interactions is facilitated when the detergent collar that is present around the hydrophobic region of membrane proteins in solution is near its solubility limit (P_{sol}). When we extend this to membrane protein-lipid interactions, membrane protein reconstitution should be facilitated when protein aggregation occurs simultaneously with liposome formation.

References

- A. R. Curran, R. H. Templer, and P. J. Booth. Modulation of folding and assembly of the membrane protein bacteriorhodopsin by intermolecular forces within the lipid bilayer. *Biochemistry*, 38:9328–9336, 1999.
- M. Dolder, A. Engel, and M. Zulauf. The micelle to vesicle transition of lipids and detergents in the presence of a membrane protein: towards a rationale for 2d crystallization. *FEBS Lett.*, 382:203–208, 1996.
- G. D. Eytan. Use of liposomes for reconstitution of biological functions. *Biochim. Biophys. Acta*, 694:185–202, 1982.
- S. M. Gruner. Intrinsic curvature hypothesis for biomembrane lipid composition: a role for nonbilayer lipids. *Proc. Natl. Acad. Sci. USA*, 82:3665–3669, 1985.
- H. Heerklotz and J. Seelig. Titration calorimetry of surfactant-membrane partitioning and membrane solubilization. *Biochim. Biophys. Acta*, 1508:69–85, 2000.
- A. Helenius, D. R. McCaslin, E. Fries, and C. Tanford. Properties of detergents. *Methods Enzymol.*, 56:734–749, 1979.
- A. Helenius, M. Sarvas, and K. Simons. Asymmetric and symmetric membrane reconstitution by detergent elimination. studies with semliki-forest-virus spike glycoprotein and penicillinase from the membrane of *Bacillus licheniformis*. *Eur. J. Biochem.*, 116:27–35, 1981.
- M. K. Jain and D. Zakim. The spontaneous incorporation of proteins into preformed bilayers. *Biochim. Biophys. Acta*, 906:33–68, 1987.
- T. C. Kaufmann, A. Engel, and H.-W. Remigy. A novel method for detergent concentration determination. *Biophys. J.*, 90:310–317, 2006.
- W. Kühlbrandt. Two-dimensional crystallization of membrane proteins. *Q. Rev. Biophys.*, 25:1–49, 1992.
- M. le Maire, P. Champeil, and J. V. Moller. Interaction of membrane proteins and lipids with solubilizing detergents. *Biochim. Biophys. Acta*, 1508:86–111, 2000.
- D. Lichtenberg. Characterization of the solubilization of lipid bilayers by surfactants. *Biochim. Biophys. Acta*, 821:470–478, 1985.
- D. Lichtenberg, R. J. Robson, and E. A. Dennis. Solubilization of phospholipids by detergents: Structural and kinetic aspects. *Biochim. Biophys. Acta*, 737:285–304, 1983.
- D. Lichtenberg, E. Opatowski, and M. M. Kozlov. Phase boundaries in mixtures of membrane-forming amphiphiles and micelle-forming amphiphiles. *Biochim. Biophys. Acta*, 1508:1–19, 2000.
- P. R. Majhi and A. Blume. Temperature-induced micelle-vesicle transitions in DMPC-SDS and DMPC-DTAB mixtures studied by calorimetry and dynamic light scattering. *J. Phys. Chem. B*, 106:10753–10763, 2002.
- A. Meister and A. Blume. Solubilization of DMPC- d_{54} and DMPG- d_{54} vesicles with octylglucoside and sodium dodecyl sulfate studied by FT-IR spectroscopy. *Phys. Chem. Chem. Phys.*, 6:1551–1556, 2004.
- J. V. Moller and M. le Maire. Detergent binding as a measure of hydrophobic surface area of integral membrane proteins. *J. Biol. Chem.*, 268:18659–18672, 1993.

- M. T. Paternostre, M. Roux, and J. L. Rigaud. Mechanisms of membrane protein insertion into liposomes during reconstitution procedures involving the use of detergents. 1. Solubilization of large unilamellar liposomes (prepared by reverse-phase evaporation) by Triton X-100, octyl glucoside, and sodium cholate. *Biochemistry*, 27:2668–2677, 1988.
- H.-W. Remigy, D. Caujolle-Bert, K. Suda, A. Schenk, M. Chami, and A. Engel. Membrane protein reconstitution and crystallization by controlled dilution. *FEBS Lett.*, 555:160–169, 2003.
- J. L. Rigaud, M. T. Paternostre, and A. Bluzat. Mechanisms of membrane protein insertion into liposomes during reconstitution procedures involving the use of detergents: 2. incorporation of the light-driven proton pump bacteriorhodopsin. *Biochemistry*, 27:2677–2688, 1988.
- J. L. Rigaud, B. Pitard, and D. Levy. Reconstitution of membrane proteins into liposomes: Application to energy-transducing membrane proteins. *Biochim. Biophys. Acta*, 1231:223–246, 1995.
- G. A. Scarborough. Large single crystals of the neurospora crassa plasma membrane H⁺-ATPase: an approach to the crystallization of integral membrane proteins. *Acta Crystallogr. D*, 50:643–649, 1994.
- W. Schaffner and C. Weissman. A rapid, sensitive and specific method for the determination of protein in dilute solution. *Anal. Biochem.*, 56:502–514, 1973.
- C. Tanford. *The Hydrophobic Effect: Formation of Micelles and Biological Membranes*. John Wiley & Sons, Inc., New York, 1980.
- M. Ueno, H. Kashiwagi, and N. Hirota. Size growth factor in the process of vesicle formation from phospholipid-detergent mixed micelles. *Chem. Lett.*, 26:217–218, 1997.
- P. K. Vinson, Y. Talmon, and A. Walter. Vesicle-micelle transition of phosphatidylcholine and octyl glucoside elucidated by cryo-transmission electron microscopy. *Biophys. J.*, 56:669–681, 1989.
- S. H. White and W. C. Wimley. Hydrophobic interactions of peptides with membrane interfaces. *Biochim. Biophys. Acta*, 1376:339–352, 1998.
- S. H. White and W. C. Wimley. Membrane protein folding and stability: physical principles. *Annu. Rev. Biophys. Biomol. Struct.*, 28:319–365, 1999.
- M. C. Wiener and S. H. White. Structure of a fluid dioleoylphosphatidylcholine bilayer determined by joint refinement of x-ray and neutron diffraction data. III. Complete structure. *Biophys. J.*, 61:434–447, 1992.
- M. Zulauf. *Crystallization of Membrane Proteins*. CRC Press, Boca Raton, FL, 1991.

In the following the publication "Controlled 2D Crystallization of Membrane Proteins Using Methyl- β -Cyclodextrin" is appended as submitted to Journal of Structural Biology 2006. Contribution to this work was the determination of the stoichiometry of detergent complexation by methyl- β -cyclodextrin.

Chapter 5

Controlled 2D Crystallization of Membrane Proteins Using Methyl- β -Cyclodextrin

Gian A. Signorell¹, Thomas C. Kaufmann¹, Wanda Kukulski¹, Andreas Engel¹ and Hervé-W. Rémigy^{1,2}

5.1 Abstract

High-resolution structural data of membrane proteins can be obtained by studying 2D crystals by electron crystallography. Finding the right conditions to produce these crystals is one of the major bottlenecks encountered in 2D crystallography. Many reviews address 2D crystallization techniques in attempts to provide guidelines for crystallographers. Several techniques including new approaches to remove detergent like the biobeads technique and the development of dedicated devices have been described (dialysis and dilution machines). In addition, 2D crystallization at interfaces has been studied, the most prominent method being the 2D crystallization at the lipid monolayer. A new approach based on detergent complexation by cyclodextrins is presented in this paper. To prove the ability of cyclodextrins to remove detergent from ternary mixtures (lipid, detergent and protein) in order to get 2D crystals, this method has been tested with OmpF, a typical β -barrel protein, and with SoPIP2;1, a typical α -helical protein. Experiments over different time ranges were performed to analyze the kinetic effects of detergent removal with cyclodextrins on the formation of 2D crystals. The quality of the produced crystals was assessed with negative stain electron microscopy, cryo-electron microscopy and diffraction. Both proteins yielded crystals comparable in quality to previous crystallization reports.

5.2 Introduction

Detergents are used to extract proteins from membranes and during subsequent purification to obtain samples suitable for crystallization. During this process the membrane protein structure and function are affected by the loss of interaction with the lipids. To reconstitute membrane proteins into

a lipid bilayer in order to obtain 2D crystals, the detergent must be removed from a protein-lipid-detergent ternary mixture. There are mainly three ways to remove detergent: Dialysis, adsorption to biobeads and dilution (Rigaud *et al.*, 1997; Hasler *et al.*, 1998; Rémigy *et al.*, 2003). However, all of these methods have their limitations. For dialysis, the rate of detergent removal is closely related to the critical micellar concentration (CMC) of the detergent (Jap *et al.*, 1992; Kuhlbrandt, 1992). For example, dialysis of low CMC detergents (such

¹M. E. Müller Institute for Microscopy, Biozentrum, University of Basel, Basel, Switzerland

²Corresponding author. Tel: +41 61 267 22 57 Fax: +41 61 267 21 09 Email: herve.remigy@unibas.ch

as Triton X-100 or dodecyl- β ,D-maltoside (DDM)) takes weeks at room temperature. Low CMC detergents are often necessary to keep the protein in its active form, as they are better substitutes for the bilayer than high CMC detergents. When low CMC detergents are required, the use of biobeads offers the advantage of a fast detergent removal. However, this can be a problem, since the high efficiency of detergent adsorption to biobeads may result in too fast detergent removal leading to aggregation primarily when small ($< 20 \mu\text{l}$) reconstitution volumes are used. Therefore a minimal initial volume of ternary mixture of $100 \mu\text{l}$ is required for removing the detergent in a controlled manner. This will lead to compromises in the selection of screening conditions, considering the limited amount of protein sample usually available. In a dilution experiment, the protein concentration should remain above 0.2 - 0.5 mg/ml and the initial detergent concentration should be as low as possible (Remigy *et al.*, 2003). An advantage inherent to dilution is the possibility to slow down or even interrupt the reconstitution process at any time, thereby allowing for slow and controlled passage through the critical phase of crystal assembly. The major drawback of the dilution approach however is the inability to remove the detergent completely.

Here we present an alternative approach to produce 2D crystals by detergent removal based on inclusion complexes with cyclodextrins. α -, β - or γ -cyclodextrins are ring shaped molecules made of 6, 7 and 8 glucose molecules, respectively. The non-polar environment inside the ring enables cyclodextrin to enclose hydrophobic or amphiphilic molecules like cholesterol or detergents. This technique was already used to perform reconstitution of active membrane proteins into membranes at a high lipid-to-protein ratio (LPR) (Degrip *et al.*, 1998; Turk *et al.*, 2000; Zampighi *et al.*, 2003). The reconstitution rate is directly related to the amount of cyclodextrin added. The higher affinity of the inclusion compounds of cyclodextrin for detergents than for lipids prevents the LPR to change during reconstitution. Affinity tests between cyclodextrin and many anionic, non-ionic and zwitterionic detergents of various CMC have been made at high LPR and have shown an almost complete lipid recovery (Degrip *et al.*, 1998). A suitable cyclodextrin (α -, β - or γ -cyclodextrin) with a sufficiently high binding affinity can be found for most detergents (Degrip *et al.*, 1998). The affinity of a detergent molecule for a cyclodextrin is largely determined by

the fit of the detergent's hydrophobic moiety with the cyclodextrin cavity (Degrip *et al.*, 1998). All alkyl-chain-containing detergents have high affinity with β -cyclodextrin. γ -cyclodextrin should be considered when a detergent with a bulky hydrophobic chain is used. Full functional reconstitution of membrane proteins with any kind of detergent is therefore possible.

The cyclodextrin approach needs to be adapted to produce proteoliposomes used for membrane protein crystallization. Finding the conditions promoting intermolecular and intramolecular interactions are mandatory, e.g. lipid-protein interactions need to be optimized by screening lipids of different nature and by varying the LPR. Since specific protein-protein interactions depend on the pH and the presence of specific counterions, the search space for optimal crystallization conditions is of an even higher dimensionality.

OmpF and SoPIP2;1 were used to test this new 2D crystallization approach. OmpF is a β -barrel membrane protein from *Escherichia coli* and SoPIP2;1 an α -helical aquaporin from spinach leaf plasma membrane, over-expressed in *Pichia pastoris*. Both proteins have their structures already determined by X-ray crystallography (Cowan *et al.*, 1992; Tornroth-Horsfield *et al.*, 2005). In the present work, methyl- β -cyclodextrin (MBCD) was selected for its high solubility and its high affinity for a wide range of detergents commonly used in membrane protein chemistry.

5.3 Materials and Methods

5.3.1 MBCD/detergent titration curves

The detergents octyl- β ,D-glucoside (OG) and dodecyl-N,N-dimethylamine-N-oxide (LDAO) were purchased from Anatrace (Ohio, USA), whereas octyl-polyoxyethylene (Octyl-POE) was purchased from Alexis (Lausen, Switzerland). All detergents were of high purity grade ($\geq 98\%$) and were used without further purification. MBCD-detergent mixtures were obtained by dilution of appropriately combined stock solutions with reagent-grade water produced by a Milli-Q filtration system ($\approx 18 \text{ M}\Omega$). The pipetted volumes were weighed on a balance (Mettler AE50) purchased from Mettler-Toledo (Greifensee, Switzerland). The different molar ratios were obtained by varying the MBCD concentration and keeping the detergent concentration constant above the corresponding CMC in

order to have a constant surface tension reduction contribution from the detergent. Contact angles between a sample droplet and the supporting Parafilm were measured using a homemade device as described by Kaufmann *et al.* (2006).

For calculation purposes the mean molecular mass of the MBCD was determined by MALDI-TOF on a Bruker Scout 26 Reflex III instrument (Bruker Daltonik, Bremen, Germany). The mass spectrometric analysis revealed an average substitution rate of 1.77 methyl groups per glucose molecule, leading to a mean molecular mass of 1310.4 Da per MBCD molecule. The molecular weight of Octyl-POE was calculated as the mean of the masses of all represented ethoxylated (EO) species ($n_{EO}=1-11$) which gives 372.52 g/mol for the hypothetical number of ethylene-oxide units $n_{EO}=5.5$. As density of Octyl-POE the value of 1.015 g/cm³, determined by Rosenbusch *et al.* (2001) was used.

5.3.2 OmpF and SoPIP 2;1 purification and reconstitution

OmpF was produced in *Escherichia coli*, purified as reported previously (Holzenburg *et al.*, 1989) and solubilized in 1% Octyl-POE. SoPIP2;1, previously referred as PM28A, expressed in *Pichia pastoris* was purified according to Karlsson *et al.* (2003). The phospholipids used to prepare proteoliposomes were dissolved in chloroform at a concentration of 10 mg/ml, dried under a stream of argon, further dried overnight in a dessicator and weighed. Reagent-grade water was added and the lipid solutions were then sonicated for 2 minutes in a cold water bath using a Branson sonifier 250 tip at 20% of the maximum output power. An aqueous solution of the same detergent used for protein solubilization was added to the lipids to get a final detergent concentration of 1% (5 mg/ml dimyristoylphosphatidylcholine (DMPC) lipids were solubilized in 1% Octyl-POE for OmpF, 5 mg/ml *E. coli* lipids in 1% OG for SoPIP2;1). To have exactly defined starting conditions, the protein-detergent mixture was dialyzed overnight against the crystallization buffer containing detergent. OmpF was dialyzed at 4°C overnight against 20 mM Hepes pH 7, 100 mM NaCl, 10 mM MgCl₂, 3 mM NaN₃, 1% Octyl-POE. SoPIP2;1 was dialyzed at 4°C overnight against 20 mM Hepes pH 7.5, 100 mM NaCl, 50 mM MgCl₂, 2 mM dithiothreitol, 3 mM NaN₃, 1% OG. After dialysis the detergent concentration was measured as described above (Kaufmann *et al.*, 2006)

and adjusted to 1% Octyl-POE for OmpF and 1% OG for SoPIP2;1 by dilution with the corresponding buffer. The final protein concentrations before lipid addition were 1.5 and 1.2 mg/ml for OmpF and SoPIP2;1 respectively. The protein concentration was determined with a BCA protein assay available from Pierce (Rockford, Ill.). DMPC was added to cover LPRs ranging from 0.15 to 1 for OmpF. *E. coli* lipids were added to the SoPIP2;1 solution to cover LPRs ranging from 0.3 to 0.4. After the detergent was removed by controlled addition of MBCD the samples were washed to eliminate the MBCD from the solution. The samples were centrifuged for 15 minutes at 55,000 rpm (100,000 g) using a Beckmann TL-100 ultracentrifuge. The supernatant was discarded and the pellet resuspended in 400 μ l detergent-free crystallization buffer. This procedure was repeated twice and after a final centrifugation the pellet was collected for cryo-electron microscopy (EM).

5.3.3 Controlled MBCD addition

MBCD was from Fluka. A dilution device described by Remigy *et al.* (2003) was used to perform the controlled addition of the MBCD. The MBCD solution is supplied to a cuvette by a micro-syringe. A valve prevents diffusion between the syringe and the cuvette. To keep the sample homogeneous, a stirrer is placed at the bottom of the cuvette. Fast reconstitutions lasting 30 minutes, 2 hours and 12 hours with initial ternary mixture volumes of 20 μ l were performed. During these experiments the samples were constantly stirred. For 30 minutes and 2 hours, 10 μ l of a 30% MBCD solution were added to the solution. For 12 hours, 25 μ l of a 10% MBCD solution were added. 30 μ l, 30 μ l and 15 μ l were recovered for the 30 minutes, 2 hours and 12 hours experiments, respectively. 72 hours and 144 hours experiments were carried out with and without stirring with an initial ternary mixture volume of 40 μ l. To overcome liquid loss during these longer experiments, bigger volumes of less concentrated cyclodextrin solutions were added. 400 μ l of a 2% MBCD solution were added over 72 hours and 600 μ l of a 1.3% MBCD solution were added over 144 hours. 200 to 230 μ l were collected after the experiments.

5.3.4 Phospholipase A2 treatment

OmpF crystals were treated with bee venom phospholipase A2 (available from Sigma) to remove

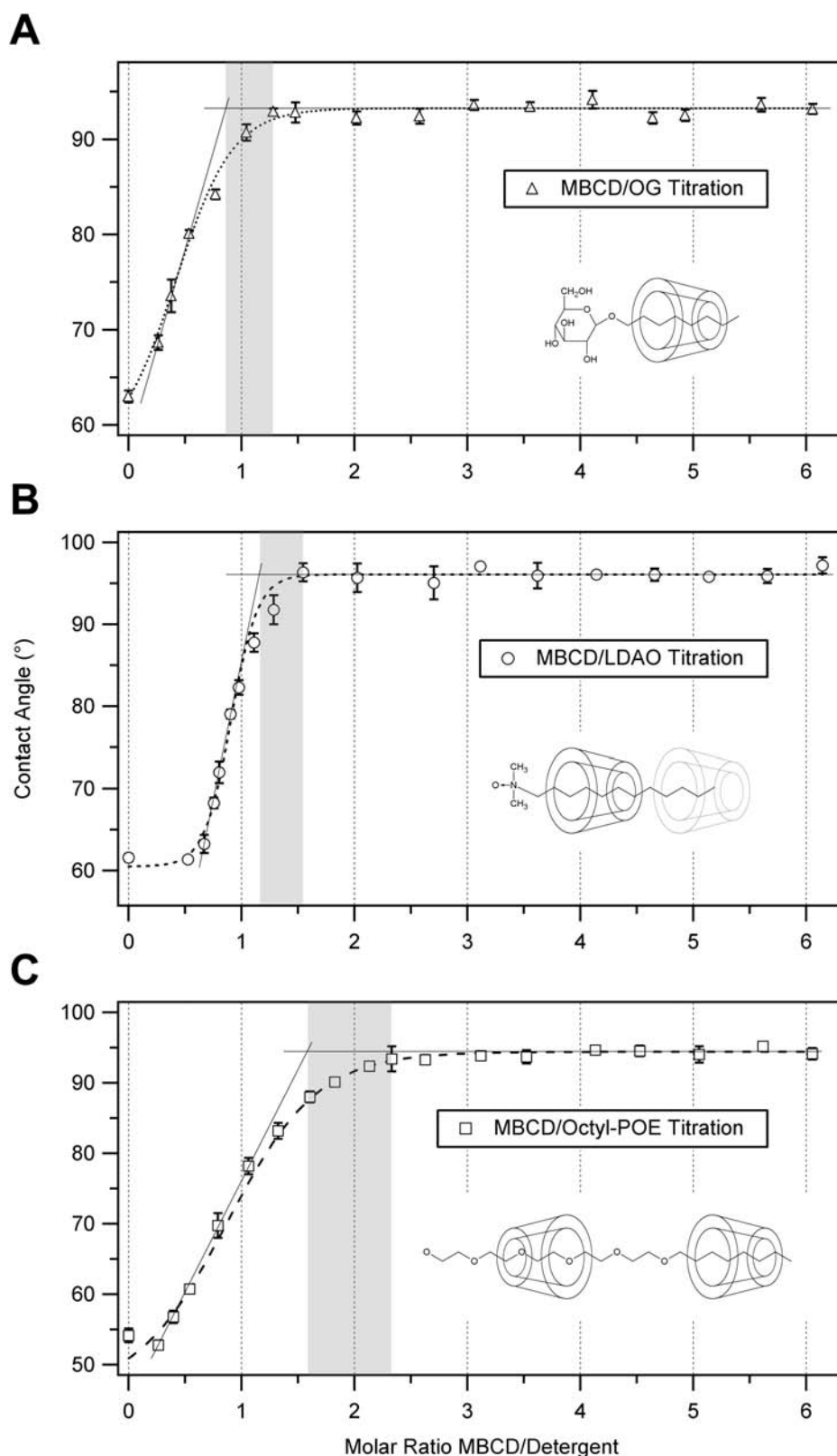


Figure 5.1: **MBCD-detergent titration curves.** The measurements were performed at constant detergent concentration above the respective CMC of the detergents. One curve represents the mean of three measurements for each MBCD-detergent pair. The possible ranges for the stoichiometry of complex formation are shaded in gray. The illustrations depict the most probable inclusion stoichiometries as deduced from the measurements. In the case of the polydisperse Octyl-POE, pentaethylene glycol monoethyl ether (C8E5) is shown as a representative structure. (A) OG at 21 mM (CMC=18 mM). (B) LDAO at 2.5 mM (CMC=1.9 mM). (C) Octyl-POE at 10 mM (CMC=6.6 mM).

lipids from the proteoliposomes and thus get closer crystal packing. This procedure was described by Mannella (1984). Loosely packed OmpF crystals (1 mg/ml) in a buffer containing 20 mM Hepes pH 7, 100 mM NaCl, 10 mM MgCl₂, 3 mM NaN₃ and 1% Octyl-POE were used to perform this treatment. 10 μ l of OmpF were added to 2 ml of low salt buffer (0.005% MBCD, 1 mM Tris HCl, 0.1 mM ethylene diamine tetra acetic acid, pH 7.5). 0, 0.3, 0.6 and 1.2 units/ml of phospholipase A2 were added to OmpF aliquoted in low salt buffer (1 mg of phospholipase corresponds to 1500 units). The mixture was incubated overnight at 4°C. The solution was centrifuged in a Beckmann TL-100 ultracentrifuge for 90 minutes at 55,000 rpm (100,000 \times g) at 4°C. The supernatant was discarded and the pellet was resuspended in the low salt buffer.

5.3.5 Electron microscopy

Specimens for negative stain electron microscopy were prepared by adsorbing proteoliposomes onto carbon films previously rendered hydrophilic by glow discharging in air. The grids were washed three times with distilled water and stained with saturated uranyl acetate (1%). Micrographs were taken on a Hitachi H-7000 transmission electron microscope operated at 100 kV using magnifications of 5,000 to 50,000. An optical bench with a laser beam was used to evaluate the diffraction quality of the micrographs. Well-ordered crystals were embedded in 2% glucose on molybdenum grids covered with a carbon film that was previously evaporated onto mica and floated on the grid. Electron diffraction patterns were recorded at low electron doses (<5 electrons per \AA^2) on a Gatan 2Kx2K CCD camera with a Philips CM-200 FEG microscope operated at 200 kV.

5.4 Results

5.4.1 MBCD/detergent titrations

The titration curves (Fig. 5.1) reveal the amount of MBCD needed for the neutralization of the respective detergents. All three curves show a sudden increase in the contact angle reflecting the MBCD-detergent complexation depleting the solution from detergent monomers, which can no more adsorb to the liquid-vapor and solid-liquid interfaces. The points at which the curves reach the plateau correspond to the molar ratios needed for complete

complexation of the detergents by MBCD, i.e., the minimal amount required in an experiment. At the same time these points correspond to the upper boundary of the complex stoichiometry. The lower boundary is given by the intersection between the extrapolated plateau and the extrapolated initial slope reflecting the highest possible association constant for the complex formation.

The obtained ranges for the stoichiometries of complex formation are 0.9 - 1.3 for MBCD/OG, 1.2 - 1.5 for MBCD/LDAO and 1.6 - 2.3 for MBCD/Octyl-POE. The results suggest a 1:1 complex for MBCD and OG. In the case of LDAO the results comply with the formation of a predominant 1:1 complex and with a fraction of the species carrying a second MBCD molecule but with much lower affinity. The mean complex stoichiometry for the polydisperse Octyl-POE levels off at a molar ratio of around 2. This suggests that while the aliphatic chain is occupied by one MBCD molecule, the polyoxyethylene chain, which is variable in length, can be decorated with different amounts of MBCD molecules.

5.4.2 2D Crystallization of the Porin OmpF

Experiments ranging from 30 minutes to 144 hours yielding OmpF crystals show that faster detergent removal rates (2 hours and less) result in low quality crystals having diameters ranging from 50 to 500 nm, with a trigonal lattice ($a=b=9\pm 0.5$ nm; $\gamma=60^\circ$), which diffracted up to 2.7 nm resolution (Fig. 5.2A). Slower rates (12 hours to 144 hours) result in the formation of large sheets having diameters ranging from 1 to 2 μ m, with a trigonal lattice ($a=b=9\pm 0.5$ nm; $\gamma=60^\circ$) diffracting up to 2.4 nm resolution (Fig. 5.2B). Stirring did not affect the crystal quality. After phospholipase A2 treatment (Mannella, 1984) on OmpF crystals obtained after 144 hours runs, crystals with a trigonal lattice ($a=b=7.2\pm 0.2$ nm; $\gamma=60^\circ$) diffracting beyond 2.2 nm resolution (Fig. 5.2C) were obtained.

5.4.3 2D Crystallization of SoPIP2;1

SoPIP2;1 reconstitution lasting 2 hours (Fig. 5.3A) and less yielded large vesicles and small sheets but no significant diffraction was observed. Large sheets comparable to those previously reported (Kukulski *et al.*, 2005) were obtained after 72 and 144 hours experiments (Fig. 5.3B). Stirring did not

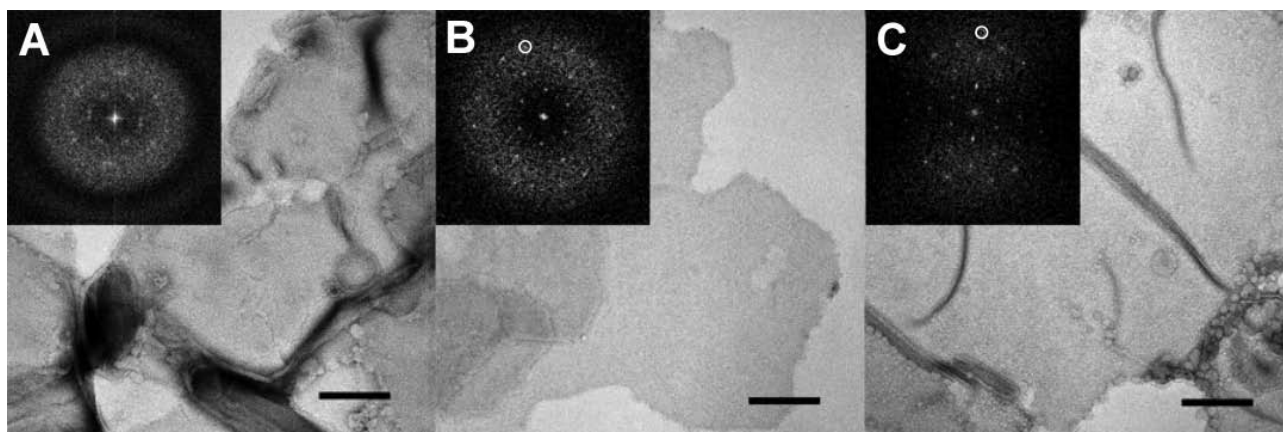


Figure 5.2: **OmpF 2D crystallization using MBCD.** Experiments ranging from 30 minutes to 144 hours show that (A) faster detergent removal rates (2 hours and less) result in low quality crystals having diameters ranging from 50 to 500 nm, with a trigonal lattice ($a=b=9\pm 0.5$ nm; $\gamma=60^\circ$). (B) Slower rates (12 hours to 144 hours) result in the formation of large sheets having a diameter ranging from 1 to 2 μm , with a trigonal lattice ($a=b=9\pm 0.5$ nm; $\gamma=60^\circ$) diffracting up to 2.4 nm resolution (spot marked by a circle). (C) After phospholipase A2 treatment on OmpF crystals obtained after a 144 hours run, crystals with a trigonal lattice ($a=b=7.2\pm 0.2$ nm; $\gamma=60^\circ$) diffracting beyond 2.2 nm resolution were obtained (spot marked by a circle). The scale bars represent 100 nm.

affect the crystal quality. The largest sheets obtained after 144 hours were used to perform direct electron diffraction. Images of electron diffraction patterns were taken from unwashed (Fig. 5.3C) and washed crystals (Fig. 5.3D). The electron diffraction patterns exhibit a $p4$ symmetry with the same lattice constants of $a=b=9.6$ nm for both, unwashed and washed samples. The indicated spots for the unwashed crystals are 24,2 (Fig. 5.3C) and 24,3 for washed crystals (Fig. 5.3D), corresponding to a resolution of 4 Å. The unwashed sample (Fig. 5.3C) displays strong additional diffraction spots, arranged in a six-fold symmetry overlaying the typical diffraction pattern of SoPIP2;1. These spots are not present in the washed sample (Fig. 5.3D).

5.5 Discussion

The capability of cyclodextrin to complex any kind of detergent molecule, independently from the CMC, is a crucial advantage over the dialysis method. The removal of detergents like Triton TX-100 or DDM can be performed. Such "mild" detergents are widely used for the purification of large and sensitive complexes like *Chlorobium tepidum* reaction center (Remigy *et al.*, 1999). The nature of the detergent, the detergent removal rate and the detergent removal technique affect size and quality of the resulting proteoliposomes and crys-

tals (Wingfield *et al.*, 1979; Hovmoller *et al.*, 1983; Chami *et al.*, 2001; Remigy *et al.*, 2003). Even if the detergent is removed in an efficient way, there is no guarantee that 2D crystals will form during the reconstitution process. For this reasons the validation of the cyclodextrin approach in its ability to produce membrane protein crystals was needed.

5.5.1 Cyclodextrin and detergent removal

To perform reconstitution with MBCD accurately, a precise evaluation of the amount of MBCD needed to remove all the detergent from a solution is required. A homemade device (Kaufmann *et al.*, 2006) to measure the detergent concentration of any solution (detergent solution, binary or ternary mixtures) was used to measure the MBCD-detergent molecular ratios after cyclodextrin addition to detergent solutions. The insets in Fig. 5.1 show the most probable complexes between MBCD and the detergents. The obtained ratios for OG (1:1), LDAO (1:1 and a weak 2:1) and Octyl-POE (2:1) are in good agreement with expected values based on the alkyl chain length. The cavity of a β -cyclodextrin molecule is about 8 Å deep, offering accommodation for a C8 chain (Fig. 5.1A). The longer chain of LDAO might be shielded by an additional cyclodextrin ring occasionally forming a 2:1 complex (Fig. 5.1B). Alternatively a 3:2

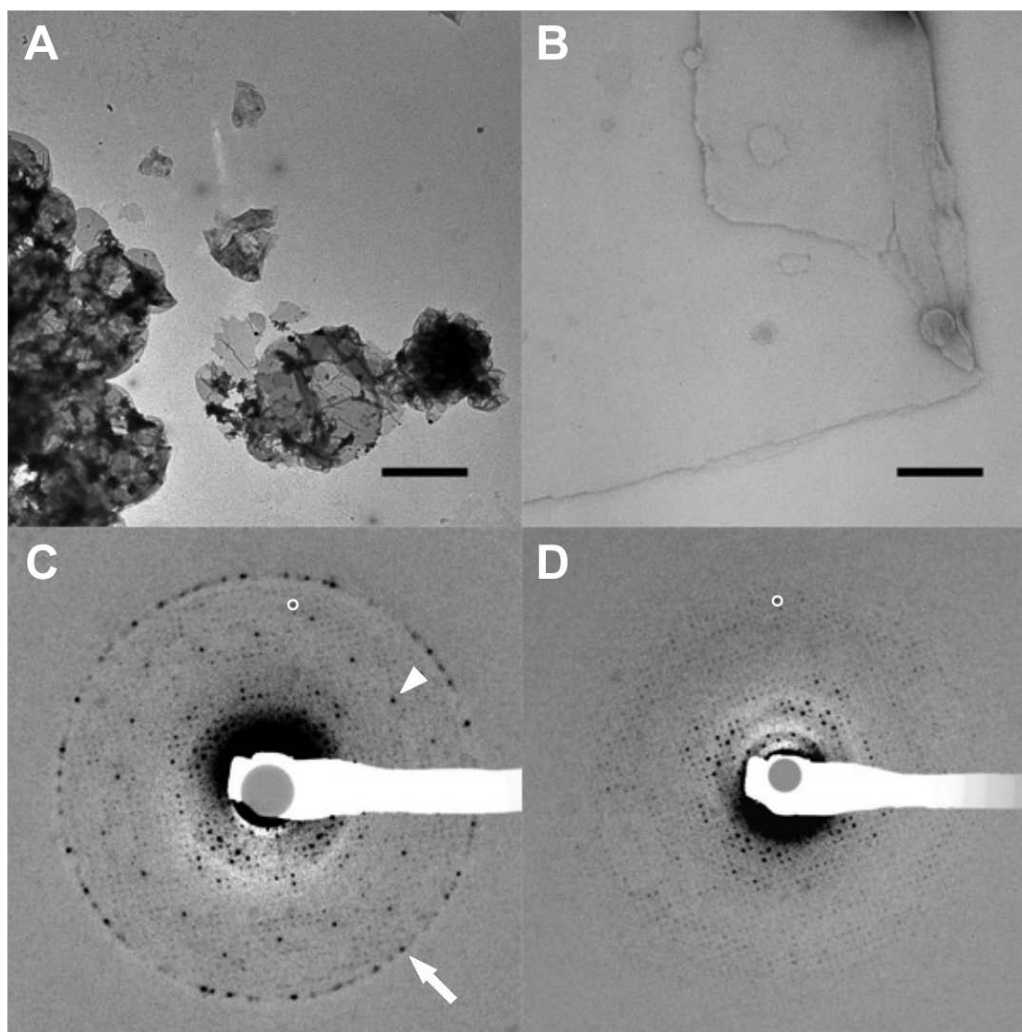


Figure 5.3: **SoPIP2;1 2D crystallization using MBCD.** (A) and (B) Electron microscopy images using negative stain. (A) overview at 5k magnification of a 2 hours run and (B) sheet at 50k magnification of a crystal obtained after a 144 hours reconstitution. The scale bar in (A) represents $1\ \mu\text{m}$ and in (B) 100 nm. (C) and (D) Electron diffraction patterns of crystals obtained after 144 hours. Both images show a p4 symmetry with lattice constants of $a=b=96\ \text{\AA}$. (C) The unwashed sample shows strong additional diffraction spots arranged in a six-fold symmetry (arrowhead). The spots arranged in circle are from water crystals (arrow). The spot marked by a circle on the diffraction image is indexed 24,2. (D) The washed sample shows no additional spot overlaying the typical diffraction pattern of SoPIP2;1. The spot marked by a circle (24,3) corresponds to a resolution of $4\ \text{\AA}$.

complex could also be envisaged, where two LDAO molecules carry one MBCD each and an additional MBCD molecule is shared between the two. This, however, is purely speculative and might not be very probable for thermodynamic reasons. Octyl-POE has a lower stoichiometry than expected. One MBCD molecule is strung onto the C8 aliphatic chain, whereas only one more is occupying the polyethylene oxide (PEO) chain (Fig. 5.1C). The latter could reflect a lower affinity for PEO fragments due to the oxygen atoms possibly hydrogen bonding with surrounding water molecules. Thus the change

of free energy is lower for PEO units. However, the polydisperse character of Octyl-POE clearly interferes with the assignment of a single stoichiometric ratio and this might be reflected in the comparatively smaller gradient of the curve. Additionally, one should keep in mind that in solution both the aliphatic chains and the polyoxyethylene chains are not only present as an extended species and therefore the geometric reasoning is of approximative nature. Schmidt-Krey *et al.* (1998) have shown that the size of microsomal glutathione transferase 2D crystals changes according to the initial deter-

gent concentration. The MBCD approach allows us to use an excess of detergent even with low CMC detergents. Having established MBCD-detergent titration curves (Fig. 5.1) we can calculate the exact amount of MBCD that needs to be added to a solution to remove all the detergent. For practical purposes one needs to add the highest molar ratio (see Results, MBCD/detergent titrations) since complete neutralization of the detergent is required. Moreover, as the detergent removal rate is directly related to the cyclodextrin addition, a mixture of detergents can be reproducibly used during crystallization. Hence, one can easily combine low and high CMC detergents without the drawbacks related to dialysis. This enables us to explore 2D crystallization conditions that could not be tested yet.

5.5.2 2D crystallization of OmpF

Using the cyclodextrin approach to remove detergent produced OmpF crystals of different qualities depending on the reconstitution time. Short reconstitution periods (up to 2 hours) yielded low quality crystals (Fig. 5.2A) similar to the crystals reported by Dorset *et al.* (1983). Longer reconstitution experiments (12 hours to 144 hours) led to bigger proteoliposomes having an average diameter of 1.5 μm that diffracted up to 2.4 nm (Fig. 5.2B). These results are in agreement (according to the size of the proteoliposomes and the lattice parameters) with previous works on OmpF (Dolder *et al.*, 1996; Remigy *et al.*, 2003) where dilution and dialysis yielded double-layered trigonal crystals. To improve the crystal packing of OmpF, we adapted the procedure using phospholipase A2 (PLA2) described by Mannella (1984) to the cyclodextrin method. PLA2 catalyzes the hydrolysis of the ester linkage in the sn-2 position of glycerophospholipids like DMPC, yielding free fatty acids and lysophospholipids. To avoid the solubilization of the proteoliposomes by these degradation products the solution is dialyzed against a low salt buffer (Mannella, 1984). The ability of cyclodextrin to bind free fatty acids and lysophospholipids allowed us to perform the PLA2 treatment without dialysis and thus to simplify the procedure. After PLA2 treatment the packing of the proteins was denser and a smaller trigonal lattice was revealed (Fig. 5.2C). These crystals are similar to the densely packed OmpF crystals that have undergone a PLA2 treatment described by Regenass *et al.* (1985) and Engel *et al.* (1992). Due

to the limitations of negative staining these crystals diffracted only up to 2.2 nm (Fig. 5.2C). Thus PLA2 treatment can be applied directly on loosely packed crystals obtained with the MBCD method given that there's enough MBCD to capture the digested lipids. This approach is appropriate when a larger than optimal initial amount of lipid is needed to keep the membrane protein stable during reconstitution.

5.5.3 2D crystallization of SoPIP2;1

Reconstitution of SoPIP2;1 lasting 2 hours and less did not yield large sheets and did not diffract in negative stain. The weak contrast in negative stained samples is due to the smooth surface of double-layered SoPIP2;1 crystals preventing negative stain to penetrate (Kukulski, personal communication). Only cryo-EM could correctly assess the quality of such crystals. Reconstitutions of SoPIP2;1 over 144 hours produced large crystals (Fig. 5.3A and B) so that electron diffraction could be performed. The diffraction patterns (Fig. 5.3C and D) correspond to one type of 2D crystal, obtained by dialysis during the determination of the 5 Å structure of SoPIP2;1 (Kukulski *et al.*, 2005). The quality of the crystals in the present work is comparable, having spots diffracting up to a resolution of 4 Å. The unwashed sample (Fig. 5.3C) displays strong additional diffraction spots arranged in a six-fold symmetry and overlaying the typical diffraction pattern of SoPIP2;1. These spots disappear when the sample is washed (Fig. 5.3D). Because washing mainly removed the MBCD from the solution, we assume that the spots in the unwashed sample result from MBCD crystallization during grid preparation.

5.5.4 Large screenings for 2D crystals using cyclodextrin

To parallelize 2D crystallization experiments to test as many conditions as possible, it is important to have the smallest possible initial volume of ternary mixtures. The accuracy in the addition of salts, lipids and other compounds impose a limit in reducing this initial sample volume. Evaporation poses the problem of keeping the sample volume constant over long time spans, which is a difficult task to handle, especially with small volumes. Using microdroplet pipettes to dispense cyclodextrin solution and water in combination with an accurate volume measurement method could overcome these drawbacks. We estimate that small volumes in the order

of 10 μl can be handled automatically. In this way up to 100 different reconstitution conditions could be tested with 1 mg of protein. This is a decisive step towards the reproducibility of 2D crystallization experiments. Still remaining is the problem of preparing and inspecting a large quantity of individual specimens by electron microscopy (Kuhlbrandt, 1992).

In our experiments crystallization mixtures were dialyzed overnight to have precise starting conditions. To diversify conditions (salts concentrations, LPRs etc.) it might be sensible to dialyze overnight batches of detergent-protein mixtures against buffers of various pHs and to subsequently add additional substances to the solution (lipids, salts, inhibitors etc.).

Short experiments (12 hours and less) yielded crystals of lower quality (small and less ordered), whereas large sheets were obtained after 72 hours and more for both OmpF and SoPIP2;1. From these results we assume that longer duration will in general increase the size and the quality of the crystals. Also, over longer experiments (72 and 144 hours) mixing did not affect crystal quality. To achieve homogeneous conditions over longer reconstitutions, a stirrer was used in our setup. In parallel experiments a shaker would be more appropriate, since shaking does not interfere with the sample directly (no contamination) and commercially available micro-plates (with 96 or 384 wells) could be used. A more sophisticated device than the dilution apparatus, controlling all pertinent parameters of the ternary mixture during crystallization would enable us to perform longer experiments promoting crystallogensis in a reproducible manner.

The transition phase temperature increases according to the ratio of saturated/unsaturated lipids. Therefore the temperature during reconstitution is a crucial parameter (Engel *et al.*, 1992). For example, the phase transition temperature of DMPC, commonly used for crystallization is beyond 23°C (Nakayama *et al.*, 1980). The effects of the temperature as parameter on the crystallization using cyclodextrins have not been investigated extensively. Since MBCD is highly soluble in water even at low temperatures, the described procedure shows no restriction in experimenting any temperature profiles during crystallization.

The reconstitution and crystallization using the cyclodextrin approach requires only small sample volumes and no additional surrounding buffer like in the dialysis method. This makes the cyclodextrin

method very suitable to screen conditions where expensive or difficult to produce compounds are used (proteins, chemicals, substrates or inhibitors). A certain protein conformation or better-ordered crystals may be achieved if such compounds (ATP, antagonists, or substrates) are added to the ternary mixture. In the dialysis method these compounds have to be added to the dialysis buffer solution to keep their concentrations constant since they are usually small enough to pass through the dialysis membrane. Many examples of co-crystallization in the 3D crystallization field involving inhibitors with high affinity, transiently bound substrates (e.g. NAD⁺), designed protein (e.g. ankyrin repeats), or other cofactors have been reported (Schindler *et al.*, 2000; Scott *et al.*, 2004; Brautigam *et al.*, 2005; Kohl *et al.*, 2005; Sundaresan *et al.*, 2005). Such conditions have not being explored by the 2D crystallization because of the limitations mentioned above. Therefore, the cyclodextrin approach appears to be a promising alternative to traditional 2D crystallization methods.

5.6 Conclusion

Cyclodextrin can be used in protein reconstitution, crystallization and to improve crystal quality in combination with phospholipase. Proteins of known structure were chosen to test this new method of 2D crystallography. The quality of both OmpF and SoPIP2;1 crystals were comparable with previously published results (Dolder *et al.*, 1996; Remigy *et al.*, 2003; Kukulski *et al.*, 2005). One advantage of this method is the accuracy of the detergent removal, allowing us to control the kinetics of the whole process in a precise way. The detergent removal rate is controlled by the amount of cyclodextrin added and therefore does not depend on the CMC of the detergent. Another advantage of the cyclodextrin method over other methods lies in its applicability in systematic screenings for crystallization conditions. The sample volume can be very small allowing to work with small amount of protein per condition and with compounds that are expensive or not available in large quantities. The possibility of large parallel screenings of 2D crystallization conditions needs to be complemented with the effort to automate electron microscopy in such a way that all the conditions can be inspected in a reasonable time. The approach needs to be explored with a large range of membrane proteins in order to acquire a solid know-how of kinetics, choice

of detergents and choice of the right cyclodextrin partner. Only these systematic experiments will give us the knowledge to produce 2D crystals of any protein in a reproducible way.

5.7 Acknowledgments

We are grateful to Per Kjellbom for providing *Pichia pastoris* over-expressing SoPIP2;1 and Mohamed Chami for fruitful feedback on membrane protein reconstitution. Heiko Heerklotz is acknowledged for critically discussing the results of detergent complexation by MBCD.

This work was supported by the NCCR Nano, the NCCR Structural Biology, the SNF grant to Andreas Engel (SNF 501 221) and the NoE 3DEM.

5.8 References

- Brautigam, C. A., Chuang, J. L., Tomchick, D. R., Machius, M., Chuang, D. T., 2005. Crystal structure of human dihydrolipoamide dehydrogenase: NAD⁺/NADH binding and the structural basis of disease-causing mutations. *J. Mol. Biol.* 350, 543-552.
- Chami, M., Pehau-Arnaudet, G., Lambert, O., Ranck, J. L., Levy, D., Rigaud, J. L., 2001. Use of octyl- β -thioglucoopyranoside in two-dimensional crystallization of membrane proteins. *J. Struct. Biol.* 133, 64-74.
- Cowan. S. W., Schirmer, T., Rummel, G., Steiert, M., Ghosh, R., Pauptit, R. A., Jansonius, J. N., Rosenbusch, J. P., 1992. Crystal structures explain functional properties of two *E. Coli* porins. *Nature* 358, 727-733.
- Degrip, W. J., Vanoostrum, J., Bovee-Geurts, P. H., 1998. Selective detergent-extraction from mixed detergent/lipid/protein micelles, using cyclodextrin inclusion compounds: a novel generic approach for the preparation of proteoliposomes. *Biochem. J.* 330, 667-674.
- Dolder, M., Engel, A., Zulauf, M., 1996. The micelle to vesicle transition of lipids and detergents in the presence of a membrane protein: towards a rationale for 2D crystallization. *FEBS Lett.* 382, 203-208.
- Dorset, D. L., Engel, A., Haner, M., Massalski, A., Rosenbusch, J. P., 1983. Two-dimensional crystal packing of matrix porin. A channel forming protein in *Escherichia coli* outer membranes. *J. Mol. Biol.* 165, 701-710.
- Engel, A., Hoenger, A., Hefti, A., Henn, C., Ford, R. C., Kistler, J., Zulauf, M., 1992. Assembly of 2-D membrane protein crystals: dynamics, crystal order, and fidelity of structure analysis by electron microscopy. *J. Struct. Biol.* 109, 219-234.
- Hasler, L., Heymann, J. B., Engel, A., Kistler, J., Walz, T., 1998. 2D crystallization of membrane proteins: rationales and examples. *J. Struct. Biol.* 121, 162-171.
- Holzenburg, A., Engel, A., Kessler, R., Manz, H. J., Lustig, A., Aebi, U., 1989. Rapid isolation of OmpF porin-LPS complexes suitable for structure-function studies. *Biochemistry* 28, 4187-4193.
- Hovmoller, S., Slaughter, M., Berriman, J., Karlsson, B., Weiss, H., Leonard, K., 1983. Structural studies of cytochrome reductase. Improved crystals of the enzyme complex and crystallization of a subcomplex. *J. Mol. Biol.* 165, 401-406.
- Jap, B.K., Zulauf, M., Scheybani, T., Hefti, A., Baumeister, W., Aebi, W., Engel, A., 1992. 2D crystallization: from art to science. *Ultramicroscopy* 46, 45-84.
- Karlsson, M., Fotiadis, D., Sjoval, S., Johansson, I., Hedfalk, K., Engel, A., Kjellbom, P., 2003. Reconstitution of water channel function of an aquaporin overexpressed and purified from *Pichia pastoris*. *FEBS Lett.* 537, 68-72.
- Kaufmann, T. C., Engel, A., Remigy, H.W., 2006. A novel method for detergent concentration determination. *Biophys. J.* 90, 310-317.
- Kohl, A., Amstutz, P., Parizek, P., Binz, H. K., Briand, C., Capitani, G., Forrer, P., Plückthun, A., Grütter, M., 2005. Allosteric inhibition of aminoglycoside phosphotransferase by a designed ankyrin repeat protein. *Structure* 13, 1131-1141.
- Kuhlbrandt, W. 1992. Two-dimensional crystallization of membrane proteins. *Q. Rev. Biophys.* 25, 1-49.
- Kukulski W., Schenk, A. D., Johansson, U., Braun, T., de Groot, B. L., Fotiadis, D., Kjellbom, P., Engel, A., 2005. The 5Å structure of heterologously expressed plant aquaporin SoPIP2;1. *J. Mol. Biol.* 350, 611-616.
- Mannella, C. A. 1984. Phospholipase-induced crystallization of channels in mitochondrial outer membranes. *Science.* 224, 165-166.
- Nakayama, A., Mitsui, T., Nishihara, M., Kito, M., 1980. Relation between growth temperature of *E. coli* and phase transition temperatures of its cytoplasmic and outer membranes. *Biochim. Biophys. Acta.* 601, 1-10.

- Regenass, M., Hardmeyer, A., Rosenbusch, J. P., Engel, A., 1985. Phospholipids in reconstituted porin membranes: Conversion of one crystal habit in another by phospholipase. *Experientia* 41, 808.
- Remigy, H.W., Stahlberg, H., Fotiadis, D., Müller, S. A., Wolpensinger, B., Engel, A., Hauska, G., Tsiotis, G., 1999. The reaction complex from the green sulfur bacterium *Chlorobium tepidum*: a structural analysis by scanning transmission electron microscopy. *J. Mol. Biol.* 290, 851-858.
- Remigy, H.W., Caujolle-Bert, D., Suda, K., Schenk, A., Chami, M., Engel, A., 2003. Membrane protein reconstitution and crystallization by controlled dilution. *FEBS Lett.* 555, 160-169.
- Rigaud, J.L., Mosser, G., Lacapere, J. J., Olofsson, A., Levy, D., Ranck, J.L., 1997. Bio-beads: an efficient strategy for two-dimensional crystallization of membrane proteins. *J. Struct. Biol.* 118, 226-235.
- Rosenbusch, J.P., Lustig, A., Grabo, M., Zulauf, M., Regenass, M., 2001. Approaches to determining membrane protein structures to high resolution: do selections of subpopulations occur? *Micron* 32, 75-90.
- Schindler, T., Bornmann, W., Pellicena, P., Miller, W. T., Clarkson, B., Kuriyan, J., 2000. Structural Mechanism for STI-571 inhibition of Abelson Tyrosine Kinase. *Science* 289, 1938-1942.
- Schmidt-Krey, I., Lundqvist, G., Morgenstern, R., Hebert, H., 1998. Parameters for the two-dimensional crystallization of the membrane protein microsomal glutathione transferase. *J. Struct. Biol.* 123, 87-96.
- Scott, E. E., White, M. A., He, Y. A., Johnson, E. F., Stout, C. D., Halpert, J. R., 2004. Structure of mammalian cytochrome P450 2B4 complexed with 4-(4-Chlorophenyl) imidazole at 1.9-Å resolution. *J. Biol. Chem.* 279, 27294-27301.
- Sundaresan, V., Chartron, J., Yamaguchi, M., Stout, C. D., 2005. Conformational diversity in NAD(H) and interacting transhydrogenase nicotinamide nucleotide binding domains. *J. Mol. Biol.* 346, 617-629.
- Tornroth-Horsfield, S., Wang, Y., Johanson, U., Karlsson, M., Tajkshohid, D., Neutze, R., Kjellbom, P., 2005. Structural mechanism of plant aquaporin gating. *Nature* 439, 688-94.
- Turk, E., Kim, O., le Coutre, J., Whitelegge, J. P., Eskandari, S., Lam, J. T., Kreman, M., Zampighi, G., Faull, K. F., Wright, E. M., 2000. Molecular characterization of *Vibrio parahaemolyticus* vSGLT: a model for sodium-coupled sugar cotransporters. *J. Biol. Chem.* 275, 25711-25716.
- Wingfield, P., Arad, T., Leonard, K., Weiss, H., 1979. Membrane crystals of ubiquinone: cytochrome c reductase from *Neurospora* mitochondria. *Nature* 280, 696-697.
- Zampighi, G. A., Kreman, M., Lanzavecchia, S., Turk, E., Eskandari, S., Zampighi, L., Wright, E. M., 2003. Structure of functional single AQP0 channels in phospholipid membranes. *J. Mol. Biol.* 325, 201-210.

Chapter 6

Development of a Tool for High Throughput Two-dimensional Crystallization Using Methyl- β -Cyclodextrin

6.1 Abstract

The aim of the present work is to provide a means for continuous addition of nanoliter amounts of a cyclodextrin solution to a detergent containing ternary mixture for crystallization. This is of special use when liposomes or proteoliposomes are to be produced. The machine allows for screening of multiple conditions for an optimal reconstitution and two-dimensional crystallization of membrane proteins with very little amount of protein. The kinetics of the reconstitution process is tightly controlled as the detergent complexation by cyclodextrins is of stoichiometric nature. The possibility of in-line optical spectroscopic analysis makes it possible to characterize the structures in the mixture as they evolve. Additionally functional assays and ligand binding experiments can be performed in succession of membrane protein reconstitution or liposome formation. Furthermore, as a result of constant liquid level monitoring, precise dilution and concentrating can be performed. This allows for systematic measurements of detergent mediated lipid solubilization. Finally, selective extraction of cholesterol from lipid membranes can also be achieved in small volumes with high precision.

6.2 Introduction

With the enormous number of membrane-associated drug targets being discovered by pharmaceutical and biotechnology companies, novel methods for screening and mode-of-action elucidation are in high demand. Both functional and binding assays provide critical data to aid the quantization and understanding of interactions of ligands with a diverse range of membrane receptors including peripheral proteins, G-protein coupled receptors, antibody receptors, cytokine receptors, viral receptors, voltage- and ligand-gated ion channels and transporter proteins. Together these proteins constitute the majority of 'druggable' targets currently addressed by marketed drugs and evaluated in drug discovery. In the literature they are said to

account for up to 70% of all drug targets (Lundstrom, 2004). They also represent a sizeable fraction of the receptor classes studied in academia in almost all areas of biochemical and physiological research.

Despite their fundamental biological and economical impact, they are still poorly understood when compared to soluble proteins. This apparent paradox is related to difficulties inevitably associated with membrane proteins: The production of large amounts of functional protein still poses a problem. Therefore membrane proteins are usually not available in abundant amounts. Additionally, due to their hydrophobic character one has to use detergents in order to keep them in solution. The detergents however, representing a non-native environment, constitute a problem as well, as they tend

to influence the structural and functional properties of membrane proteins.

Membrane proteins are purified in their detergent solubilized form. In order to perform functional assays and certain structural investigations one has to eliminate the detergent and re-incorporate the proteins into lipid bilayers. This process is commonly referred to as reconstitution of the membrane protein into proteoliposomes. This is usually achieved by continuous detergent removal from ternary mixtures consisting of detergent solubilized protein and detergent solubilized lipid molecules (or detergent destabilized vesicles (Paternostre et al., 1988; Rigaud et al., 1988)). Several methods exist for detergent removal, such as dialysis against detergent-free buffer (Engel et al., 1992), adsorption of detergent molecules to hydrophobic beads (Bio-Beads) (Rigaud et al., 1997) or dilution of the corresponding mixture below the critical micellar concentration (cmc) of the respective detergent (Rémigy et al., 2003).

However, these methods all bear limitations with respect to the amount of protein necessary to conduct reconstitution experiments, reproducibility of detergent removal kinetics and feasibility of high throughput implementation. An alternative way of detergent removal is given by the formation of inclusion complexes with host molecules (such as cyclodextrins), thereby suppressing their solubilizing capacity. Topologically, most of these host molecules can be represented as toroids. The interior of the toroid is considerably less hydrophilic than the aqueous environment and thus able to host the hydrophobic part of detergent molecules within the apolar cavity, thereby preventing hydrophobic interactions with other partners such as membrane proteins or lipids. Depending on the nature of the hydrophobic moiety of the detergent, most prominently the length of the alkyl chain, inclusion complexes of different molar ratios (host molecules/detergent) are formed. The longer the alkyl chain, the higher molar ratios will be displayed by the inclusion complexes. Compounds suitable for detergent inclusion comprise macrocyclic compounds exhibiting a cavity that is large enough to accommodate a detergent molecule, such as cyclodextrins, cucurbiturils and calixarenes, as well as cyclic peptides, α -cyclophanes, crownethers, (hemi-)carcerands, cavitands, cryptands and spherands might work too). Moreover, any (nano-)particulate polymer featuring hydrophobic cavities could possibly be used.

It has been demonstrated that reconstitution of solubilized membrane proteins can be achieved by addition of cyclodextrins to a ternary mixture (De-Grip et al., 1998). Additionally, we have shown previously that 2D crystallization is feasible with the use of MBCD (Signorell et al., 2006). The stoichiometric complex formation between a specific detergent molecule and a cyclodextrin is a tremendous advantage in view of reproducibility and control of the reconstitution kinetics.

6.3 Machine for High Throughput Two-dimensional Crystallization

6.3.1 Requirements

To construct a device that continuously delivers nanoliter quantities of a cyclodextrin solution for protein reconstitution in well plates suitable for high throughput screening several requirements have to be met: (see Fig. 6.1)

- The cyclodextrin addition should be performed by non-contact dispensing. This is required when working with detergent containing samples, which exhibit enhanced wetting behavior. Progressive addition of nanoliter amounts of cyclodextrin has to be ensured for a fine control of the kinetics.
- Preferably, the well plate resides on a shaker for optimal mixing of the constituents of the ternary mixtures.
- The level of the liquid within a well is monitored using a sensor and corrected for evaporation by addition of water as necessary.
- Optical spectroscopic devices for in-line analysis of the events occurring inside a well would be of great use. Spectroscopic techniques could comprise turbidimetry, fluorescence spectroscopy, Raman spectroscopy, Infrared/Ultraviolet spectroscopy and polarization analysis. Using a specially designed shaker unit that leaves the optical pathway free for spectroscopic and other optical analyses is thus a prerequisite.
- A preceding automated mixing station for the preparation of the ternary mixtures would warrant high throughput and high accuracy, and prevent user induced errors.

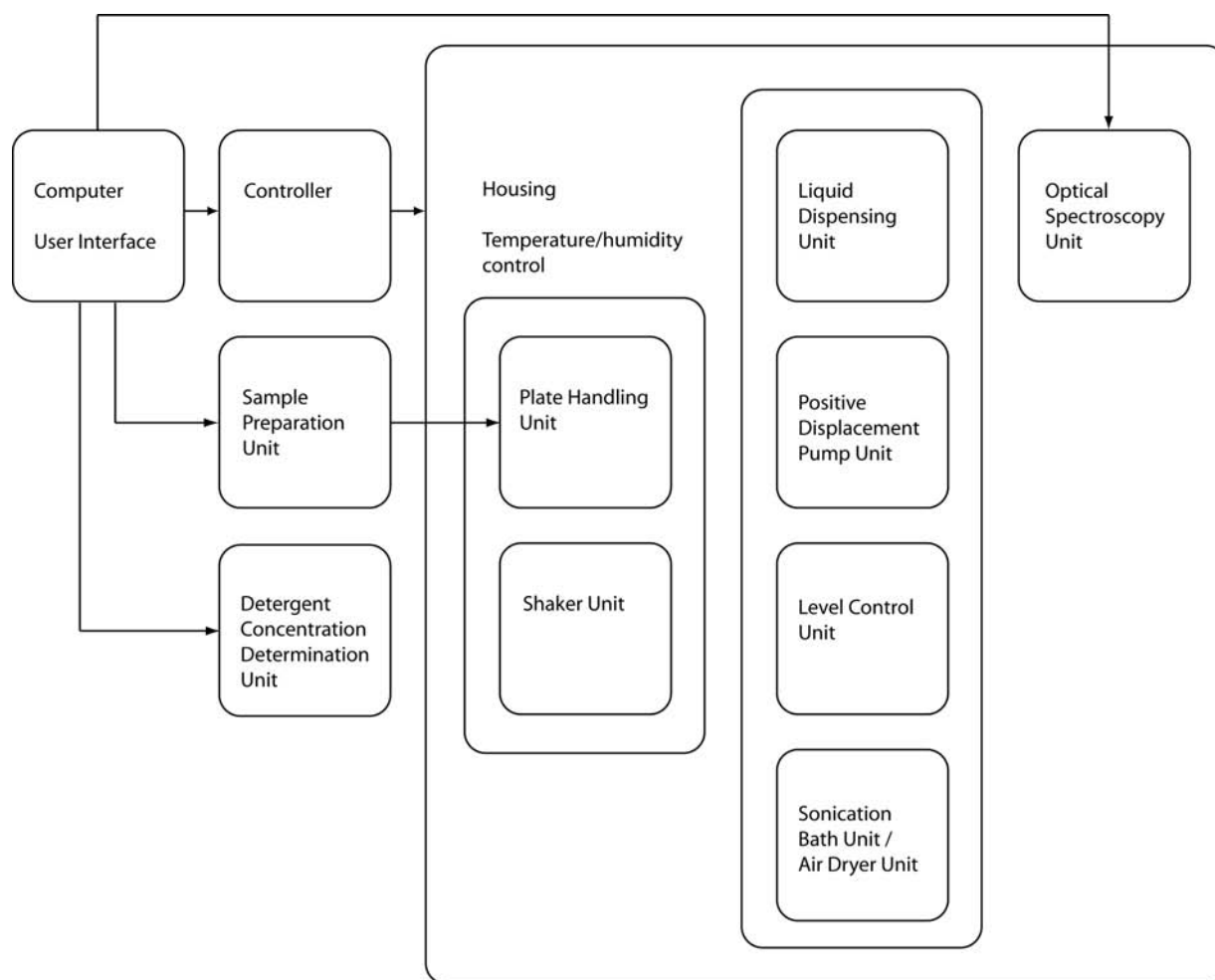


Figure 6.1: **Conceptual layout of the cyclodextrin-driven reconstitution machine.**

- An in-line detergent concentration measuring device would allow for determination of the amount of cyclodextrin needed to completely neutralize the detergent.
- All of these modules should preferably be contained within a housing allowing for temperature and humidity control.
- A computer would assemble and send all necessary commands to a controller, thus serving as interface for the user.

6.3.2 Construction of the Machine

One solution for achieving quantitative non-contact dispensing is a system in which a positive-displacement pump unit is used to supply reagent to a non-contact dispense element. Suitable non-contact dispense elements include piezoelectric displacement nozzles, solenoid time-open valves, orifice, or aerosol units. Such systems combine the quantitative characteristics of a positive-

displacement pump unit with the non-contact ejection characteristics of the selected dispense element. Here we have chosen the solenoid time-open valves as they provide high fidelity provided that the back pressure is constantly monitored.

The liquid level within the wells is constantly monitored using a capacitive sensor. The sensor measures the level by changes in capacity near the liquid surface as compared to air without contacting the surface. This provides a means of performing accurate dilutions as well as concentrating the sample by controlled evaporation. In principle any available capacitive sensor can be implemented, however here we have chosen a setup in which the electrodes are placed next to each other, giving the advantage of leaving the optical pathway beneath the well plate free for spectroscopic analyses. Alternatively, the level control could be achieved using ultrasonic liquid level detection.

The liquid handling unit may include a sonication bath unit and an air dryer unit for automatic cleaning of the dispense elements if partial or complete

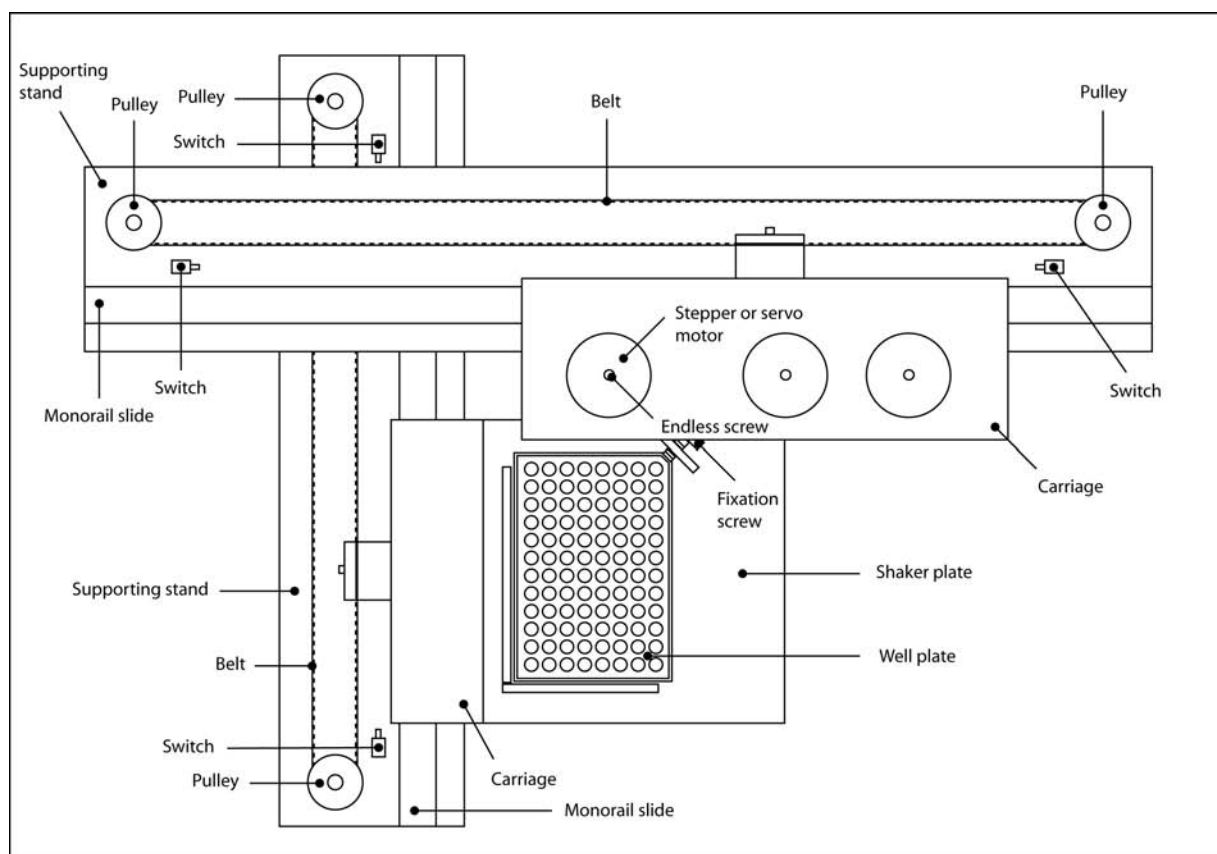


Figure 6.2: Schematic top view of the machine.

clogging thereof occurs.

Both, the liquid dispensing units and the level control unit, are attached to a single carriage. This carriage is fixed to a supporting stand through a monorail slide system and coupled to a belt passing around two pulleys of which one is directly coupled to a stepper motor (or servo motor) allowing for movement along the X axis. Movement of the individual dispensing heads and the level control sensor along the Z axis is mediated through individual stepper motors (or servo motors) carrying endless screws connected to the respective supports driving these items along vertical monorail slide systems.

The carriage of the shaker unit too is fixed to a supporting stand through a monorail slide system and coupled to a belt passing around two pulleys and of which one is directly coupled to a stepper motor (or servo motor) allowing for movement along the Y axis.

All of the drive systems are equipped with two switches at either end of the rails providing control of the boundaries of the movement. Alternatively, light pathway detectors could be used.

The agitation of the shaker is accomplished by a stepper motor (or servo motor) coupling its ro-

tation eccentrically to the shaker plate through a crank shaft and a ball bearing. Two monorail slides mounted on top of each other, one allowing for movement in the X direction and the other allowing for movement in the Y direction, guide the agitation. The stepper motor (or servo motor) and the monorail slides are fixed on the periphery of the carriage in order to leave the optical pathway beneath the well plate free for in-line spectroscopic analyses. The stepper motor (or servo motor) and the monorail slides are fixed in proximity to each other to ensure that the drive torque is close to the moveable axes. The coupling between the stepper motor (or servo motor) and the shaker plate includes a small plate interrupting the path of a fork light barrier enabling the shaker to automatically come back to its initial position.

6.3.3 Operation of the Machine

The well plate is manually fastened in position by a screw. However, this system can be easily adapted for robotic transfer of the well plate from an upstream sample preparation unit and for multiple well plates to be processed in parallel.

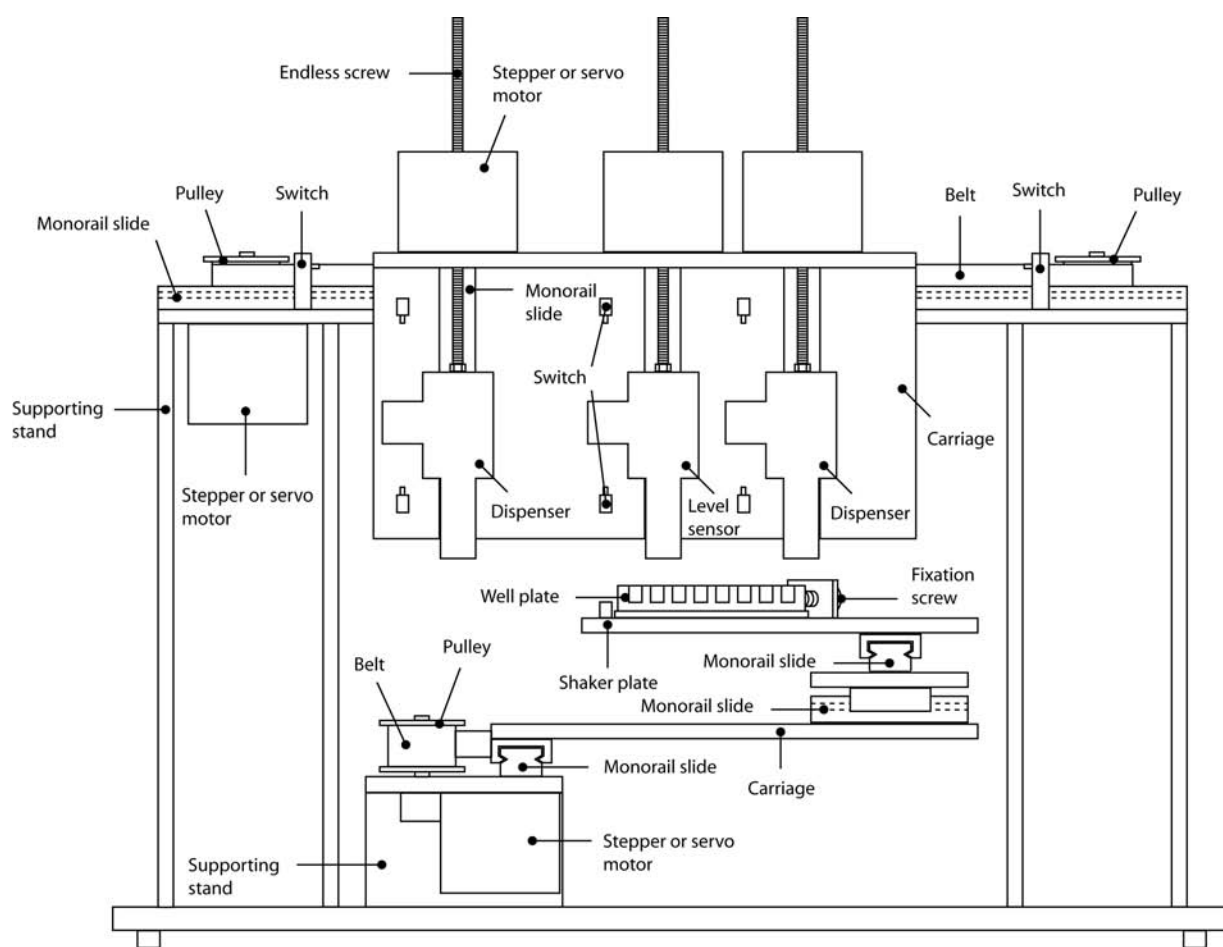


Figure 6.3: Schematic front view of the machine.

In principle any cyclodextrin and derivatives thereof can be used for complexation of detergents. However, the β -cyclodextrin has proven to be most useful in conjunction with detergents carrying alkyl chains as hydrophobic moiety. Detergents such as CHAPS, which represent larger structures to be contained within the cavity, are more efficiently complexed by γ -cyclodextrins. Preferably, methylated derivatives of the corresponding cyclodextrins are used for their higher solubility in aqueous solutions. In some cases however, the use of less water-soluble derivatives can be advantageous as they form insoluble precipitates which can easily be removed. The kinetics of detergent neutralization is controlled by the amount of cyclodextrin dispensed with each addition.

At the beginning, the wells are loaded with equal protein amounts and different lipids, all compounds being solubilized, and the solutions containing counter ions and other compounds being adjusted to a certain pH. The computer driven injection of detergent absorber proceeds sequentially for each well, with the liquid level being measured and

adjusted. All pertinent parameters such as temperature, turbidity and liquid level are acquired and stored in a data file together with the starting conditions.

6.4 Screening Strategy for High Throughput Crystallization

In the following possible strategies for high throughput screening are discussed. The multidimensional space that has to be experimentally covered is enormous, and therefore the key parameters (axes of the multidimensional space, showing the most important variations) have to be identified first. In order to search for optimal conditions efficiently, an initial screen is necessary. Several approaches for generating an experimental matrix can be used:

- Empirical approach: This takes previous, successful crystallization conditions for other proteins into account and simply applies them to new candidates.

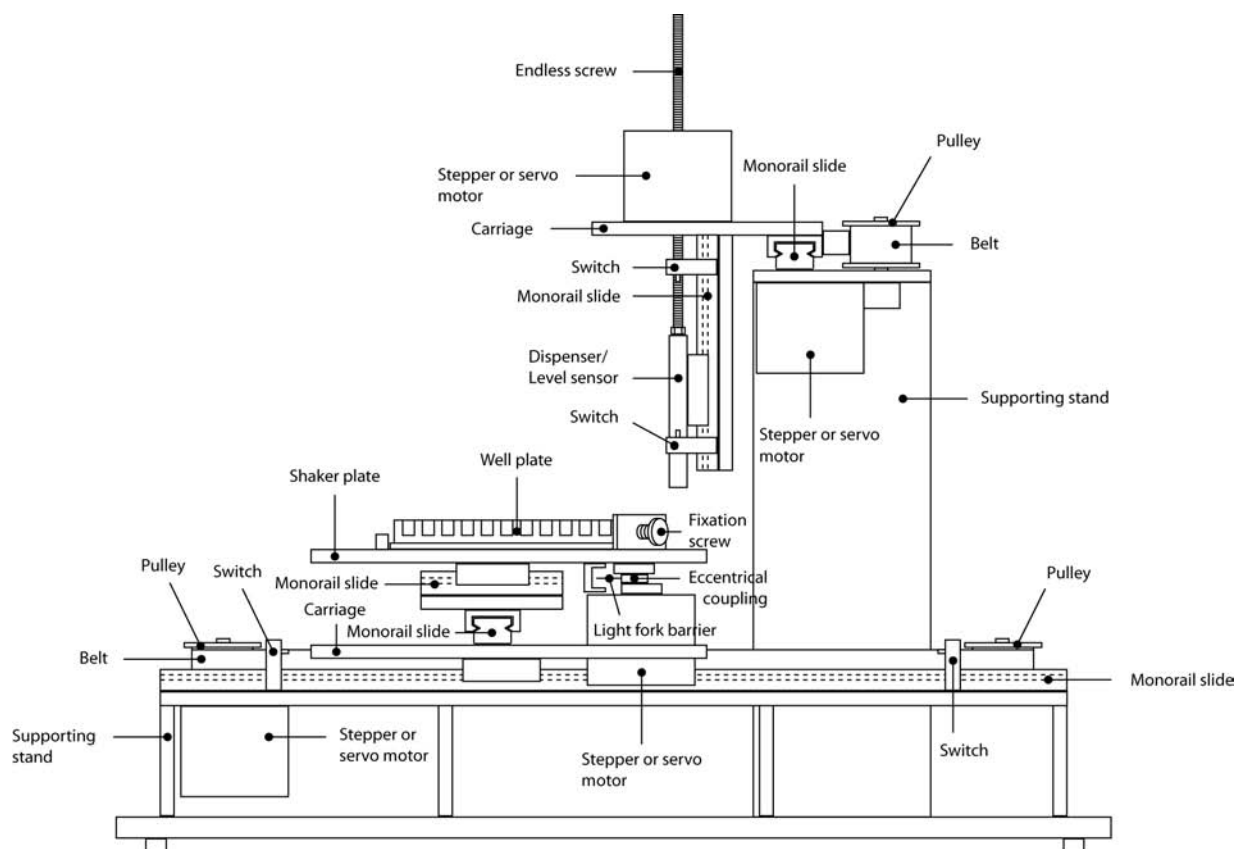


Figure 6.4: Schematic side view of the machine.

- Statistical approach: This analyzes previously successful conditions statistically and establishes a screen matrix covering the range of most successful conditions.
- Rational approach: This represents the most difficult approach to crystallization. Even though a lot of effort is invested in understanding the process of crystal assembly by studying more simple systems (e.g., binary mixtures), the whole process still remains a black box. It is all but trivial to extrapolate data of such studies to more complex (multidimensional) systems. However, it might be sufficient to perform a few systematic measurements in order to guess promising starting conditions.

A combination of the above approaches seems best suitable to cover most of the experimental space in two-dimensional crystallography:

Empirical approaches are indispensable in the early selection for possible candidate proteins. It is advisable to screen for the most stable member within homologs of different organisms. Additionally, it can be very helpful to use stable mutants blocked in a specific state (see e.g., lactose perme-

ase (Abramson et al., 2003)). Often, the addition of a high affinity ligand (e.g., inhibitor) is stabilizing the protein structure. Even antibodies have been successfully used to stabilize proteins (Hunte and Michel, 2002).

At this point the screening can be subdivided into several optimization steps:

Detergent type and amount for solubilization

Solubilize the biological membranes in different detergents and choose the detergent giving the best yield.

Detergent type and amount for purification (stability)

Check the stability of the protein in different detergents. In the best case the protein is best extracted from the membranes by the detergent it is most stable in. Unfortunately, this is not always the case and different detergents have to be chosen for extraction and further purification. This can be done by exchanging the detergent for extraction by another detergent on the column, as discussed in more detail in Chapter 3.

It should always be kept in mind that applying selective pressure quite early bears the danger of leaving out possible candidates. Therefore, the three best detergents should be tested as follows.

Detergent type and amount for lipid

Detergents that need to be tested are the ones that keep the protein in solution over weeks. Additionally, high-cmc detergents like octyl- β ,D-glucoside can be promising if they are used at the lowest concentration required to solubilize the lipids. This minimizes possible adverse effects on the protein.

For this purpose systematic lipid solubilization measurements need to be accomplished (see Chapter 3).

Lipid type for best yield in reconstitution

This step is crucial as different proteins require a specific type of lipid for stability. However, if the purification protocol has not been too harsh there is a good chance for native lipids to remain on the protein surface. Additionally, one strategy is to use lipid mixtures, e.g., from natural sources, with different compositions, trying to identify the type of lipid providing the best yield in reconstituted material. In subsequent refinement steps the length and saturation of the alkyl chain can be tested further.

In this context a standard protocol for the rapid assessment of reconstitution efficiency would be of great use for relative quantization, but such a method still remains to be developed.

pH range

The solubility minimum of a protein is at its isoelectric point (pI), where the protein has no net charge. The pI is defined experimentally as that pH at which the protein does not migrate in an electric field. Crystallization of a protein at its pI does not require the presence of additional ions. Away from its pI, however, the concentration of net neutral protein decreases in the absence of added ions. Crystallization of the charged protein away from its pI requires that counter-ions bind to the protein to produce a net neutral species.

The more the pH of the crystallization solution is away from the pI, the higher is the protein net charge and its solubility, and the larger is the number of counter-ions necessary for electrostatic compensation.

When statistically analyzing the pH range successfully used in 2D as well as 3D crystallization

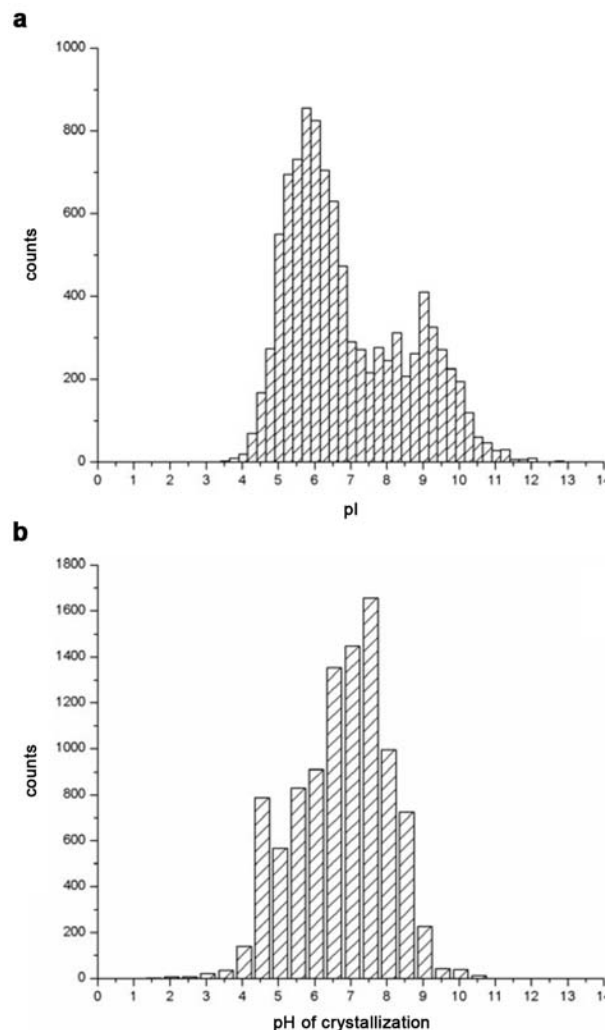


Figure 6.5: **Frequency distributions.** (Kantardjiev and Rupp, 2004) (a) pI of successfully crystallized proteins. (b) Reported pH of crystallization for proteins.

experiments one realizes that most proteins crystallize around the physiological pH of 7 - 7.5. Fig. 6.5 indicates that there is no statistically significant direct correlation between the pI of a crystallized protein and the pH of crystallization. However, there is a good correlation ($R^2 = 0.62$) between the pI of a crystallized protein and the difference between the pH of crystallization solution and pI (Fig. 6.6). It is apparent that acidic proteins crystallize with highest likelihood $\sim 0 - 2.5$ pH units above their pI, whereas basic proteins preferably crystallize $\sim 0.5 - 3$ pH units below their pI. Extreme values of pH do not contribute significantly to successful crystallization for most proteins, except for those that have unusually high or low pI values.

Thus, in order to improve the efficiency of the pH screening one can determine the protein's pI in

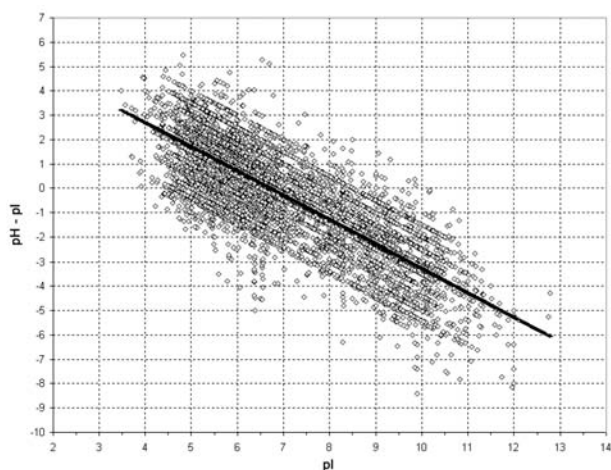


Figure 6.6: **Correlation between pI and pH.** (Kantardjieff and Rupp, 2004) Correlation between calculated pI of successfully crystallized protein and difference between reported crystallization pH and pI. $R^2 = 0.62$.

SDS and/or in the best detergent. Depending on the protein's pI, one should screen 2 - 3 pH units below or above, but within the range of pH 4 - 9.

Salt type and amount

The Hofmeister series provides a good basis to choose different types of salts with respect to their effects on the water structure (chaotropic/kosmotropic).

The effect of salt on the structural stability of proteins (both acidic and basic) becomes important at moderate salt concentrations (0.01-1.0 M) at neutral pH, and the effect is dominated by the anions (37).

Salt solutions have large effects on the structure and properties of proteins, including their solubility, denaturation, dissociation into subunits, and the activity of the enzymes. These effects are sensitive to the nature of the salt and may vary over a wide range, even for the salts of the same type. The order of effectiveness of different salts on proteins is generally similar to the Hofmeister series which was described for the salting out of the proteins more than a century ago (37).

Anions have been shown to affect the solubility of negatively charged proteins (Carbonnaux et al., 1995) according to the Hofmeister series:

sulfate (phosphate) > fluoride > chloride > bromide > iodide (perchlorate) > thiocyanate,

but in the reverse order for positively charged proteins (Ries-Kautt and Ducruix, 1989).

Cations	B	Anions	B
<i>Kosmotropes (strongly hydrated ions)</i>			
Mg ²⁺	0.385	PO ₄ ³⁻	0.590
Ca ²⁺	0.285	CH ₃ CO ₂ ⁻	0.250
Ba ²⁺	0.22	SO ₄ ⁻	0.208
Li ⁺	0.150	F ⁻	0.10
Na ⁺	0.086	HCO ₂ ⁻	0.052
<i>Chaotropes (weakly hydrated ions)</i>			
K ⁺	-0.007	Cl ⁻	-0.007
NH ₄ ⁺	-0.007	Br ⁻	-0.032
Rb ⁺	-0.030	NO ₃ ⁻	-0.046
Cs ⁺	-0.045	ClO ₄ ⁻	-0.061
		I ⁻	-0.068
		SCN ⁻	-0.103

Table 6.1: **Jones-Dole viscosity B coefficients follow the Hofmeister series.** Data from (Collins, 2004). The gradients indicate the tendency of stabilizing (green) and destabilizing (red) proteins.

Interestingly, this is also the order in which these ions elute from a Sephadex G-10 column (Collins and Washabaugh, 1985). The ions preceding chloride are polar kosmotropes, polar water-structure makers, and stabilize protein against denaturation whereas those following it, water-structure breaker ions, destabilize, i.e., denature proteins. The chloride ion in the concentration range of 0.1-0.7 M has little effect on protein stability (Collins and Washabaugh, 1985).

Proteins are stabilized by high concentrations of strongly hydrated anions and destabilized by high concentrations of weakly hydrated anions or strongly hydrated cations (see Table 6.1). Stabilization and crystallization are both associated with a decrease in the solvent accessible surface of a protein; destabilization and solubilization are both associated with an increase in the solvent accessible surface of a protein.

Looking at Table 6.1, we see first that the Jones-Dole viscosity *B* coefficient separates the ions into the same two groups as the Hofmeister series (*B* is a direct measure of the strength of ion-water interactions normalized to the strength of water-water interactions in bulk solution). Within each group the ions are also ordered in the same manner, according to the surface charge density on the atoms

to which the water molecules are attached. Second, we see that the negative charges on proteins (carboxylates) are strongly hydrated, whereas the positive charges on proteins (derivatives of ammonium) are weakly hydrated. And third, we see that the major intracellular anions (carboxylates and phosphates) are strongly hydrated whereas the major intracellular monovalent cations (K^+ and the positively charged amino acid side chains) are weakly hydrated. This mismatch in water affinity between the major intracellular anions and cations is important because it ensures that the charges on macromolecules remain free of counterions; this increases the solubility of the macromolecules (since only net neutral complexes crystallize) and functionally allows their charges to be used as binding determinants.

In a first step where only protein reconstitution is assessed, the use of two or three standard salts (NaCl/KCl/ev. $MgCl_2$) and concentrations (physiological ionic strength 150 - 200 mM) are sufficient. Further refinement in salt type and amount can be done when optimizing short range interactions between proteins. From a statistical point of view a reasonable range for screening would lie between 0 - 500 mM.

It might be possible to measure contact angles of buffer compositions used for crystallization in order to get a qualitative ranking of whether overall buffer compositions are kosmotropic or chaotropic.

6.5 Discussion

Here we present a machine that provides a means of parallel high throughput quantitative reconstitution of membrane proteins using detergent complexation by cyclodextrins. Applications range from high throughput membrane protein reconstitution, including two-dimensional crystallization of membrane proteins, to functional assays as well as ligand binding assays. Furthermore it allows to minimize the amounts of scarcely available membrane proteins required for their successful reconstitution. Monitoring of the formation of larger structures as well as ligand interactions and functional assays could all be performed by implementation of in-line spectroscopic measurements. Selective extraction of cholesterol from membranes and simultaneous monitoring of target protein function could also be accomplished by the use of cyclodextrins. One should keep in mind that the latter could represent a major drawback for cholesterol dependent

proteins.

However, advantageous to this new setup are the small volumes needed to perform successful reconstitutions, the precise control of the detergent removal rate as a result of the stoichiometric association of cyclodextrins with detergent molecules and the parallel reconstitution in industrially standardized well plates amenable for further high throughput analysis.

We propose to combine a screening strategy based on a (near) full factorial design with a careful step-by-step identification of key parameters for crystallization, such as detergent type and amount, and lipid type (see Fig. 7.1).

Thanks to automated liquid handling, the constant monitoring of the assays and the small volumes required for reconstitution, this represents a powerful setup providing high reproducibility and high throughput for the production of 2D crystals.

References

- J. Abramson, I. Smirnova, V. Kasho, G. Verner, H. R. Kaback, and S. Iwata. Structure and mechanism of the lactose permease of *Escherichia coli*. *Science*, 301: 610–615, 2003.
- C. Carbonnaux, M. Ries-Kautt, and A. Ducruix. Relative effectiveness of various anions on the solubility of acidic *Hypoderma lineatum* collagenase at pH 7.2. *Protein Sci.*, 4:2123–2128, 1995.
- K. D. Collins. Ions from the Hofmeister series and osmolytes: effects on proteins in solution and in the crystallization process. *Methods*, 34:300–311, 2004.
- K. D. Collins and M. W. Washabaugh. The Hofmeister effect and the behaviour of water at interfaces. *Q. Rev. Biophys.*, 18:323–422, 1985.
- W. J. DeGrip, J. VanOostrum, and P. H. M. Bovee-Geurts. Selective detergent-extraction from mixed detergent/lipid/protein micelles, using cyclodextrin inclusion compounds: a novel generic approach for the preparation of proteoliposomes. *Biochem. J.*, 330:667–674, 1998.
- A. Engel, A. Hefti, A. Hoenger, C. Henn, R. C. Ford, J. Kistler, and M. Zulauf. Assembly of 2-d membrane protein crystals: Dynamics, crystal order and fidelity of structure analysis by electron microscopy. *J. Struct. Biol.*, 109:219–234, 1992.
- C. Hunte and H. Michel. Crystallisation of membrane proteins mediated by antibody fragments. *Curr. Opin. Struct. Biol.*, 12:503–508, 2002.

- K. A. Kantardjieff and B. Rupp. Protein isoelectric point as a predictor for increased crystallization screening efficiency. *Bioinformatics*, 20:2162–2168, 2004.
- K. Lundstrom. Structural genomics on membrane proteins: mini review. *Comb. Chem. High Throughput Screen.*, 7:431–439, 2004.
- M. T. Paternostre, M. Roux, and J. L. Rigaud. Mechanisms of membrane protein insertion into liposomes during reconstitution procedures involving the use of detergents. 1. Solubilization of large unilamellar liposomes (prepared by reverse-phase evaporation) by Triton X-100, octyl glucoside, and sodium cholate. *Biochemistry*, 27:2668–2677, 1988.
- M. Ries-Kautt and A. Ducruix. Relative effectiveness of various ions on the solubility and crystal growth of lysozyme. *J. Biol. Chem.*, 264:745–748, 1989.
- J. L. Rigaud, M. T. Paternostre, and A. Bluzat. Mechanisms of membrane protein insertion into liposomes during reconstitution procedures involving the use of detergents. 2. Incorporation of the light-driven proton pump bacteriorhodopsin. *Biochemistry*, 27:2677–2688, 1988.
- J. L. Rigaud, G. Mosser, J. J. Lacapere, A. Olofsson, D. Levy, and J. L. Ranck. Bio-beads: an efficient strategy for two-dimensional crystallization of membrane proteins. *J. Struct. Biol.*, 118:226–235, 1997.
- H.-W. Rémigy, D. Caujolle-Bert, K. Suda, A. Schenk, M. Chami, and A. Engel. Membrane protein reconstitution and crystallization by controlled dilution. *FEBS Lett.*, 555:160–169, 2003.
- G. A. Signorell, T. C. Kaufmann, W. Kukulski, A. Engel, and H.-W. Rémigy. Controlled 2D crystallization of membrane proteins using methyl- β -cyclodextrin. *Biophys. J.*, 2006. submitted.

Chapter 7

General Discussion and Conclusions

7.1 Scope of this Thesis

This thesis represents an attempt to enlighten the role of the detergent in reconstitution and more specifically in two-dimensional (2D) crystallogenesis of membrane proteins. The construction of a tool for precise and routine measurements of detergent concentrations provided a valuable tool for better understanding and controlling the detergent issue. Additionally, a novel approach for detergent removal in 2D crystallization, i.e. the use of cyclodextrins was explored and a nanoliter dispensing high throughput tool was developed allowing for profound and sophisticated screening of optimal conditions for protein reconstitution and crystallization.

7.2 Combining Electron Microscopy and Atomic Force Microscopy

Although electron crystallography has proven to be a powerful approach to structure determination of membrane proteins (for a recent example see (Gonen et al., 2005)) successes are somehow restricted to certain classes of membrane proteins (e.g., outer membrane porins, aquaporins, naturally occurring crystalline proteins). This is mainly due to the stability of these proteins with respect to biochemical manipulation. One can not exclude however, that these are simply more amenable to crystallization due to the nature of their molecular surfaces.

2D crystallization exhibits several advantages compared to 3D crystallization of membrane proteins: The simple fact that the proteins are allowed to reside in a native-like environment, i.e., the membrane and that their function is not impaired by the lateral crystal contacts is of considerable interest. If structural investigations shall not be restricted to static snapshots of different conformations and moreover structure-function relationships shall be established, then electron microscopy (EM) in combination with atomic force microscopy (AFM) surely represent a valuable approach.

In Chapter 2 the combination of such data has

been successfully applied to the ammonium transporter AmtB from *Escherichia coli*. The aim was to determine the crystal packing of the double-layered 2D crystals of AmtB by AFM in order to process the cryo EM data. Additionally, the AFM images, due to their outstanding signal-to-noise ratio, enabled the direct visualization of trimers in the reconstituted membranes. The topographical data from the AFM allowed the assessment of a single layer within the double layered crystals.

7.3 Investigating the Role of the Detergent

In Chapter 3 the development of a fast and precise method for detergent concentration determination is presented. The robustness and wide application range of this method has been demonstrated by comparing concentrations of radioactively labeled dodecyl- β ,D-maltoside (DDM) with measured contact angles, by measuring the amount of DDM bound to the proton/galactose symporter GalP from *E. coli*, by measuring the effects of 100 mM NaCl on the cmc of dodecyl-N,N-dimethylamine-N-oxide, by characterizing the surface energy of Parafilm, and finally by revealing the stoichiometry of complex formation between methyl- β -cyclodextrin (MBCD) and different de-

tergents. The possibility of performing such measurements routinely in membrane biochemistry is unique compared to all other methods available to date.

Chapter 4 addresses the major aspects of detergent use in membrane protein purification and crystallization. First, the stability of GalP in different detergents is assessed, unveiling profound differences in the capacity of detergents to keep the protein in solution. Second, it is demonstrated, that the amount of a detergent, i.e., dodecyl- β ,D-maltoside, bound to a protein can be controlled during purification. At last the amount of different detergents for solubilization of *E. coli* lipids is determined, showing differences in the mechanisms by which detergents promote solubilization.

Banerjee *et al.* (Banerjee *et al.*, 1995) examined the preferential affinity of detergents for different lipids in mixed membranes (such as biological membranes). They showed that different detergents extract the serotonin 5-HT1A receptor from native membranes along with different lipids. The effect is considerable and might explain why different detergents exhibit such a different ability to keep a protein in its native state, because some might simply not be able to co-solubilize native lipids essential for the stability (and function) of the protein.

The amount of detergent bound to a protein is of special interest when using dialysis or dilution for detergent removal. Furthermore, in most cases the protein must not be exposed to excess detergent which anyway fails to satisfactorily mimic the native bilayer. As pointed out in the discussion of Chapter 4, protein reconstitution is facilitated when the detergent collar that is present around the hydrophobic region of membrane proteins in solution is near its solubility limit (P_{sol}).

The same is true for the lipid: Reconstitution is likely to happen when liposomes are forming, therefore an excess of detergent is not desirable either. Additionally, even detergents known to have adverse effects on protein stability can be used for lipid solubilization, given that they are present at a minimal concentration. The use of detergent mixtures in crystallization can also have the effect of reducing the size of the detergent collar around the protein. Moreover, the free detergent concentration in detergent mixtures is altered by the presence of the second species and can be crucial to the formation of crystals in some cases (Koning, 2003).

When using minimal amounts of detergent in a crystallization mixture, special care should be taken

with respect to the formation of ternary micelles. Ideally, equilibration of the ternary mixtures prior to detergent removal needs to be completed.

7.4 The Use of Cyclodextrins for High Throughput 2D Crystallization of Membrane Proteins

Chapter 5 demonstrates the feasibility of the cyclodextrin-based detergent removal for two-dimensional crystallization. The possibility of choosing different kinetics, simply by adding different amounts of cyclodextrin at various time intervals is one of the major advantages of this method. By implementing optical spectroscopy, it would be possible to slow down the detergent removal rate at the onset of proteoliposome and 2D crystal formation. As pointed out by Lichtenberg *et al.* (Lichtenberg *et al.*, 2000) the rate of detergent removal has to be slow enough to allow for detergent-induced vesicle size growth, a process which is usually quite slow. This aspect is important to keep in mind as one defines the rate of detergent neutralization (in contrast to dialysis). At a first glance one might think that in this respect the cyclodextrin approach bears no advantage compared to dialysis. However, the rate of low-cmc detergent removal using dialysis can be too slow, thereby keeping the protein out from its native environment for too long, ultimately promoting its precipitation.

In Chapter 6 we present an apparatus for parallel quantitative reconstitution and 2D crystallization of membrane proteins. Cyclodextrin provides a unique opportunity for high throughput implementation compared to other methods available today. Protein concentrating through controlled evaporation with concomitant detergent neutralization (to prevent detergent concentrating) is advantageous compared to commercially available protein concentrating devices which very often concentrate detergent micelles too. Moreover, the possibility of using one protein preparation for wide screening ensures that inconsistencies in results arising from preparative differences are excluded. Often, the detergent and lipid concentration of the purified protein are ill characterized, and this variability may be a cause for much of the irreproducibility and failure in crystallization (Wiener, 2004).

So far the use of wide screening matrices (sparse matrix design) in 2D crystallography was restricted by the enormous number of experiments and

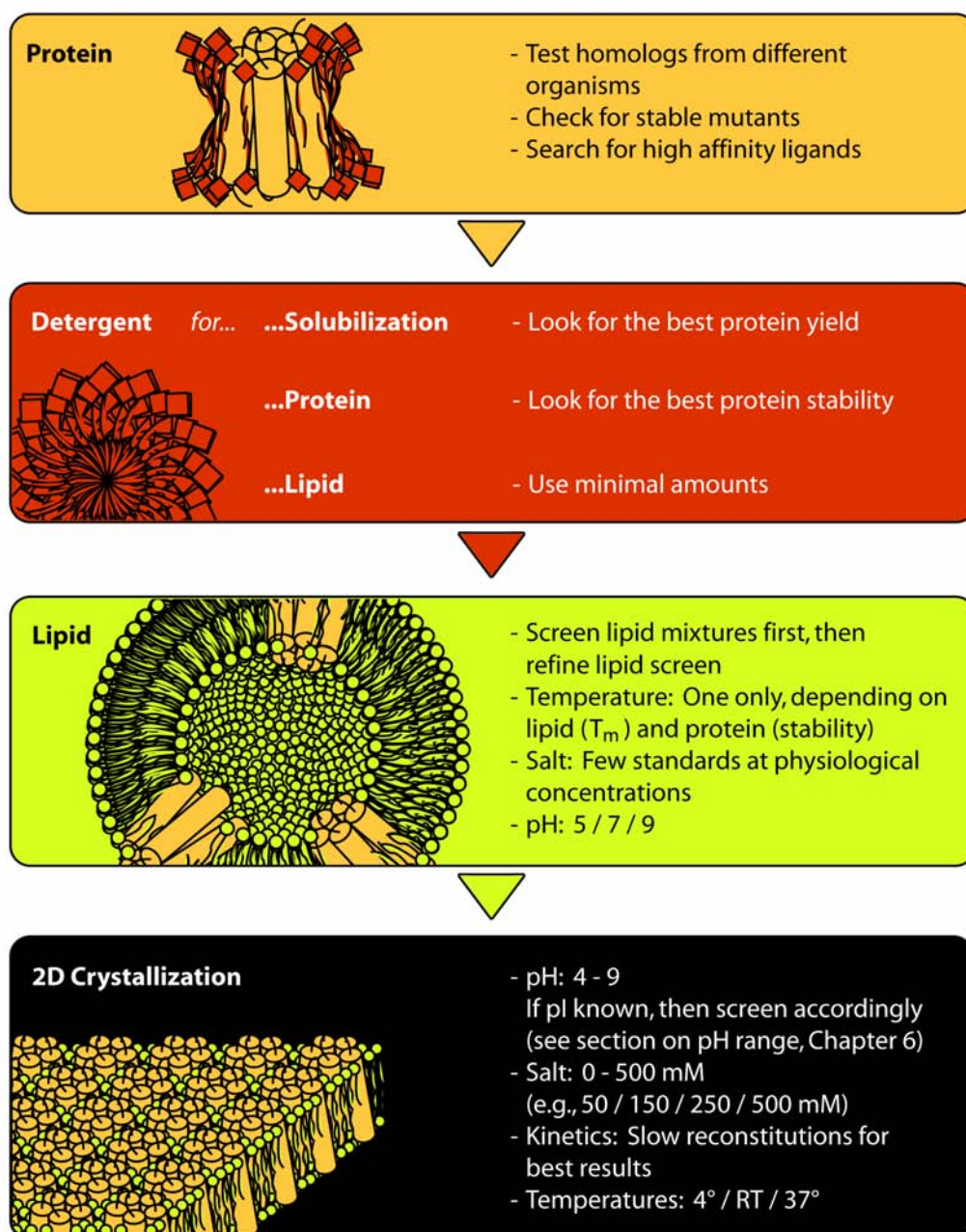


Figure 7.1: **Strategy for high throughput screening in 2D crystallography.** Prior to the wide screening of conditions promoting crystallization, key parameters should be sequentially analyzed in order to confine the multidimensional space to a meaningful range.

amount of protein needed for a rigorous screening. The presented machine makes it possible to partially compensate for the first bottleneck in protein structure elucidation, which is the over-expression of membrane proteins.

Fig. 7.1 summarizes the screening strategy based on the criteria discussed in Chapter 6 and above. Screening efficiency is provided by the subdivision of the problem into multiple subproblems and by their sequential screening.

With the high throughput approach however, a

new bottleneck arises as one will produce a large number of crystallization trials, which have to be screened for their outcome. Therefore –in analogy to the x-ray community– the development of automated sample preparation and automated electron microscopic analysis would provide substantial support to the 2D crystallographer.

Combining step-by-step identification of key values necessary for crystallization (and/or efficient reconstitution) together with high throughput screening matrices opens up new prospects in the en-

deavor to membrane protein structure and function determination. Now it is possible to apply a semi-rational screening strategy and this might contribute to transform 2D crystallization from art to science (Jap et al., 1992).

References

- P. Banerjee, J. B. Joob, J. T. Buseb, and G. Dawson. Differential solubilization of lipids along with membrane proteins by different classes of detergents. *Chem. Phys. Lipids*, 77:65–78, 1995.
- T. Gonen, Y. Cheng, P. Sliz, Y. Hiroaki, Y. Fujiyoshi S. C. Harrison, and T. Walz. Lipid-protein interactions in double-layered two-dimensional AQP0 crystals. *Nature*, 438:633–638, 2005.
- B. K. Jap, M. Zulauf, T. Scheybani, A. Hefti, W. Baumeister, U. Aebi, and A. Engel. 2D crystallization: from art to science. *Ultramicroscopy*, 46: 45–84, 1992.
- R. I. Koning. *Cryo-Electron Crystallography: from Protein Reconstitution to Object Reconstruction*. PhD thesis, Rijksuniversiteit Groningen, 2003.
- D. Lichtenberg, E. Opatowski, and M. M. Kozlov. Phase boundaries in mixtures of membrane-forming amphiphiles and micelle-forming amphiphiles. *Biochim. Biophys. Acta*, 1508:1–19, 2000.
- M. C. Wiener. A pedestrian guide to membrane protein crystallization. *Methods*, 34:364–372, 2004.

Appendix A

Acknowledgements

First, I'd like to thank Prof. Andreas Engel for the opportunity to conduct my PhD thesis in his group. You always consigned me with challenging projects, what I have regarded as a sign of confidence and trust in what I do and consequently I am grateful for.

A great big "thank you" to Hervé "Go Go Gadgeto" Rémigy for providing me with so many solutions to my many problems encountered during this work. You have been a great support not only in scientific terms, but also in motivational and many other issues. Your great sense of humor (and justice) helped me to overcome many obstacles, as you turned my attention to self-reflection and more importantly to the essentials. I admire your pioneering spirit!

I thank Dimitrios Fotiadis for sharing his outstanding skills in atomic force microscopy with me. I am very glad that we surmounted our initial discordance. After all, we are quite alike in terms of our understanding of science. Exactness and diligence are of utmost significance for our both work.

I thank Mohamed Chami for inspiring discussions on all matters of 2D crystallography and for the wonderful images he took with the cryoelectron microscope.

I thank Kitaru Suda for unequaled experimental advice and support. Your knowledge seems to be infinite as I can't remember having asked you a question without getting a conclusive answer.

I thank Wanda, Nora and Marco for all the good moments we shared in the lab, in the mensa and most importantly in the bars. I wish you all a lot of success for the continuation of your (scientific?) careers.

I thank Heiko Heerklotz for being a referee for my thesis. I very much appreciate your spontaneous readiness to read through my work albeit having an overfull calendar yourself.

Ultimately I'd like to thank my family for being my family. Needless to say that without you I wouldn't be where I am now or even who I am. This thesis is dedicated in its entirety to you!

Appendix B

Curriculum Vitae

B.1 Personal Details

Gender Male

Date of birth 03.06.1979

Place of birth São Paulo, Brazil

Present Citizenships Swiss, Brazilian

B.2 Education

1984 - 1985 English Junior School, Göteborg, Sweden

1985 - 1987 Domhofschule, Arlesheim, Switzerland

1987 - 1991 École Européenne I, Bruxelles, Belgium

1991 - 1997 Gymnasium Bäumlhof, Basel, Switzerland: Matura Typus A (emphasis on latin and ancient greek)

1997 - 2001 University of Basel, Basel, Switzerland: Studies in Biology II (Biochemistry).

Diploma thesis topic: "Expression, Purification and 2D-Crystallization of Lactose Permease from *Escherichia coli* (LacY) and Mechanosensitive Channel of Large Conductance from *Mycobacterium tuberculosis* (Tb-MscL)" (in the group of Prof. A. Engel)

2001 - 2006 University of Basel, Basel, Switzerland: PhD thesis in Biophysics (Structural Biology).

PhD thesis topic: "Detergent-Protein and Detergent-Lipid Interactions: Implications for Two-dimensional Crystallization of Membrane Proteins and Development of Tools for High Throughput Crystallography" (in the group of Prof. A. Engel)

B.3 Teaching

2001 Instructor in the "Blockkurs in Biophysik und Strukturbiologie" for the atomic force microscopy experiments.

2002 Tutoring "Übungen zu Grundlagen der Biologie" for students of Biology at the Biozentrum, University of Basel, Switzerland.

Instructor in the "Blockkurs in Biophysik und Strukturbiologie" for the atomic force microscopy experiments.

2003 Tutoring in the ethics-tutorial for students of Biology and Pharmacology at the Biozentrum, University of Basel, Switzerland.

Instructor in the "Blockkurs in Biophysik und Strukturbiologie" for the atomic force microscopy experiments.

2004 Tutoring "Übungen zu Grundlagen der Biologie" for students of Biology at the Biozentrum, University of Basel, Switzerland.

Tutoring in the ethics-course for students of Biology and Pharmacology at the Biozentrum, University of Basel, Switzerland.

Teacher at the 3rd NCCR Practical Course: "Membrane protein expression, purification, 2-D crystallization and imaging" at the Biozentrum, University of Basel, Switzerland.

Instructor in the "Blockkurs in Biophysik und Strukturbiologie" for the atomic force microscopy experiments.

2005 Instructor in the "Blockkurs in Biophysik und Strukturbiologie" for the atomic force microscopy experiments.

B.4 Publications

Articles

Conroy MJ, Jamieson SJ, Blakey D, Kaufmann T, Engel A, Fotiadis D, Merrick M, Bullough PA. 2004. Electron and atomic force microscopy of the trimeric ammonium transporter AmtB. *EMBO Reports*, 5(12): 1153-1158

Kaufmann TC, Engel A, Rémigy H-W. 2006. A Novel method for detergent concentration determination. *Biophysical Journal*. 90(1): 310-317

Signorell GA, Kaufmann TC, Kukulski W, Engel A, Rémigy H-W. 2006. Controlled 2D crystallization of membrane proteins using methyl- β -cyclodextrin. *submitted to: Journal of Structural Biology*

Book chapters

Braun T, Kaufmann T, Rémigy H, Engel A. 2006. Two-dimensional crystallization of membrane proteins. in: *Encyclopedic Reference of Genomics and Proteomics in Molecular Medicine*. Eds: Ganten D, Ruckpaul K. Springer-Verlag Berlin Heidelberg New York. *in press*

Kukulski W, Kaufmann T, Braun T, Rémigy H, Fotiadis D, Engel A. 2006. Assessing Structure and Dynamics of Native Membrane Proteins. in: *Structural Biology of Membrane Proteins*. Eds: Grishammer R, Buchanan S K. Royal Society of Chemistry Cambridge. *in press*

Patent applications

Engel A, Rémigy H-W, Kaufmann TC. 2005. Method and equipment for the determination of surfactant concentrations in aqueous solutions. European Patent Application Nr. EP05011904 and US Provisional Patent Application Nr. US60/702,261

Engel A, Rémigy H-W, Kaufmann TC. 2006. Equipment for high throughput reconstitution of membrane proteins using detergent complexation by nanoparticles. European Patent Application and US Provisional Patent Application. *in preparation*

B.5 Courses

2001 FEBS Advanced Course: Molecular dynamics of membrane biogenesis, June 18-30, Cargese, Corsica, France.

2004 EMBO Course: Cryoelectron microscopy and digital image processing, September 5-14, EMBL Heidelberg, Germany.

